BNL 19302
(ENDF-202)

ENDF-202
CROSS SECTION EVALUATION WORKING GROUP
BENCHMARK SPECIFICATIONS

November 1974

MASTER

NATIONAL NEUTRON CROSS SECTION CENTER

BROOKHAVEN NATIONAL LABORATORY
ASSOCIATED UNIVERSITIES, INC.
UNDER CONTRACT NO. AT(30-1)-16 WITH THE
UNITED STATES ATOMIC ENERGY COMMISSION

Research supported by the United States Atomic Energy Commission.

Printed in the United States of America

November 1974 600 copies

FAST REACTOR BENCHMARK CONTENTS

CSEWG FAST REACTOR BENCHMARK COMPILATION

June 1973

Contributors:

H. Alter
R. B. Kidman
R. LaBauve
R. Protsik
B. A. Zolotar

I. INTRODUCTION

The utilization of integral experiments has been widely accepted by the CSEWG community as a mechanism for validation of the ENDF/B data files. Over the past half dozen years a number of fast integral experiments have been given recognizance as CSEWG Fast Reactor Benchmarks. These benchmarks have been specified at various times by various people. These efforts are recognized as having been very worthwhile.

This report represents an attempt by the CSEWG community to systematically present specifications for the currently accepted Fast Reactor Benchmarks. Specifications for these benchmarks conform to an agreed upon format. All accepted benchmarks have been reviewed for completeness and accuracy of the experimental information. It is anticipated that from time to time additional benchmarks will be generated from now available integral experiments. With the establishment and acceptance of a standard specification format, it is believed that the problems of passing from experiment to benchmark will be minimized.

II. CONTRIBUTORS

In 1971 E. M. Pennington, ANL and J. D. Jekins, ORNL, were assigned the task of producing an acceptable standard format for specifying CSEWG Fast Reactor Benchmarks. Their success is documented in Section III.

Upon acceptance of the above standard, members of the CSEWG Data Testing Subcommittee were assigned Fast Reactor Benchmarks for re-specification according to the accepted format, and to verify wherever possible, the accuracy of the given experimental data for these benchmarks. The responsible personnel, their affiliation and the benchmarks so specified are as follows:

CSEWG BENCHMARK ASSEMBLY	RESPONSIBILITY	
JEZEBEL	R. LaBauve	LASL
GODIVA		
VERA-11A	H. Alter*	AI
ZEBRA-3		
VERA-1B		
ZEBRA-2		
ZPR-3-48	B. A. Zolotar**	ANL
ZPR-6-7		
ZPR-6-6A		
ZPR-3-6F	R. B. Kidman ***	HEDL
ZPR-3-11		
ZPR-3-56B		
ZPR-3-12	R. Protsik	GE
ZPPR-2		
SEFOR		

New addresses:
*Divs. of Reactor Research & Development, USAEC, Washington, D. C. 20545
**Electric Power Research Institute, 3412 Hillview Avenue, Palo Alto, CA 94304
***Los Alamos Scientific Laboratory, P. O. Box 1663, Los Alamos, New Mexico 87544

III. BENCHMARK SPECIFICATION FORMAT

CSEWG benchmark problems are intended to allow the assessment of the validity of microscopic nuclear data by comparison of integral experiments and calculations. CSEWG benchmarks should therefore be selected for usefulness and ease of calculation and representation, and should be as free as possible from effects ascribable to computational techniques and modeling.

A CSEWG benchmark should provide a logically ordered description of the system which will allow the user to determine if the problem is of interest, to set up the problem in an unambiguous fashion with a reasonable amount of effort, to compare calculated results directly to the experiment with a minimum application of correction factors, and where such factors are unavoidable, to apply correction factors in an unambiguous and clearly described fashion. The benchmark description should contain sufficient information and suitable documentation to permit the user to form an independent assessment of the validity of the calculational models described. Benchmark descriptions lacking comments and documentation in this regard are unacceptable.

In accord with the broad requirements above, the following format for benchmark specifications is required:

A. Benchmark name and type., e.g., JEZEBEL - a bare sphere of plutonium; SEFOR Doppler benchmark.

B. System Description: This should be a description in English of the physical system and the general reasons for its selection as a benchmark. The section should include, for example, specific cross section and energy range sensitivities of the system.

C. Model Description:

1. One-Dimensional Model: If at all possible, the system should be described as a one-dimensional homogeneous model.

Such a prescription should include:

a. model dimensions and a figure;

b. boundary conditions;

c. atom densities in each region in units of atoms/barns cm;

d. the perpendicular bucklings, which may be energy - and region-dependent, if the geometry is not spherical;

e. the suggested geometrical mesh description;

f. the suggested calculational method, i.e., diffusion theory, S_n with n specified, etc.;

g. the suggested energy group structure;

h. details on special calculational techniques, i.e., if central worth data are available, then the size of the region over which such a calculation is to be effective might be specified, or if resonance shielding for a particular nuclide is important, then this fact might be noted;

i. an estimate of the suitability of the simple model to represent the actual system, with some estimated uncertainty in k_{eff} ascribable to the model.

2. Other more complicated models: Two- and three-dimensional models for the system may be prescribed as outlined above. Exact specifications can be useful for those wishing to perform Monte Carlo calculations.

D. Experimental Data:

Experimental data with error estimates should be presented for all available quantities of interest. Errors should be represented as one standard deviation and so described.

Experimental data should include:

a. measured eigenvalue with error estimates. It is permissible to give correction factors to be applied to the calculated eigenvalue to allow for heterogeneous-homogeneous, transport-diffusion, 2D-1D, etc., corrections.

b. experimental spectral indices at the core center with error estimates wherever possible. Correction factors may be required to allow for heterogeneity effects.

c. material worths at the core center including error estimates wherever possible. These should be given in units of $10^{-5} \Delta k/k$/mole. It may be necessary to give correction factors to allow for the differences between the simplified one-dimensional and actual models.

d. other quantities for optional analysis such as central activation cross sections, Doppler effects, Rossi alpha, and leakage spectra should be included. Error estimates should be given if possible. Wherever corrections are necessary to relate calculated and experimental results, detailed instructions on their application should be given together with a numerical example.

E. Calculated Results:

An optional section giving CSEWG calculated results using version N data would be helpful in establishing both model validity data trends. Individual results should be given for specific codes and calculational procedures rather than averaged results. This allows assessment of the merits of various codes. Comments on the committee's experience with the specific benchmark could be included here.

F. Comments and Documentation:

This section should contain sufficient information to allow the user first, to comprehend the approximations inherent in the benchmark representation and how they were resolved, and second, to trace back through references the detailed calculation basis for the model. In particular, this section should cover:

a. the method used for converting the actual three-dimensional geometry to one-dimensional geometry should be briefly described, and an error estimate should be given for the process.

b. a brief description should be presented of the method for converting from heterogeneous to homogeneous regions including an error estimate.

c. some discussion should be given of any corrections which were made to experimental spectral indices and central worths for flux depressions by fission chambers, sample size effects, etc. In the case of central worths, the values of inhours per $\% \Delta k/k$ used for converting the experimental measurements should be given, along with a reference to the delayed neutron parameters involved. The persons providing the benchmark description should be aware of the fact that central worths calculated for the simplified 1D-system may be considerably different from those of the actual system, and that calculations to investigate this fact should be made.

d. finally, the section must include references to the sources of information presented. The references should be to published documents or papers rather than internal memoranda.

G. Limitations:

The benchmark descriptions should not require any specifications which are pertinent only to individual multigroup cross-section production codes such as MC^2 or ETOX for example. Such specifications include weighting spectra within groups, ordinary or consistent P_1 or B_1 options, etc. However, generally applicable problem qualifications, i.e., order of S_n or broad group structure, may appear as suggestions in the model description, Section C.

FAST REACTOR BENCHMARK NO. 1

A. Benchmark Name and Type: JEZEBEL, a bare sphere of plutonium.

B. System Description

JEZEBEL is a bare sphere of plutonium metal. The single-region, simple geometry and uniform composition conveniently facilitate calculational testing, especially for the plutonium isotope cross sections in the fission source energy range.

C. Model Description

The spherical homogeneous model has a core radius of 6.385 cm and the following composition.[1]

Isotope	Density, 10^{24} a/cc
^{239}Pu	0.03705
^{240}Pu	0.001751
^{241}Pu	0.000117

The recommended mode of calculation is one-dimensional transport theory, S_{16}, with 40 mesh intervals in the core, a vacuum boundary condition on the core boundary (6.385 cm) and a 26 energy group structure with half-lethargy unit widths and an upper energy of 10 MeV.

D. Experimental Data[a]

1. Measured Eigenvalue: $k = 1.000 \pm 0.003$

2. Spectral Indices at Core Center

a. Central Fission Ratios[2]

$\sigma_f(^{238}U)/\sigma_f(^{235}U)$	0.205 ± 0.008
$\sigma_f(^{233}U)/\sigma_f(^{235}U)$	1.61 ± 0.10
$\sigma_f(^{239}Pu)/\sigma_f(^{235}U)$	1.49 ± 0.03
$\sigma_f(^{237}Np)/\sigma_f(^{235}U)$	0.99 ± 0.05

b. Central Activation Cross Sections[3]

Isotope	$\sigma_{(n,\gamma)}$, barns (spectrum average at core center)	Thermal Normalization Value, barns
^{51}V	0.0028 ± 0.0002	4.8
^{55}Mn	0.0029 ± 0.0002	13.3
^{63}Cu	0.0122 ± 0.0006	4.5
^{93}Nb	0.0276 ± 0.0030	1.15
Au	0.1012 ± 0.0025	98.8

3. Rossi Alpha[5]

$\alpha = -\beta_{eff}/\ell = -0.65\times10^{6}\ sec^{-1}$

4. Central Reactivity Worths[4]

Isotope	Central Worth, 10^{-5} $\Delta k/k$/mole
H	119 ± 2
Be	29 ± 1

[a]See Section F for a discussion of some of the experimental data.

Isotope	Central Worth, 10^{-5} $\Delta k/k$/mole
^{10}B	-477 ± 20
C	-13.1 ± 0.4
N	-43 ± 1
O	-18.8 ± 0.6
Al	-26.8 ± 0.8
Ti	-49 ± 2
V	-29 ± 1
Fe	-41 ± 1
Ni	-91 ± 4
Zr	-68 ± 2
Mo	-84 ± 3
Ta	-190 ± 6
Au	-165 ± 4
Th	-124 ± 4
^{233}U	2582 ± 20
^{235}U	1528 ± 15
^{238}U	217 ± 8
^{237}Np	1499 ± 40
^{239}Pu	3025 ± 30
^{240}Pu	1972 ± 190

NOTE: These central worths have been effectively normalized by use of an empirically derived, normalized effective delayed neutron fraction. See Section F.

5. Leakage Spectrum[6]

The spectrum of neutrons emitting from the surface of the core is represented below in the 1/2 lethargy group structure (E_{MAX} = 10 MeV) with an arbitrary normalization to the value 20 in group 5.

Energy Group	Lower Lethargy Limit	Relative Flux
1	0.5	3.1
2	1.0	11.7
3	1.5	17.7
4	2.0	20.0
5	2.5	16.5
6	3.0	13.6
7	3.5	9.7

E. Calculated Results

Calculated results may be appended to these specifications.

F. Comments and Documentation

The composition and configuration specifications were taken from Ref. 1. The actual JEZEBEL composition included gallium at a density of 0.001375×10^{24} a/cc. In these specifications, gallium has been deleted and its effect on k_{eff} (-0.0035), based on reactivity worth measurements of gallium compared to plutonium, has been included.

For the mode of calculation suggested, S_{16}, it is estimated that the eigenvalue is calculated 0.08% too high compared to a hypothetical S-infinity calculation. This result is based on transport-calculation studies for Godiva as reported in ANL-7416.[7]

The central fission and capture ratios given here are those evaluated by Hansen and reported in Ref. 2.

The central activation cross sections were measured with a comparative activation technique that relied upon knowledge of a standard activation cross section and upon thermal activation cross sections for each isotope for normalization purposes.[3] The ^{235}U fission cross section was selected as the standard activation cross section. Thermal normalization cross sections were determined from measurements and in conjunction with the value assigned to the standard activation cross section in this assembly. Thus, the central activation cross sections reported here are effectively normalized to a value assigned to the ^{235}U fission cross section in this assembly and to values determined for the thermal normalization cross sections. The data for the central activation cross sections was originally reported in Ref. 3. Subsequently, some of the thermal normalization values and, consequently, the activation cross sections, have been re-evaluated by LASL.

The measured central reactivity worths, corrected for sample size effects, were taken from Ref. 4. The measured values were reported in units of a dollar (cents/mole). These measured values were then converted to units of $\Delta k/k$ with a value of 0.0019 for the effective delayed neutron fraction obtained

from Ref. 5. It should be noted, however, that this value of β_{eff} is actually a value normalized to a reference calculation. The procedure used was based upon a measurement (Rossi-α) of the increment in mass added to the surface of the assembly that would bring the assembly from delayed to prompt critical. The computed (S_4) change in multiplication for this mass increment was then equated to β_{eff}. Thus, the central worth values specified here are, in fact, normalized to a measured worth.

The data listed for the leakage spectrum was derived from Ref. 6. A finer energy mesh representation for the spectrum may be found in Ref. 6 along with statistical uncertainties (which are large at higher energies) in each energy range.

REFERENCES

1. G. E. Hansen and H. C. Paxton, "Reevaluated Critical Specifications of Some LASL Fast Neutron Systems", LA-4208, 1969.
2. G. E. Hansen, "Status of Computational and Experimental Correlation for Los Alamos Fast Neutron Critical Assemblies", Proc. of Seminar on Physics of Fast and Intermediate Reactors, Vol. I, IAEA, Vienna (1962).
3. C. E. Byers, "Cross Sections of Various Materials in the Godiva and Jezebel Critical Assemblies", Nucl. Sci. and Eng. 8, No. 6, p. 608 (Dec. 1960).
4. Engle, et al., "Reactivity Contributions of Various Materials in Topsy, Godiva, and Jezebel," Nucl. Sci. and Eng., 8, No. 6, p. 543, (Dec. 1960).
5. G. A. Jarvis, et al., "Two Plutonium Metal Critical Assemblies", Nucl. Sci. and Eng. 8, 525-531 (1960).

6. L. Stewart, "Leakage Neutron Spectrum from a Bare Pu-239 Critical Assembly", Nucl. Sci. and Eng. 8, No. 6, p. 595. (Dec. 1960).

7. Argonne Code Center, "Numerical Determination of Space, Time, Angle, and Energy Distribution of Particles in an Assembly," ANL-7416 (1968).

FAST REACTOR BENCHMARK NO. 2

A. Benchmark Name and Type

VERA-11A, a plutonium-plus-graphite assembly.

B. System Description

VERA-11A was a cylindrically shaped critical assembly fueled with plutonium and diluted with graphite. Assembly core height was 21.7 cm and the effective core diameter was 26.9 cm. The core region was surrounded by a blanket consisting of depleted uranium and stainless steel. This assembly was designed to explore the accuracy of the plutonium 239 neutron cross section data.

C. Model Description

1. One-Dimensional Model Description

A one-dimensional spherical model of VERA-11A is given in Figure 1. A vacuum boundary condition should be applied at the outer reflector boundary. Material atom densities for the core and reflector regions are given in Table 1. The standard calculation mode is an S_8 transport theory calculation using a multigroup structure composed of 26 groups, each of lethargy width equal to 0.5 and with E_{max} set to 10 MeV. The number of mesh are 40 in the core and 40 in the reflector.

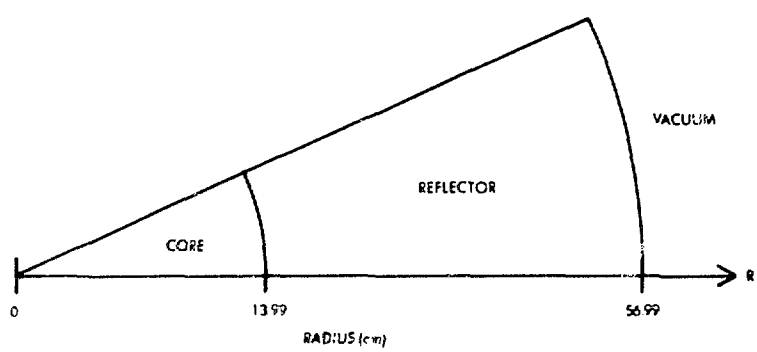

Figure 1. Spherical Model of VERA-11A Assembly

2. Two-Dimensional Model Description

A two-dimensional (R-Z) cylindrical model of the VERA-11A assembly is given in Figure 2. Zero return current boundary conditions should be applied to the top and the right side of the model; a symmetry boundary condition should be applied along the model bottom. It is suggested the assembly be calculated using a two-dimensional diffusion theory code. Suggested mesh is 40 radial and axial intervals in the core and 40 intervals for the reflector thickness.

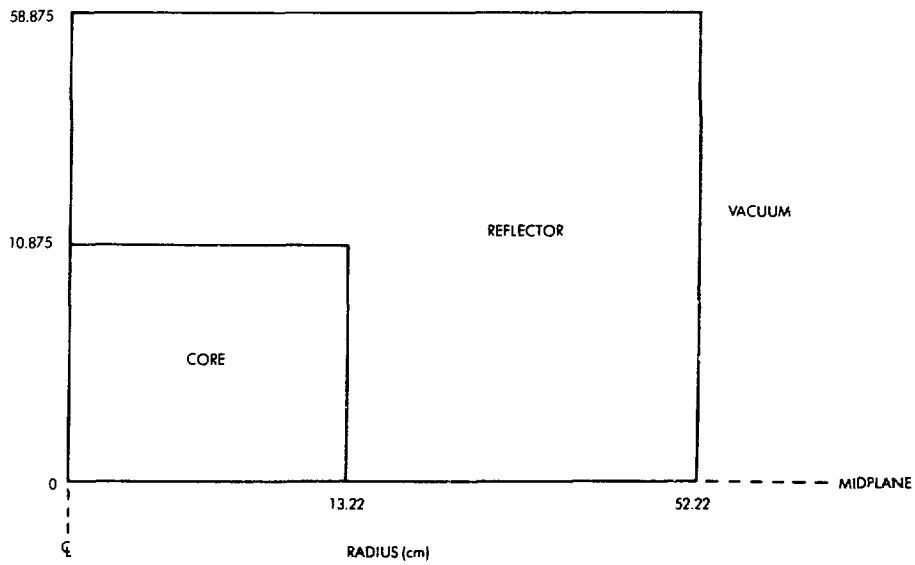

Figure 2. Two-Dimensional (R-Z) Model of VERA-11A Assembly

Table 1.

VERA-11A Region Compositions

(Atoms/Barn-cm)

Material	Core	Reflector*	
		(a)	(b)
Pu-239	0.007213	-	-
Pu-240	0.000370	-	-
Pu-241	0.000028	-	-
Ga	0.000449	-	-
C	0.046204	-	-
Fe	0.006084	0.0065	0.006582
Cr	0.001579	0.0017	0.001713
Ni	0.000665	0.00071	0.000721
Cu	0.007402	-	-
U-235	-	0.00025	0.00026
U-238	-	0.03440	0.03610
Pb	0.000035	-	-
Sn	0.000043	-	-

*Composition (a) should be used for calculations.

D. Experimental Data

1. Experimental Critical Mass — 33.81±0.06 Kg Pu-239

Corrections for Edge Irregularities	-0.97±0.3
Finite Fuel Plate Thickness	+1.37±0.3
Homogeneous Cylinder Critical Mass	34.2±0.4 Kg Pu-239
Experimental Eigenvalue	1.000±0.003

2. Experimental Spectral Indices at Core Center Relative to σ_f (U-235)

σ_f (U-238) = 0.007±0.002
σ_f (Pu-239) = 1.07±0.02
σ_f (Pu-240) = 0.475±0.020
σ_f (N_p-237) = 0.43±0.02
σ_f (U-233) = 1.49±0.03

3. Material Worths at Core Center

The measured reactivity coefficients for U-235, U-238, and Pu-239 at the core center of VERA-11A were equated[3] to perturbation cross sections by normalizing to a value of 1.901 barns for U-235 calculated using the FD1 cross section library.

Material	Reactivity Coefficient, mb, (normalized to 1901 for U-235)
U-235	1901±20
U-238	24±1
Pu-239	3448±38

F. Comments and Documentations

VERA-11A was a cylindrical critical assembly fueled with plutonium and diluted with graphite. Detailed descriptions of the experimenta have not been published. Model specifications are those derived by McTaggart.[1]

The experimental critical mass is 33.81±0.06 Kg Pu-239. Corrections for edge irregularities (-0.97±0.3) and for finite fuel plate thickness (+1.37±0.3) produce a homogeneous cylindrical critical mass of 34.2±0.4 Kg Pu-239. Plates in the fuel elements in VERA-11A form continuous planes perpendicular to the axis of the cylindrical core. It was therefore possible to estimate corrections for heterogeneity (~ 1.0% in k) from infinite slab calculations. Applying a shape factor of 0.959 produces a homogeneous spherical critical mass of 32.8±0.5 Kg Pu-239, with the radius of the critical sphere equal to 13.99±0.07 cm. Experimental results were derived from results quoted by McTaggart, Baker[2] and Smith.[3] R. W. Smith[4] provided the following comment on the experiment: The correction for heterogeneity in VERA-11A is 1.37 Kg Pu-239, McTaggart of AWRE has pointed out that heterogeneity measurements on the current re-build of VERA-11A suggest a heterogeneity correction nearer 1.0 Kg Pu-239; the atom densities for lead and tin arise from the solder in the plutonium can; a figure of 95±15 p.p.m. of hydrogen in the graphite has been suggested to allow for possible moisture content in the graphite, the effect of this moisture or k_{eff} for VERA-11A is about +0.03% $\Delta k/k$.

The estimated correction to the S_8 eigenvalue for the "S_∞" is -0.0024. For example, if the transport theory, k_{eff} (S_8), result was 0.9990, then the k_{eff} (S_∞) result would be 0.9990-0.0024 = 0.9876.

REFERENCES

1. M. H. McTaggart, Internal Report VERA/OP113, (January 1967).
2. A. R. Baker, "Comparative Studies of the Criticality of Fast Critical Assemblies," Proc. of International Conf. in Fast Critical Experiments and Their Analysis, ANL-7320 (1966)
3. R. D. Smith, et al, "Fast Reactor Physics Including Results from U. K. Zero Power Reactors," Proc. 3rd Int. Conf. Peaceful Uses of Atomic Energy, 6 pg 166, IAEA (1964)
4. Private Communication, R. W. Smith (UKAEA) to H. Alter, (Nov. 1970).

FAST REACTOR BENCHMARK NO. 3

A) ZPR-3 Assembly 48 - A Plutonium Fueled Fast Critical Assembly

B) System Description

The ZPR-3 consists of two halves, each a horizontal matrix of 2.2 in. square stainless steel tubes into which are loaded perforated stainless steel drawers containing fuel and diluent materials of various types. Assembly 48 was a small (400 liter) fast critical assembly with a soft spectrum and other characteristic representative of current LMFBR designs. The drawers contained plates of plutonium, Pu/U/Mo alloy, sodium, depleted uranium, and graphite. The atomic ratio of uranium to plutonium was approximately 4:1, with the ^{240}Pu isotopic fraction of 6%. The L/D ratio was approximately unity and the blanket was 12 in. of depleted uranium.[1] Figure 1 shows the loading of a core drawer as well as several other special drawers. Figures 2 and 3 show the cross sectional views of the as-built reference assembly, which had an excess reactivity of 61 Ih. The equivalent cylindricalized representation of the as-built reference assembly is shown in Fig. 4.

C) Model Description

1. One-Dimensional Model: A one-dimensional model with spherical geometry has been used in the analysis of many measurements in this assembly. The spherical homogeneous model was defined with reference to a two-dimensional finite cylindrical, heterogeneous model which will be described in Section C.2, and a spherical, heterogeneous model. The radius of the core in the spherical, heterogeneous model was chosen such that the multiplication constant was the same as for the two-dimensional model. The spherical, homogeneous model used the same core radius as the spherical heterogeneous model. The resulting core

radius and blanket thickness were 45.245 cm and 30.0 cm, respectively. The appropriate compositions for use with the spherical model are given in Table I.

An energy group structure with 27 energy groups, as given in Table II, is suggested. Such a structure has sufficient detail at low energies to afford accurate computations of material worths and Doppler effects.

Because of the simplicity of the two-region, homogeneous spherical model the macroscopic flux distributions across the reactor may be computed with diffusion theory, and a relatively coarse mesh of 2 cm should be adequate.

Central material reactivity worths and Doppler reactivity worths may be computed by perturbation theory. If the material sample is optically thin and if the material is contained in the core, the homogeneous core cross section for the material are fairly appropriate to the sample. If the material sample is optically thin and if the material is not contained in the core, then infinite dilution cross sections are appropriate for the sample.

The major flaw in the homogeneous spherical model for this geometrically simple system is in the neglect of heterogeneities in the unit cell. Sections D and F indicate the uncertainties arising from the use of homogeneous cross sections. The error in material worth or Doppler worth introduced by flux distortions depends strongly upon the nature of the sample.

2. Other More Complicated Models: A two-dimensional finite cylindrical representation of the system is closer to the physical configuration than a spherical representation. In defining the finite cylindrical

model, the as-built loading was corrected for excess reactivity, edge smoothing, spiking of the control and safety rods with extra fuel and for the stainless steel interface between the halves of the assembly. The resulting region dimensions and compositions for the zero-excess reactivity, heterogeneous, two-dimensional model are given in Tables III and IV, respectively.

D) Experimental Data

1. Measured Eigenvalues: The measured eigenvalue corresponding to the models of Section C is 1.000 ± 0.001. Calculations indicate a 0.0183 heterogeneity correction.[2]

2. Unit-Cell Reaction Rates: Foils of enriched uranium and depleted uranium were irradiated at the center of Assembly 48 to obtain ratios of capture and fission in ^{238}U to fission in ^{235}U. The foils, 0.39 in. in diam by 0.01 in. thick were wrapped in aluminum foil for placement between plates at 12 locations in the unit cell. The fission and capture activations were determined by radiochemical methods.[3]

   Table V gives the cell-averaged values of the capture and fission ratios obtained from these measurements together with the heterogeneity correction. To be clear, these unit-cell reaction rate values correspond to the reactions actually taking place in the unit-cell in the assembly, and not, for example, to a cell-average defined as the value of the flux at every point in the cell multiplied by the cross section of the foil material. We use the term to refer to the flux and volume weighted reaction rates as they actually occur in the unit-cell. Hence, a per atom unit-cell reaction rate ratio is converted to the actual

ratio of the number of reactions taking place in the cell simply by multiplying the former ratio by the appropriate atom density ratio.

3. Material Worth at the Center of the Core: Central reactivity worths of several heavy and structural materials were measured in a small diameter (0.45 in.) steel carrier cylinder. The reactivity of the carrier with a sample as compared on empty carrier was obtained from the change in position of the autorod. The plutonium and uranium samples were clad annuli while the structural material samples were generally 0.42 in. cylinders. Table VI gives the experimental worths of several isotopes together with the results of calculations using the homogeneous, spherical model.

E) Calculated Results

The calculations described in this section were made using ENDF/B-III data and the standard one-dimensional, homogeneous spherical model of the assembly. The fundamental mode option of the SDX[4] code was used to compute homogeneous cross sections. This model yielded a multiplication constant of 0.9744 for the critical. The addition of the heterogeneity and the transport corrections gives a k_{eff} of 0.9999.

Table VII gives the comparison of the multiplication constant, reaction rate ratios and several central worths computed with several models. First-order perturbation theory was used in the central worth calculations.

F) Comments and Documentation

To assess the limitations of the homogeneous, spherical Benchmark model, the multiplication constant, reaction rate ratios and central reactivity worths

were calculated with a one-dimensional spherical heterogeneous model and with a two-dimensional finite cylindrical model. In this way, the errors arising from homogenization can be separated from the errors arising from the simplified geometric representation. The heterogeneous cross sections were computed with the plate unit cell option of the SDX code, which uses the NR approximation to obtain resonance cross sections and integral transport methods to obtain spatial weighting factors. The model used to represent the unit cell in these SDX problems as described in Ref. 5.

The results of calculations with the three models are compared in Table VII. The one-dimensional and the two-dimensional heterogeneous models are in good agreement. From comparison of the spherical homogeneous and heterogeneous results, heterogeneities account for a difference of about 1.8% in the multiplication constant and differences up to 10% in the central worths. For the central worth measurements, the conversion factor 1% $\Delta k/k$ = 981 Ih was used to convert the measured periods to the desired reactivity units. The delayed neutron data of Keepin[6] were used in computing this conversion factor.

References

1. A. M. Broomfield, A. L. Hess, P. I. Amundson, et al., "ZPR-3 Assemblies 48, 48A and 48B: The Study of a Dilute Plutonium-Fueled Assembly and Its Variants," ANL-7759 (1970).
2. B. A. Zolotar, E. M. Bohn, and K. D. Dance, "Benchmark Tests and Comparisons Using ENDF/B Version III Data," Applied Physics Division Annual Report, July 1, 1971 to June 30, 1972, ANL-8010 (in press).
3. R. J. Armani et al., "Improved Techniques for Low-Flux Measurements of Prompt-Neutron Lifetime, Conversion Ratio, and Fast Spectra," IAEA Symp. on Exponential and Critical Experiments, Vienna (1964).
4. W. M. Stacy, Jr., H. Henryson II, B. J. Toppel, and B. A. Zolotar, "MC^2-2/SDX Development - Part II," Applied Physics Division Annual Report, July 1, 1971 to June 30, 1972, ANL-8010 (in press).
5. J. E. Marshall, "The Unit-Cell Composition Model Developed for SDX Input Preparation and the Resulting Cell Specifications for the ZPR/ZPPR Benchmark Assemblies," Applied Physics Division Annual Report, July 1, 1971 to June 30, 1972, ANL-8010 (in press).
6. G. R. Keepin, "Physics of Nuclear Kinetics," Addison-Wesley, Reading, Mass. (1965), Table 4-7.

TABLE I. ZPR-3 Assembly 48 Spherical Model Atom Densities, atom/barn-cm

Isotope	Core Radius = 45.245 cm	Blanket Thickness = 30.0 cm
^{239}Pu	0.001645	-
^{240}Pu	0.000106	-
^{241}Pu	0.000011	-
^{242}Pu	0.0000004	-
^{235}U	0.000016	0.000083
^{238}U	0.007405	0.03969
C	0.02077	-
Na	0.006231	-
Fe	0.01018	0.004925
Cr	0.002531	0.001225
Ni	0.001119	0.000536
Mo	0.000206	-
Al	0.000109	-
Mn	0.000106	0.000051
Si	0.000124	0.000060

TABLE II. Specifications of 27-Group Structure

Group	ΔU	E_{upper}, keV	Group	ΔU	E_{upper}, keV
1	0.5	10000	14	0.5	15.034
2	0.5	6065.3	15	0.5	9.1188
3	0.5	3678.8	16	0.5	5.5308
4	0.5	2231.3	17	0.5	3.3546
5	0.5	1353.4	18	0.5	2.0347
6	0.5	820.85	19	0.5	1.2341
7	0.5	497.87	20	0.5	0.74851
8	0.5	301.97	21	0.5	0.45400
9	0.5	183.16	22	1	0.27536
10	0.5	111.09	23	1	0.10130
11	0.5	67.379	24	1	0.03727
12	0.5	40.868	25	1	0.01371
13	0.5	24.787	26	2	0.00504
			27	-	0.00068

TABLE III. Dimensions for the Zero-Excess Reactivity, Cylindrical Version of ZPR-3 Assembly 48

Core radius, cm	41.59
Core height, cm	76.352
Radial blanket thickness, cm	34.47
Radial blanket height, cm	137.16
Axial blanket thickness, cm	31.144
Core volume, liters	415

TABLE IV. Mean Atom Densities for the Zero-Excess Cylindrical Model of Assembly 48, atoms/barn-cm

	Core	Axial Blanket	Radial Blanket
^{239}Pu	0.001645	-	-
^{240}Pu	0.000106	-	-
^{241}Pu	0.000011	-	-
^{242}Pu	0.0000004	-	-
^{235}U	0.000016	0.000082	0.0000803
^{238}U	0.007405	0.03933	0.038497
C	0.02077	-	-
Na	0.006231	-	-
Fe	0.01018	0.005633	0.005871
Cr	0.002531	0.001401	0.001460
Ni	0.001119	0.000613	0.000639
Mo	0.000206	-	-
Al	0.000109	-	-
Mn	0.000106	0.000059	0.000061
Si	0.000124	0.000069	0.000072

TABLE V. Unit-Cell Reaction Rate Ratios in ZPR-3 Assembly 48

	Measurement[a]	Calculated Heterogeneity Correction Factors[b]
$^{28}c/^{25}f$	0.131 ± 0.007	1.057
$^{28}f/^{25}f$	0.0321 ± 0.0016	1.017

[a]Flux-weighted average of seven unit-cell locations.
[b]Homogeneous/heterogeneous.

TABLE VI. Central Reactivity Worths Measured in ZPR-3 Assembly 48, 10^{-5} $\Delta k/k$/mole

Isotope[a]	Measured Worth 1σ Inprecision[b]	Calculated Worth[c]
^{239}Pu	108.4 ± 1.0	138.06
^{235}U	80.0 ± 1.2	103.10
^{238}U	-5.72 ± 0.17	-6.894
^{23}Na	-0.148 ± 0.007	-0.2543
^{10}B	-90.96 ± 0.61	-93.57
Fe	-0.700 ± 0.023	
Cr	-0.652 ± 0.079	
Ni	-1.09 ± 0.01	
Mn	-1.28 ± 0.06	
Al	-0.432 ± 0.022	
Ta	-30.25 ± 0.92	
Mo	-4.24 ± 0.04	
C	-0.055 ± 0.015	

[a]See Table 35 of Ref. 1 for further description of samples.
[b]Measured period converted to reactivity with use of conversion factor 1% $\Delta k/k$ = 981 Ih.
[c]FOP calculation based on ENDF/B-III data and central spherical, homogeneous fluxes.

TABLE VII. Comparison of Calculations for ZPR-3 Assembly 48 with Several Models

		1-Dimensional Homogeneous	1-Dimensional Heterogeneous	2-Dimensional Heterogeneous
	k_{eff}	0.9744	0.9927	0.9927
Reaction Rates	$^{28}c/^{25}f$	0.1359	0.1285	
	$^{28}f/^{25}f$	0.03187	0.03135	
Central Worths, 10^{-5} $\Delta k/k$/mole	^{239}Pu	138.06	136.38	134.95
	^{235}U	103.10	102.33	
	^{238}U	-6.894	-7.715	-7.654
	^{23}Na	-0.2543	-0.2522	-0.2482
	^{10}B	-93.57	-103.53	-102.61

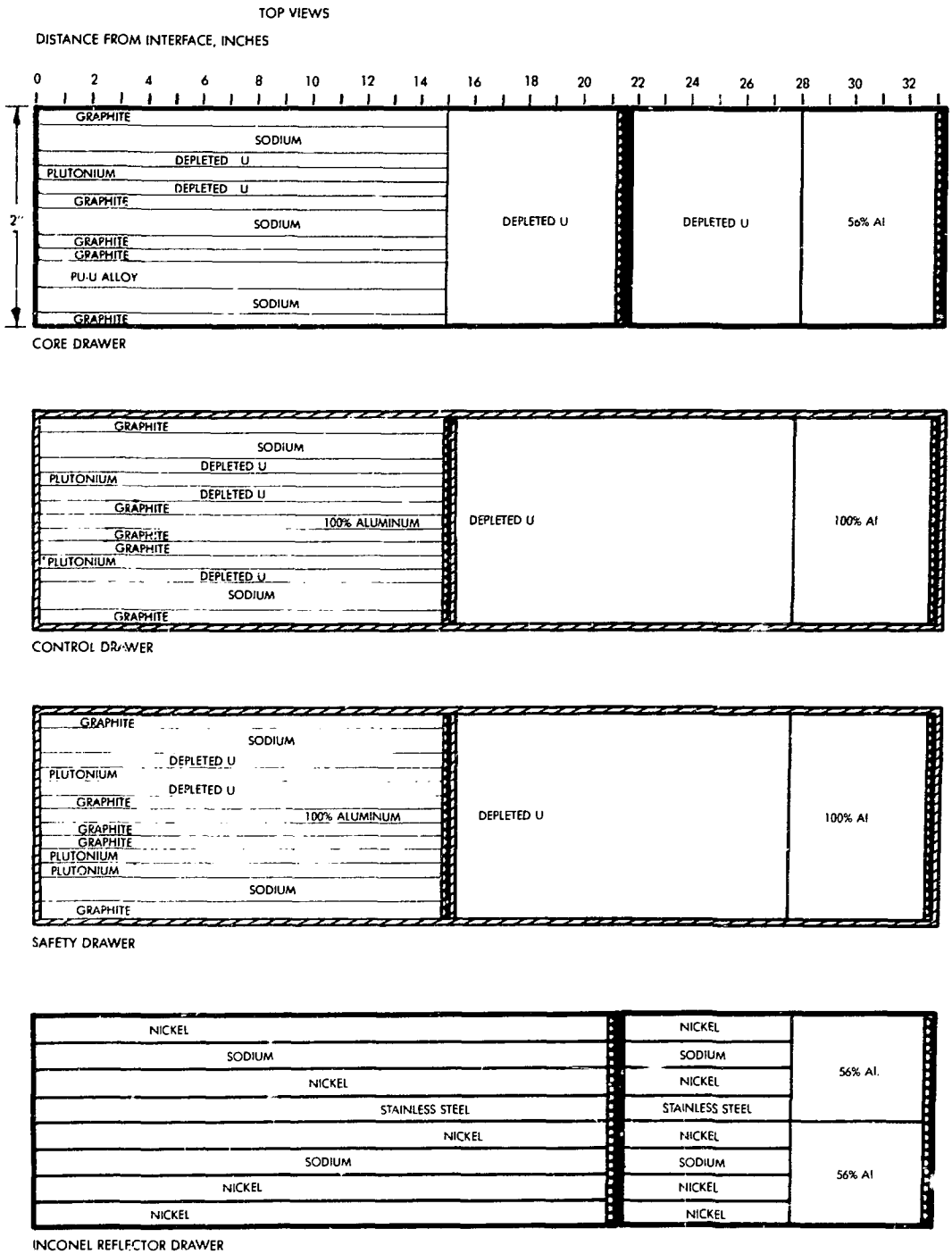

Figure 1. Basic Drawer Arrangements for Assemblies 48, 48A, and 48B

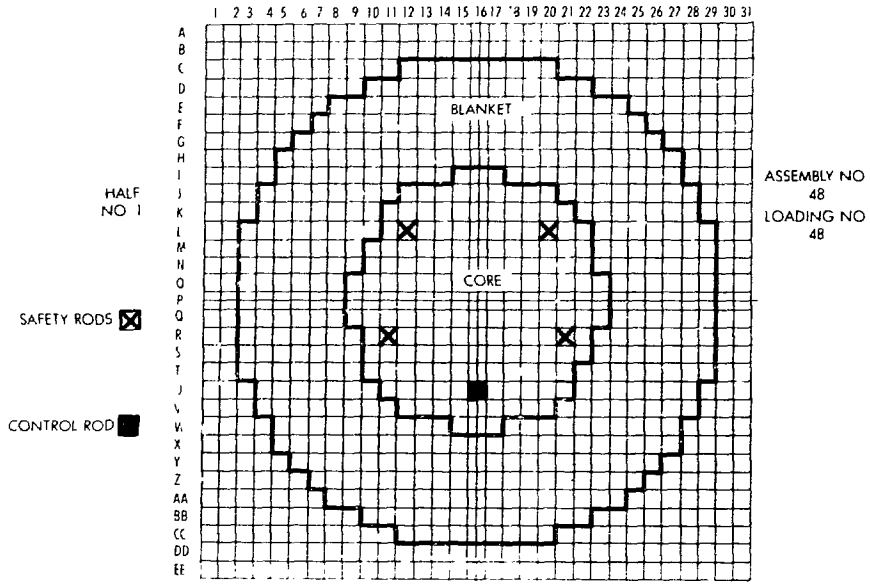

Figure 2. Assembly 48 Drawer Arrangement in Half No 1

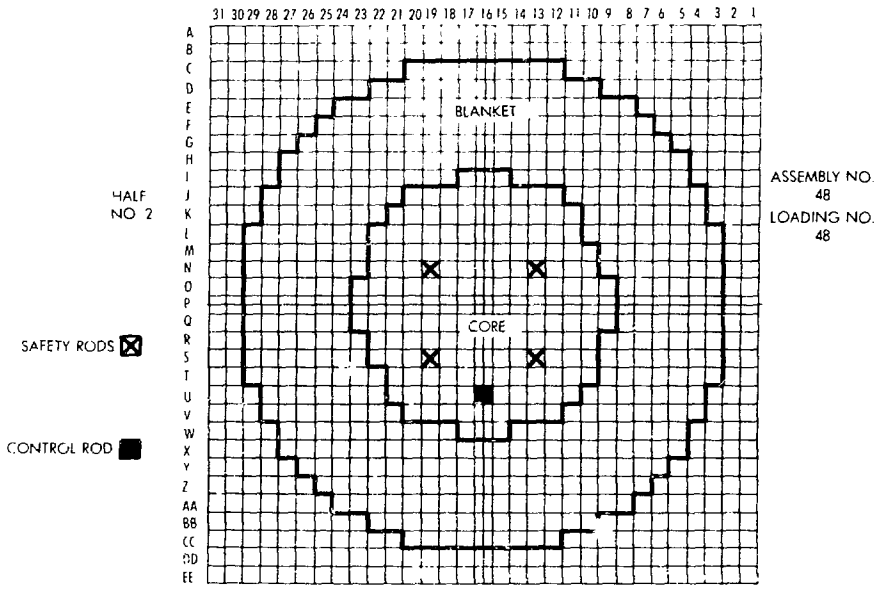

Figure 3. Assembly 48 Drawer Arrangement in Half No. 2

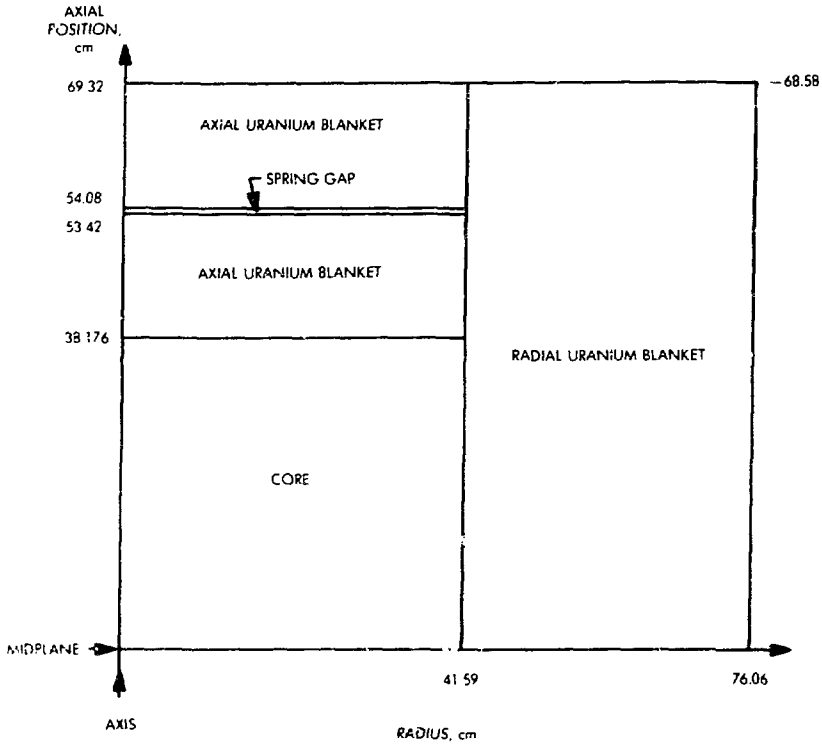

Figure 4. Critical Geometry for Heterogeneous Core Assembly 48 Represented as Circular Cylinder

FAST REACTOR BENCHMARK NO. 4

A. Benchmark Name and Type

ZEBRA-3, a 9:1 uranium/plutonium metal assembly.

B. System Description

The ZEBRA facility consists of stainless steel tubes containing reactor materials mounted vertically on a 3 meter square base plate. A pin at the lower end of each element fits into the base plate and the elements are restrained laterally by 3 steel lattice plates. The central 27 cm square of the base plate is removable so large experiments may be mounted in the reactor center. A concrete shield and steel containment vessel complete the structure.

ZEBRA-3 was a cylindrical critical assembly with a core height of 35.04 cm, an effective diameter of 46.24 cm and a core volume of 58.86 liters. The core is surrounded by a blanket of natural uranium having an axial thickness of 30.54 cm and an effective radial thickness of 34.04 cm.

The assembly has a hard spectrum with more than 80% of the neutron flux being at energies over 100 kev. The assembly is useful for testing the high energy U-238 and Pu-239 cross section data.

C. Model Description

1. One-Dimensional Model Description

A one-dimensional spherical model of ZEBRA-3 is given in Figure 1. A vacuum boundary condition should be applied to the outer reflector boundary. Atom densities for the materials in the core and reflector are given in Table 1. The standard calculational mode is an S_8 transport theory calculation using a multigroup structure composed of 26 groups, each of lethargy width equal to 0.5 and with E_{max} set at 10 MeV. The number of mesh intervals for core and reflector are 40 and 30, respectively.

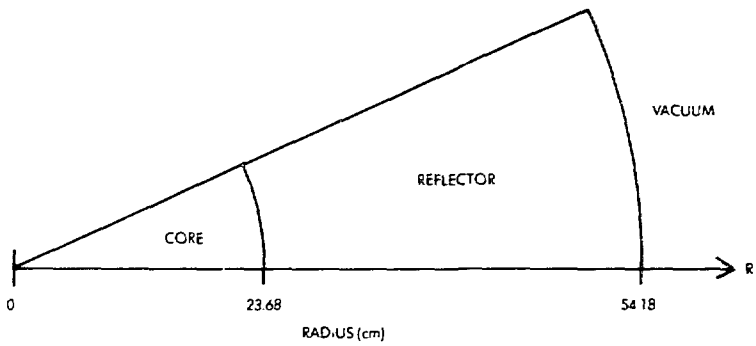

Figure 1. Spherical Model of ZEBRA-3 Assembly

2. Two-Dimensional Model Description

A two-dimensional (R-Z) cylindrical model of the ZEBRA-3 assembly is given in Figure 2. A zero return current boundary condition should be applied to the top and right side of the model; a symmetry boundary condition shouldbe applied along the model bottom. The standard calculation mode is two-dimensional diffusion theory with mesh as follows: 40 radial and axial intervals in the core; 30 intervals for the reflector thicknesses.

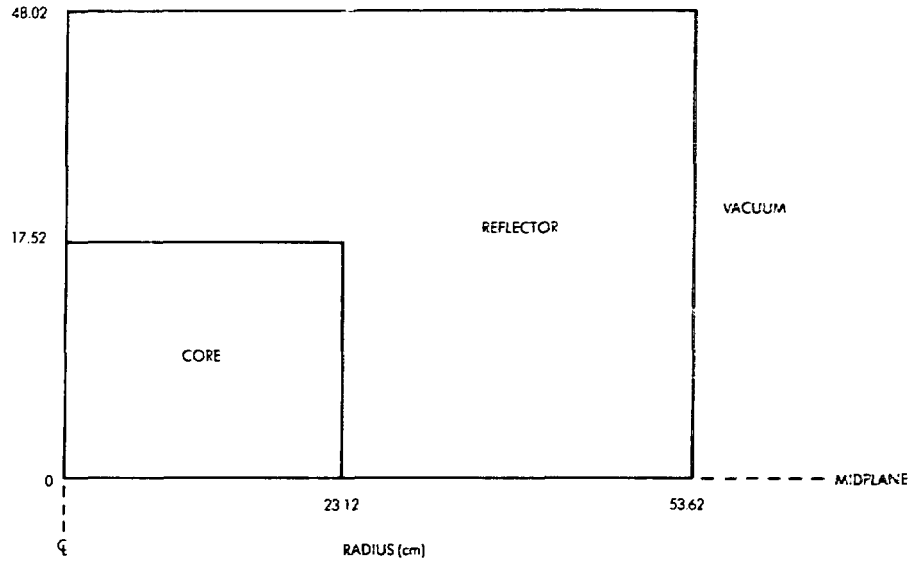

Figure 2. Two-Dimensional (R-Z) Model of ZEBRA-3 Assembly

Table 1.

ZEBRA-3 Region Compositions*

(Atoms/Barn-cm)

Material	Core	Reflector
Pu-239	0.003466	-
Pu-240	0.0001834	-
Pu-241	0.0000127**	-
U-235	0.0002264	0.000298
U-238	0.031775	0.041269
Cu	0.0043702	0.000004
Fe	0.004578	0.003323
C	0.000042	0.000042
Cr	0.000864	0.000864
Mo	0.000008	0.000008
Mn	0.000064	0.000064
Ni	0.000483	0.000483
Aℓ	0.000019	0.000019
Ti	0.000016	0.000016
Si	0.000054	0.000054
V	0.000005	0.000005

*Revised by R. W. Smith 11/70

**As of Jan./Feb. 1965, $T_{1/2}$ = 13.2 years.

D. Experimental Data

1. Experimental Critical Mass — 80.1±0.2 Kg (Pu-239 + Pu-241)

Corrections for Edge Irregularities	-1.6±0.1
Finite Plate Thickness (fuel + diluent)	+2.9* ±0.8
Homogeneous Cylinder Critical Mass	81.4±0.9 Kg (Pu-239 + Pu-241)
	81.0 Kg Pu-239
	0.4 Kg Pu-241
Experimental Eigenvalue	1.000±0.003

2. Experimental Spectral Indices at Core Center Relative to σ_f U-235

σ_f (U-238) = 0.0461±0.0008

σ_f (U-233) = 1.542±0.019

σ_f (U-234) = 0.346±0.009

σ_f (U-236) = 0.099±0.005

σ_f (Pu-239) = 1.190±0.014

σ_f (Pu-240) = 0.373±0.005

σ_f (Np-237) = 0.353±0.004

*This value is the mean of the measured and calculated value: (measured 2.5 Kg; calculated 3.3 Kg)

3. Material Worths at Core Center

Material	Reactivity Coefficient (10^{-5} $\Delta k/k$/mole)
U-235	197±4
Pu-239	318±8
U-238	-9.95±0.48
B-10	-105±5
B	-26.7±0.6
Ta	-30±1
Li-6	-85±4
Au	-26±1
Cu	-6.4±0.3
C	-3.8±0.2
Na	-2.8±0.3
Aℓ	-3.4±0.4
Pb	-3.9±0.4
H	-32±1

The reactivity coefficients given above are values for effective zero size samples as quoted in Reference 1. The conversion from in-hours to $\Delta k/k$ for ZEBRA-3 is given as 860 Ih = 0.01 $\Delta k/k$.

F. Comments and Documentation

Experimental information on the ZEBRA-3 assembly is detailed in AEEW-R-461.[1] The experimental critical mass was 80.1±0.2 Kg (Pu-239 + Pu-241). Corrections for edge irregularities and heterogeneity effects were -1.6±0.1 and +2.9±0.8 Kg (Pu-239 + Pu-241), respectively, resulting in a homogeneous cylinder critical mass of 81.0 Kg Pu-239 + 0.4 Kg Pu-241. This critical mass for the equivalent homogeneous cylinder was obtained from the measured values by allowing for partially inserted control rods and counter holes as well as irregular edge and heterogeneity effects.

Applying a shape factor of 0.944±-.005 gives a homogeneous spherical critical mass of 76.8±1.0 Kg (Pu-239 + Pu-241), or 76.4 Kg Pu-239 and 0.4 Kg Pu-241. The corresponding critical sphere radius is 23.68±0.12 cm.

The correction to the S_8 eigenvalue result to extrapolate to an "S_∞" value is estimated to be -0.001. For example, if k_{eff} (S_8) is 1.003, then k_{eff} (S_∞) would be 1.002.

REFERENCES

1. J. Adamson, et al., "The Third Core of ZEBRA", AEEW-R-461 (1965).
2. Private Communication, R. W. Smith (AEEW) to H. Alter (11/70).

FAST REACTOR BENCHMARK NO. 5

A. Benchmark Name and Type: GODIVA, a bare sphere of enriched uranium.

B. System Description

GODIVA, as a bare sphere of enriched uranium metal, is especially suited for testing ^{235}U and ^{238}U cross sections in the fission source energy range. The single-region, simple geometry and uniform composition conveniently facilitate calculational testing.

C. Model Description

The spherical homogeneous model has a core radius of 8.741 cm and the following composition:[1]

Isotope	Density, 10^{24}a/cc
^{235}U	0.04500
^{238}U	0.002498
^{234}U	0.000492

The recommended mode of calculation is one-dimensional transport theory, S_{16}, with 40 mesh intervals in the core, a vacuum boundary condition at the core boundary (8.741 cm) and a 26 energy group structure with half-lethargy unit widths and an upper energy of 10 MeV.

D. Experimental Data*

1. Measured Eigenvalue: $k = 1.00 \pm 0.003$

2. Spectral Indices at Core Center

a. Central Fission and Capture Ratios[2]

σ_f(U-238)/σ_f(U-235)	0.156 ± 0.005
σ_f(Pu-239)/σ_f(U-235)	1.42 ± 0.02
σ_f(U-233)/σ_f(U-235)	1.63 ± 0.10
$\sigma_{n,\gamma}$ (Au)/σ_f(U-235)	0.105 ± 0.010
σ_f(U-234)/σ_f(U-238)	5.0 ± 0.2
$\sigma_{n,\gamma}$ (U-238/σ_f(U-238)	0.47 ± 0.02
σ_f(Th-232)/σ_f(U-238)	0.234 ± 0.005

b. Central Activation Cross Sections[3]

Isotope	$\sigma(n,\gamma)$, barns (spectrum average at core center)	Thermal Normalization Value barns
^{55}Mn	0.0033 ± 0.0002	13.3 ± 0.2
^{59}Co	0.0461 ± 0.0050	19.9 ± 0.9
^{63}Cu	0.0144 ± 0.0006	4.5 ± 0.2
^{65}Cu	0.0092 ± 0.0005	2.3 ± 0.3
^{93}Nb	0.0371 ± 0.0030	1.15 ± 0.05
^{181}Ta	0.159 ± 0.007	22 ± 1
^{185}Re	0.248 ± 0.015	110 ± 5
^{187}Re	0.197 ± 0.018	75 ± 4
^{197}Au	0.123 ± 0.003	98.8

3. Rossi Alpha[2]

$\alpha = -\beta_{eff}/\ell = -1.10\times10^{6}\ \mathrm{sec}^{-1}$

*See Section F for a discussion of some of the experimental data.

4. Central Reactivity Worths[4]

Isotope	Central Worth, 10^{-5} $\Delta k/k$/mole
H	316 ± 7
Be	48 ± 2
^{10}B	- 365 ± 7
C	15.8 ± 1.3
Aℓ	3.3 ± 1.2
Fe	- 1.3 ± 1.3
Co	- 4.0 ± 1.3
Ni	- 29 ± 1
Cu	- 12 ± 1
Au	- 49 ± 2
Th	- 9 ± 1
^{235}U	983 ± 7
^{238}U	160 ± 2
^{239}Pu	1881 ± 13
^{240}Pu	1122 ± 130

Note: These central worths have been effectively normalized by use of an empirically derived, normalized effective delayed neutron fraction. See Section F.

5. Leakage Spectrum[5]

The spectrum of neutrons emitting from the surface of the core is represented below in the 1/2-lethargy group structure (E_{MAX} = 10 MeV) with an arbitrary normalization to the value 18 in group 5.

Energy Group	Lower Lethargy Limit	Relative Flux
1	0.5	2.0
2	1.0	7.1
3	1.5	13.6
4	2.0	16.8
5	2.5	18.0
6	3.0	18.8
7	3.5	11.5
8	4.0	8.0

E. Calculated Results

Calculated results may be appended to these specifications.

F. Comments and Documentation

The composition and configuration specifications were taken from Ref. 1. The central fission and capture ratios given here are those evaluated by Hansen and reported in Ref. 2.

The central activation cross sections were measured with a comparative activation technique that relied upon knowledge of a standard activation cross section and upon thermal activation cross sections for each isotope for normalization purposes.[3] The ^{235}U fission cross section was selected as the standard activation cross section. Thermal normalization cross sections were determined from measurements and in conjunction with the value assigned to the standard activation cross section in this assembly. Thus, the central activation cross sections reported

are effectively normalized to a value assigned to the ^{235}U fission cross section in this assembly and to values determined for the thermal normalization cross sections. The data for the central activation cross sections was originally reported in Ref. 3. Subsequently, some of the thermal normalization values and, consequently, the activation cross sections, have been re-evaluated by LASL.

The measured central reactivity worths, corrected for sample size effects, were taken from Ref. 4. The measured values were reported in units of a dollar (cents/mole). These measured values were then converted to units of $\Delta k/k$ with a value of 0.0066 for the effective delayed neutron fraction obtained from Ref. 5. It should be noted, however, that this value of β_{eff} is actually a value normalized to a reference calculation. The procedure used was based upon a measurement (Rossi-α) of the increment in mass added to the surface of the assembly that would bring the assembly from delayed to prompt critical. The computed (S_4) change in multiplication for this mass increment was then equated to β_{eff}. Thus, the central worth values specified here are, in fact, normalized to a measured worth.

The data listed for the leakage spectrum was derived from Ref. 6. A finer energy mesh representation for the spectrum may be found in Ref. 6 along with statistical uncertainties (which are large at higher energies) in each energy range.

REFERENCES

1. G. E. Hansen and H. C. Paxton, "Reevaluated Critical Specifications of Some LASL Fast Neutron Systems", LA-4208, 1969.
2. G. E. Hansen, "Status of Computational and Experimental Correlation for Los Alamos Fast Neutron Critical Assemblies", Proc. of Seminar on Physics of Fast and Intermediate Reactors, Vol. I, IAEA, Vienna (1962).
3. C. E. Byers, "Cross Sections of Various Materials in the Godiva and Jezebel Critical Assemblies", Nucl. Sci. and Eng. 8, No. 6, p. 608 (Dec. 1960).
4. Engle, et al., "Reactivity Contributions of Various Materials in Topsy, Godiva, and Jezebel," Nucl. Sci. and Eng., 8, No. 6, p. 543, (Dec. 1960).
5. G. A. Jarvis, et al., "Two Plutonium Metal Critical Assemblies", Nucl. Sci. and Eng. 8, 525-531 (1960).
6. L. Stewart, "Leakage Neutron Spectrum from a Bare Pu-239 Critical Assembly", Nucl. Sci. and Eng. 8, No. 6, p. 595. (Dec. 1960).

FAST REACTOR BENCHMARK NO. 6

A. Benchmark Name and Type

VERA-1B, an enriched uranium-plus-graphite system.

B. System Description

VERA-1B is a cylindrically shaped critical assembly fueled with enriched uranium and diluted with graphite. The assembly core was 27.2 cm in height and the effective core diameter was 38.1 cm. The assembly core was surrounded by a blanket of natural uranium and stainless steel. VERA-1B was designed to explore the accuracy of U-235 neutron cross section data.

C. Model Description

1. One-Dimensional Model Description

A one-dimensional spherical model of VERA-1B is given in Figure 1. A vacuum boundary condition should be applied at the outer reflector boundary. Material atom densities for the core and reflector are given in Table 1.

The standard calculation mode is an S_8 transport theory calculation using a multigroup structure composed of 26 groups, each of lethargy width equal to 0.5 and with E_{max} set at 10 MeV. Forty mesh intervals are used for both core and reflector regions.

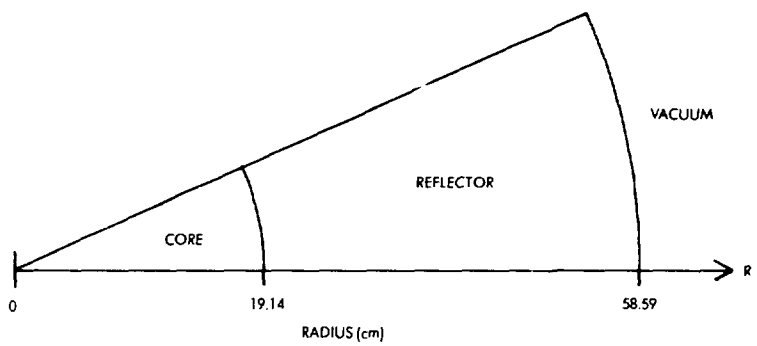

Figure 1. Spherical Model of VERA-1B Assembly

Table 1.

VERA-1B Region Compositions

(Atoms/Barn-cm)

Material	Core	Reflector*	
		(a)	(b)
U-235	0.007349	0.00025	0.00026
U-236	0.000014	-	-
U-234	0.000092	-	-
U-238	0.000455	0.03440	0.03610
C	0.057540	-	-
H	0.000058	-	-
Fe	0.006283	0.006464	0.006582
Ni	0.001635	0.001682	0.001713
Cr	0.000689	0.000708	0.000721

*Use Composition (a) in calculations

2. Two-Dimensional Model Description

A two-dimensional (R-Z) cylindrical model of the VERA-1B assembly is given in Figure 2. Zero return current boundary conditions should be applied to the top and right side of the model; a symmetry boundary condition should be applied along the model bottom. The suggested calculational mode is two dimensional diffusion theory with 40 mesh intervals for the radial and axial core dimensions and 40 mesh intervals for the reflector thickness.

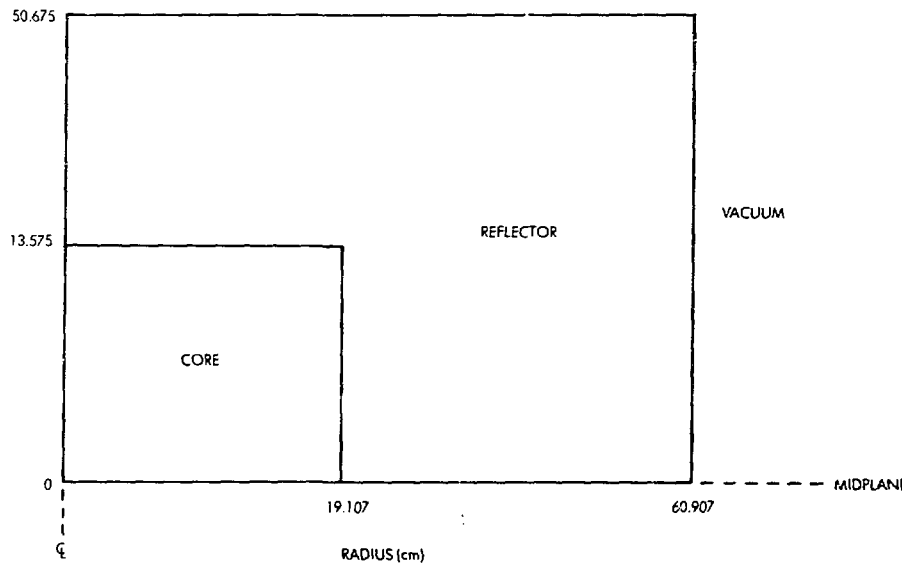

Figure 2. Two-Dimensional (R-Z) Model of VERA-1B Assembly

D. Experimental Data

1. Experimental Critical Mass — 86.3±0.15 Kg U-235

Corrections for Edge Irregularities	-0.6±0.2
Finite Fuel Plate Thickness	+3.6±0.4
Homogeneous Cylinder Critical Mass	89.3±0.4 Kg U-235
Experimental eigenvalue	1.0000±0.0028

2. Experimental Spectral Indices at Core Center Relative to σ_f U-235

σ_f (U-238)	=	0.0665±0.0010
σ_f (U-233)	=	1.433±0.047
σ_f (U-236)	=	0.134±0.010
σ_f (Pu-239)	=	1.070±0.026
σ_f (Pu-240)	=	0.399±0.032
σ_f (Np-237)	=	0.38±0.012
σ_c (U-238)	=	0.131±0.006 (cell average)
	=	0.126±0.006 (average over U-238 in cell)

3. Material Worths at Core Center

Material	Reactivity Coefficient 10^{-5} Δk/k/mole
U-235	221±3
U-238	7.5±0.3
Pu-239	387±5
U-233	378±5
Np-237	28±3
B-10	-237±50
Au	-26±1
Stainless Steel	2.1±0.3
Aℓ	3.5±0.4
Na	13±1
C	5.95±0.12
H	90±2

Sample size corrections were made using experimental worth vs. size and/or S_n calculations. Errors quoted do not include those due to delayed neutron data. The conversion from inhours to $\Delta k/k$ is 416 Ih = 0.01 $\Delta k/k$.

4. Rossi Alpha

At delayed critical, $\alpha = -6.9 \times 10^4 \text{ sec}^{-1}$. Extrapolation to $\alpha = 0$ gave 336±10 inhours per dollar.

F. Comments and Documentation

In VERA-1B a figure of 95±15 p.p.m. of hydrogen in graphite[1] has been suggested to allow for possible moisture content in the graphite. The effect of this moisture on k_{eff} for VERA-1B is about 0.15%. This moisture content has not been included in the core composition data for VERA-1B.

Details and experimental results of the VERA-1B experiments have been described by McTaggart.[2] The experimental critical mass is 86.3±0.15 Kg U-235. Corrections for edge irregularities (-0.6±0.2) and for finite fuel plate thickness (+3.6±0.4) produce a homogeneous cylindrical critical mass of 89.3±0.4. This critical mass for the equivalent homogeneous cylinder was obtained from the measured values by allowing for partially inserted control rods and counter holes as well as irregular edge and heterogeneity effects.

Applying a shape factor of 0.943 produces a homogeneous spherical critical mass of 84.2±0.6 Kg U-235 with the radius of the critical sphere equal to 19.14±0.05 cm.

The correction to the S_8 eigenvalue to extrapolate to an "S_∞" eigenvalue is estimated to be -0.001. For example, if the k_{eff} (S_8) result was 1.0000, then the k_{eff} (S_∞) result would be 0.9990.

REFERENCES

1. Private communication, R. W. Smith (UKAEA) to H. Alter, Nov. 1970.

2. M. H. McTaggart, et al, "Interim Report on Uranium Fueled VERA Reactor Experiments", AWRE-R5/66 (1966).

FAST REACTOR BENCHMARK NO. 7

A. Name and Type: ZPR-III 6F, a dilute ∿ 1:1 fertile to fissile U system.

B. System Description:

Several early assemblies on ZPR-III (6F, 1B, 2, 2B, 5, and 13) used a core composition with a U-238 to U-235 ratio of about 1:1. The reflector of these assemblies was composed mostly of U-238.

Reasons for creating a benchmark to represent these assemblies are as follows: 1) The measurements on all of the source assemblies form an extensive set of experimental results which represents a relatively simple system; 2) The 1:1 fertile to fissile ratio provides an important interval in the range of such ratios being tested by the benchmark program; 3) And it provides an opportunity to test the U-235 and U-238 cross section sensitivities in the intermediate spectrum region.

C. Model Description:

1. One-Dimensional Model (sphere)

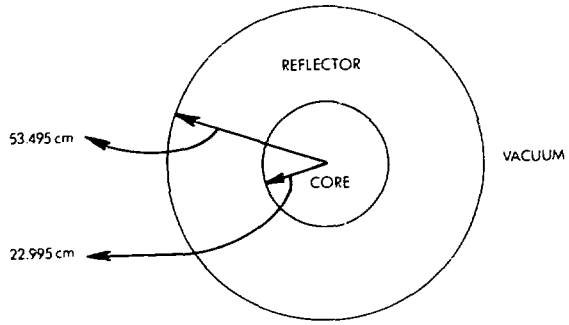

Suggestions:

Code..... 1-D transport theory with S_4.

Mesh..... 40 intervals in the core, 30 in the reflector.

2. Two-Dimensional Model (cylinder)

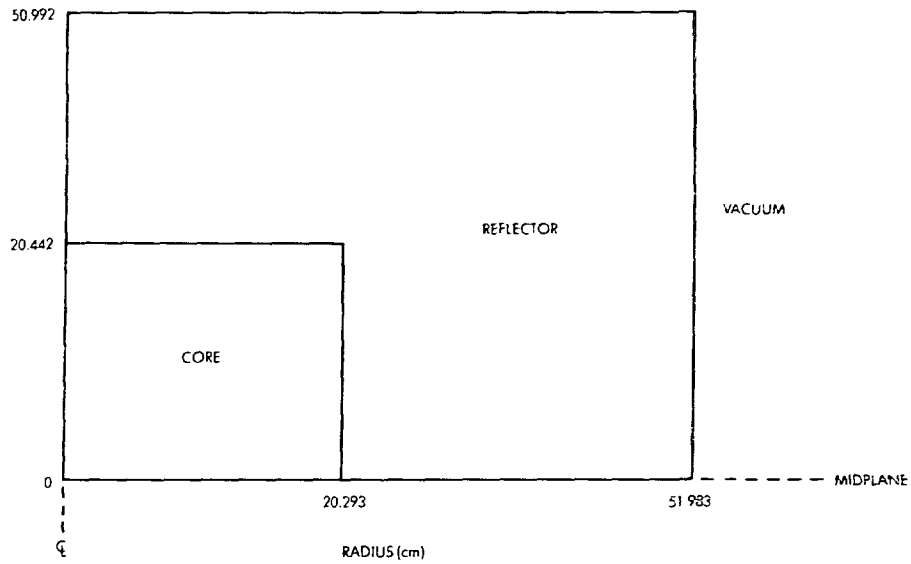

Suggestions:

Code..... 2-D diffusion theory

Mesh..... 40 radial intervals, core

40 axial intervals, core

30 radial intervals, radial reflector

30 axial intervals, axial reflector

3. Atom Densities

Material	Density, 10^{24} atoms/cc	
	Core	Reflector
U-235	0.006727	0.000089
U-238	0.007576[a]	0.040026
U-234	0.000069	- - -
Al[b]	0.019019	0.001359
Fe	0.007712	0.004539
Cr	0.001918	0.001129
Ni	0.000839	0.000494
Mn	0.000080	0.000047

a. Includes 0.000029 for U-236.

b. Includes atom density for Si in steel.

4. Techniques

All calcualtions should be performed with appropriately resonance-shielded cross sections. A suggested multigroup structure is 26 half-lethargy width groups with E_{max} = 10 MeV.

D. Experimental Data: (all errors are one standard deviation)

1. Eigenvalue = 1.0000 ± 0.0015

2. Central Spectral Indices

σ_f (U-238) / σ_f (U-235) = 0.078 ± 0.002

σ_f (U-234) / σ_f (U-235) = 0.451 ± 0.020

σ_f (U-233) / σ_f (U-235) = 1.53 ± 0.03

σ_f (Pu-239)/ σ_f (U-235) = 1.22 ± 0.03

σ_f (Pu-240)/ σ_f (U-235) = 0.53 ± 0.02

$\sigma_{n,\gamma}$ (U-238) / σ_f (U-235) = 0.104 ± 0.003

3. Material Worths at Core Center

Material	Reactivity Coeff. 10^{-5} $\Delta k/k/mole^a$	Material	Reactivity Coeff. 10^{-5} $\Delta k/k/mole^a$
U-235[b]	175 ± 5	Fe	-0.9 ± 0.3
U-238	1.5 ± 0.5	Cr	-0.55 ± 0.19
Pu(4.5%240)[b]	251 ± 12	Ni	-1.7 ± 0.5
U-233[b]	244 ± 24	Mn	-0.65 ± 0.24
Th	-12 ± 2	V	+1.2 ± 0.4
B-10[b]	-86 ± 5	Nb	-5.8 ± 1.2
Hf	-14 ± 5	Al	+0.23 ± 0.35
Ta	-17 ± 3	Na	+3.2 ± 0.9
W	-7.4 ± 1.6	C	+2.8 ± 1.2
Mo	-3.6 ± 0.6	Be	+4.9 ± 1.6
Zr	-0.1 ± 0.2	H	+56 ± 23

a. Derived from worths in inhours using calculated factor of 430 Ih/%k.

b. Approximately corrected for sample-size effects.

4. Rossi Alpha at Delayed Critical = -9.85×10^4 sec^{-1}

E. Comments and Documentation:

The specifications for the 1-D model were derived from the 6F critical mass while the 2-D model was based on Assembly 2. Large probable errors have been assigned to the reactivity coefficients to cover the possible discrepancies between the measurements (with massive samples) and "zero-

size" coefficients which would be comparable to perturbation theory. The primary information source has been internal ZPR-III memos written during the conduct of these assemblies. Some results have been published, as by Long[1], but there may be differences from results quoted here because of later-established corrections to the critical mass, reaction ratios, and material worths, or from using more accurate composition breakdowns. A more recent reference[2] contains a convenient compilation of all the pertinent experimental details and measurements for these source assemblies.

According to Baker[3], for Assembly 6F

$$k_{eff}\ (S_4) - k_{eff}\ (\text{diffusion theory}) = 0.023$$

and

$$k_{eff}\ (S_\infty) - k_{eff}\ (S_4) = -.023/6 = -.0038.$$

Thus, for example, if a 1-D diffusion theory calculation gave an eigenvalue of .9900, the corrected eigenvalue would be .9900 + .023 (corrected to S_4) -.0038 (corrected to S_∞) = 1.0092.

References:

1. J. K. Long et al., "Fast Neutron Power Reactor Studies with ZPR-III," Proc. 2nd Int. Conf. on Peaceful Uses of Atomic Energy, Vol. 12, p. 119 (1958).

2. P. F. Palmedo, editor, "Compilation of Fast Reactor Experiments," BNL-15746, Brookhaven National Laboratory, Upton, New York, June 1, 1971.

3. A. R. Baker, "Comparative Studies of the Criticality of Fast Critical Assemblies," ANL-7320, Argonne National Laboratory, Argonne, Illinois, October 1966.

FAST REACTOR BENCHMARK NO. 8

A. Name and Type: ZPR-III 11, an ∿ 7:1 fertile to fissile uranium metal system.

B. System Description:

Several fast reactor experiments (ZPR-III Assembly 11, ZPR-III Assembly 22, ZEBRA Core 1, and ZPR-6 Assembly 1) were all cylindrical critical assemblies constructed with very nearly identical core compositions. The cores were fueled with uranium metal such that the ratio of U-238 to U-235 was ∿ 7:1. The reflectors were composed mostly of U-238.

Reasons for creating a benchmark to represent these assemblies are as follows: 1) the measurements on all of the source assemblies form a rather extensive set of experimental results which represents a relatively simple system; 2) the 7:1 fertile to fissile ratio provides an important interval in the range of this ratio being tested by the benchmark program; and 3) it provides an opportunity to test the U-235 and U-238 cross section sensitivities in the soft spectrum region.

C. Model Description:

1. One-Dimensional Model (sphere)

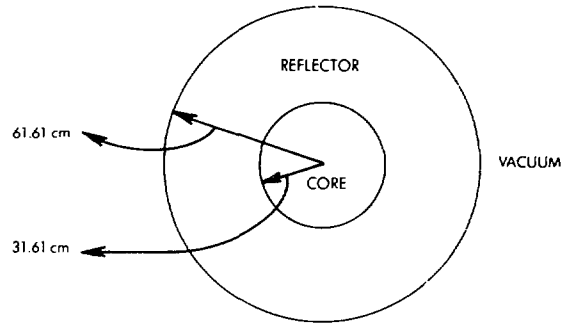

Suggestions:

Code..... 1-D transport theory with S_4

Mesh..... 30 intervals in the core, 20 in the reflector.

2. Two-Dimensional Model (cylinder)

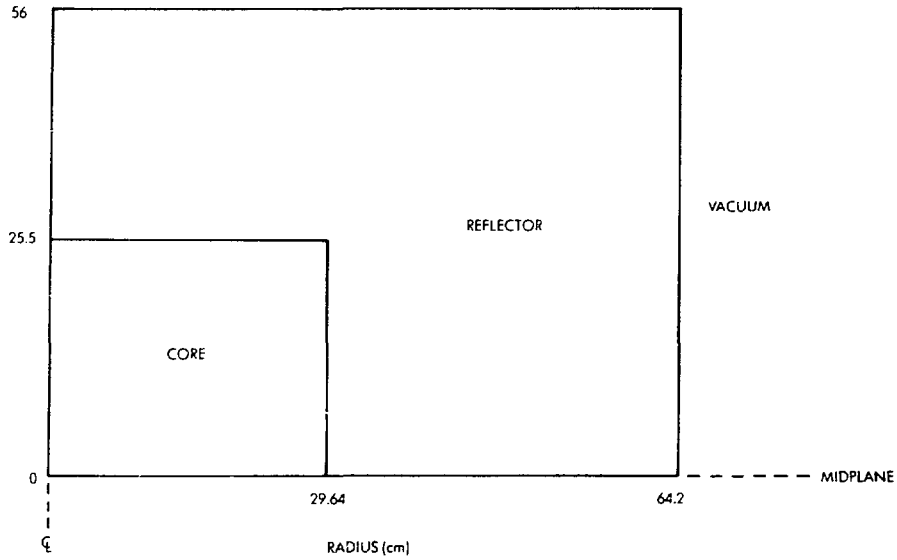

Suggestions:

Code..... 2-D diffusion theory

Mesh..... 30 radial intervals, core

30 axial intervals, core

20 radial intervals, reflector

20 axial intervals, reflector

3. Atom Densities

Material	Density, 10^{24} atoms/cc	
	Core	Reflector
U-235	0.004567	0.000089
U-238	0.034392*	0.040025
U-234	0.000046	- - -
Fe	0.005681	0.004925
Cr	0.001486	0.001196
Ni	0.000718	0.000536
Mn	0.00208	0.000111

*Includes 0.000019 for U-236.

4. Techniques

All calculations should be performed with appropriately resonance-shielded cross sections. A suggested multi-group structure is 26 half-lethargy width groups with E_{max} = 10 MeV.

D. Experimental Data: (all errors are one standard deviation)

1. Eigenvalue = 1.0000 ± 0.0025

2. Spectral Indices at Core Center

σ_f (U-238) / σ_f (U-235) = 0.038 ± 0.001

σ_f (U-234) / σ_f (U-235) = 0.31 ± 0.03[a]

σ_f (U-233) / σ_f (U-235) = 1.52 ± 0.02

σ_f (Pu-239)/ σ_f (U-235) = 1.19 ± 0.02

σ_f (Pu-240)/ σ_f (U-235) = 0.34 ± 0.02

σ_f (U-236) / σ_f (U-235) = 0.12 ± 0.02[b]

σ_f (Np-237)/ σ_f (U-235) = 0.33 ± 0.02[b]

$\sigma_{n,\gamma}$ (U-238) / σ_f (U-235) = 0.112 ± 0.005[c]

a. Measured ratio plus 5% wall-effect correction

b. Measured in ZEBRA Core 1

c. For Assembly 22, from ZPR-3 internal memo.

3. Material Worths at Core Center

Material	Reactivity Coefficient 10^{-5} $\Delta k/k/mole^a$	Material	Reactivity Coefficient, 10^{-5} $\Delta k/k/mole^a$
U-235[b]	123 ± 3	Fe	-1.7 ± 0.1
U-238	-6.6 ± 0.2	Cr	-1.7 ± 0.1
U-233	221 ± 4	Ni	-2.4 ± 0.1
Pu-239[b]	209 ± 5	Na	-0.7 ± 0.1
B-10[b]	-72 ± 2	Al	-1.0 ± 0.1
Ta	-19.6 ± 0.6	O	-0.87 ± 0.15
Mo	-5.1 ± 0.2	C	-0.85 ± 0.13
Mn	-1.8 ± 0.1		

a. Derived from measurements in inhours using conversion of 470 inhours per % $\Delta k/k$.

b. Approximately corrected for sample-size effects.

4. Rossi Alpha at Delayed Critical

$\alpha = -10.4 \pm 0.3 \times 10^4 \text{ sec}^{-1}$.

E. Comments and Documentation:

The 1-D and 2-D models are based on the Assembly 11 composition and a heterogeneous critical mass of 237.4 kg U-235, (adjusted for edge irregularities and the interface-gap effect) as quoted by Davey[1]. A heterogeneity advantage of +0.8 ±0.2% k, based on fuel-bunching experiments in all the cited assemblies, was applied to derive the homogeneous critical size of the cylinder. For the sphere size, a

calculated shape factor of 0.94[1] was utilized. Except as noted, central spectral indices were taken from a report by Davey[2]. The Zebra values cited are from a report by Ingram[3]; this Zebra report also gives measured Rossi Alpha values. Material worths at the core center were derived from internal ZPR-3 and ZPR-6 memos and also from the UKAEA reports on measurements in Zebra[3,4]. Data from Zebra investigations into sample-size effects were used to correct some reactivity coefficients to values comparable to perturbation theory. A more recent reference[5] contains a convenient compilation of all the pertinent experimental details and measurements for the ZPR source assemblies.

According to Baker[6], for Assembly 11,

$$k_{eff}\ (S_4) - k_{eff}\ (\text{diffusion theory}) = 0.008$$

and

$$k_{eff}\ (S_{oo}) - k_{eff}\ (S_4) = -.008/6 = -.0013.$$

Thus, for example, if a 1-D diffusion theory calculation gave an eigenvalue of .9900, the corrected eigenvalue would be .9900 + .008 (corrected to S_4) - .0013 (corrected to S_{oo}) = .9977.

References:

1. W. G. Davey, "k Calculations for 22 ZPR-3 Fast Reactor Assemblies Using ANL Cross Section Set 635," ANL-6570 (May 1962).

2. W. G. Davey and P. I. Amundson, "A Re-evaluation of Fission Ratios Measured in ZPR-3 Critical Assemblies," ANL-6941 (October 1964).

3. G. Ingram et al., "The First Core of Zebra," AEEW-R315 (1963).

4. G. Ingram et al., "Central Perturbation Cross Sections in Zebra Cores 1 and 2," AEEW-R373 (1964).

5. P. F. Palmedo, editor, "Compilation of Fast Reactor Experiments," BNL-15746, Brookhaven National Laboratory, Upton, New York, June 1, 1971.

6. A. R. Baker, "Comparative Studies of the Criticality of Fast Critical Assemblies," ANL-7320, Argone National Laboratory, Argonne, Illinois, October 1966.

FAST REACTOR BENCHMARK NO. 9

A. Benchmark Name and Type

ZPR-III Assembly 12, a 4:1 uranium-graphite system, source experiment.

B. System Description

ZPR-III Assembly 12 was designed as a fast reactor benchmark source experiment on a 4:1 uranium-graphite system. The graphite was included to produce the softer spectra characteristic of larger power reactors. The core was approximately cylindrical composed from a repetition of a one-drawer unit cell. A blanket, consisting primarily of depleted uranium, surrounded the core. The polonium-beryllium neutron sources were removed before measurements were made.

C.1 One-Dimensional Model Description

A one-dimensional spherical model of ZPR-III Assembly 12 is shown in Figure 1, including model dimensions and suggested mesh. Zero return current boundary conditions should be applied at the outer boundary. The atom densities in both regions (atoms/barn-cm) are given in Table I. S_4 transport theory calculations are suggested in any suitable fast reactor energy group structure, but with groups no coarser than 0.5 lethargy width down to a lethargy of 12.5. The estimated uncertainty in k_{eff} ascribable to the model is $\Delta k/k = \pm 0.0023$.

C.2 Two-Dimensional Model Description

A two-dimensional (R-Z) model of ZPR-III Assembly 12 is shown in Figure 2, including model dimensions and suggested mesh. Zero return current boundary conditions are to be applied along the top and right sides; a symmetry boundary condition should be applied along the bottom. The atom densities in both regions (atoms/barn-cm) are given in Table I. Diffusion theory is suggested with cross sections in any suitable fast

reactor energy-group structure.* The estimated uncertainty in k_{eff} ascribable to the model $\Delta k/k = 0.0015$.

D. Experimental Data

1. Measured $k_{eff} = 1.0000$, uncertainty unknown

2. Experimental spectral indices at the core center, relative to σ_f (U-235) are as follows:

σ_f (U-238) = 0.047 ± 0.002
σ_f (U-234) = 0.305 ± 0.012
σ_f (U-233) = 1.48 ± 0.03
σ_f (Pu-239) = 1.12 ± 0.02
$\sigma_{n,\gamma}$ (U-238) = 0.123 ± 0.005

3. Material worths at the core center are as follows:

Material	Reactivity Coefficient 10^{-5} $\Delta k/k$/mole
U-235**	157±.5
U-238	-6.7±1.0
Plutonium**(4.5% Pu-240)	244±7
U-233**	269±7
Ta**	-31±1
Ru**	-16±1
Nb	-10±1
Mo**	-7±0.5
Ni	-2.7±0.5
Fe	-1.5±0.4
Al	-0.4±0.1
C	2.0±0.3

* If the two-dimensional problem is run with a group structure that contains groups broader than 0.5 lethargy, these cross sections should be generated by regionwise collapsing, using representative spectra for each of the regions i.e., Figure 2, from a structure that has no groups greater than 0.5 lethargy width down to a lethargy of 12.5

** Approximately corrected for sample size effects.

4. Rossi Alpha at delayed critical = $-(6.84 \pm 0.20) \times 10^4 sec^{-1}$.

F. Comments and Documentation

The primary source of information for this benchmark has been one internal ZPR-III memo giving details and results of experiments on Assembly 12. Much of the data have been reported by Long[1]; however, some of the originally published values have been adjusted with later determined corrections, including heterogeneity effects on critical mass and chamber wall effects on fission ratios. The reactivity coefficients listed have been assigned high uncertainties because of the large sample sizes used.

The eigenvalue for the one-dimensional model from the prescribed S_4 calculations differs from a hypothetical $S_{infinity}$ eigenvalue by an estimated $\Delta k/k = 0.0018$.

The conversion from inhours to $\Delta k/k$ is 427 Ih = .01 $\Delta k/k$.

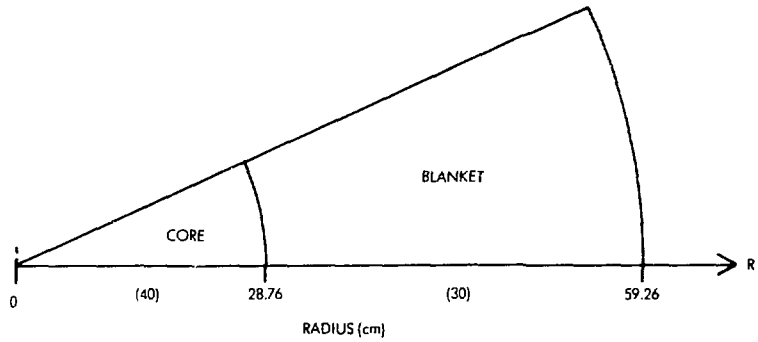

Figure 1. Spherical Model of ZPR-III Assembly 12.
Suggested Number of Mesh Intervals in ( ).

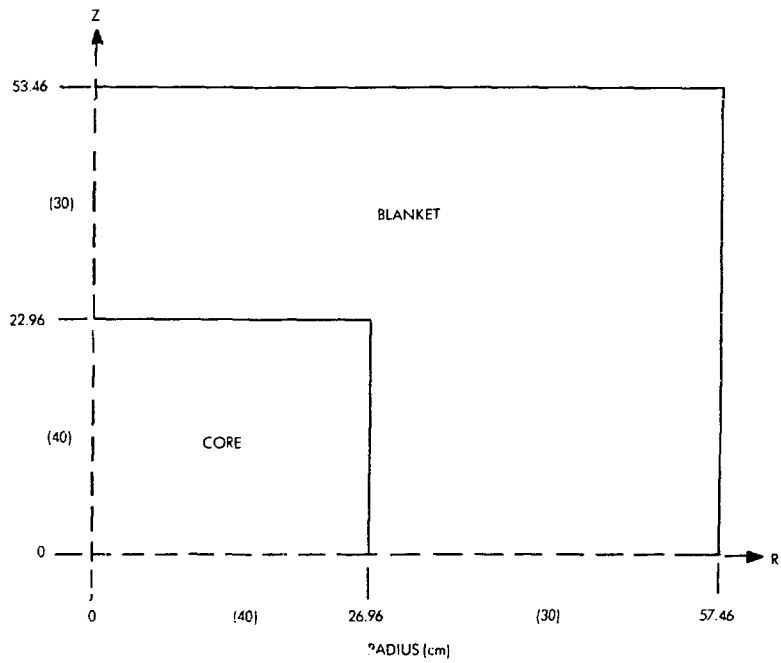

Figure 2. Two-Dimensional (R-Z) Model of ZPR-III Assembly 12.
Suggested Number of Mesh Intervals in ( ).

TABLE I

ZPR-III ASSEMBLY 12 REGION COMPOSITIONS (ATOMS/BARN-CM)

Material	Core	Blanket
U-235	0.004516	0.000089
U-238	0.016948*	0.040026
U-234	0.000046	-
C	0.026762	-
Fe	0.005704	0.004971
Cr	0.001419	0.001237
Ni	0.000621	0.000541
Mn	0.000059	0.000052
Si	0.000069	0.000060

* Including U-236.

FAST REACTOR BENCHMARK NO. 10

A. Benchmark Name and Type

ZEBRA-2, a 6:1 uranium-plus-graphite system.

B. System Description

The ZEBRA facility consists of stainless steel tubes containing reactor materials mounted vertically on a 3-meter square base plate. A pin at the lower end of each element fits into the base plate and the elements are restrained laterally by 3 steel lattice plates. The central 27 cm square of the base plate is removable so large experiments may be mounted in the reactor center. A concrete shield and steel containment vessel complete the structure.

ZEBRA Core 2 was a cylindrical critical assembly with a core height of 83.82 cm and an effective core diameter of 80.26 cm. The core is surrounded by a blanket of natural uranium having an axial thickness of 30.48 cm and an effective radial thickness of 33.26 cm. A complete detailed description of this assembly is found in the report AEEW-R410, "The Second Core of ZEBRA", by A. M. Broomfield, et al published in 1965.

ZEBRA-2 was designed to explore the accuracy of neutron cross section data for U-235 and U-238. The core contains some graphite and has a neutron spectrum similar to that of a large power reactor.

C. Model Description

A one-dimensional spherical model of ZEBRA-2 is given in Figure 1. A vacuum boundary condition should be applied to the outer reflector boundary. Material atom densities for the core and reflector regions are given in Table 1. The standard calculational mode is an S_4 transport theory calculation using a multigroup structure composed of 26 groups, each of lethargy width equal to 0.5 and with E_{max} set to 10 MeV. The number of mesh intervals for core and reflector are 40 and 30, respectively.

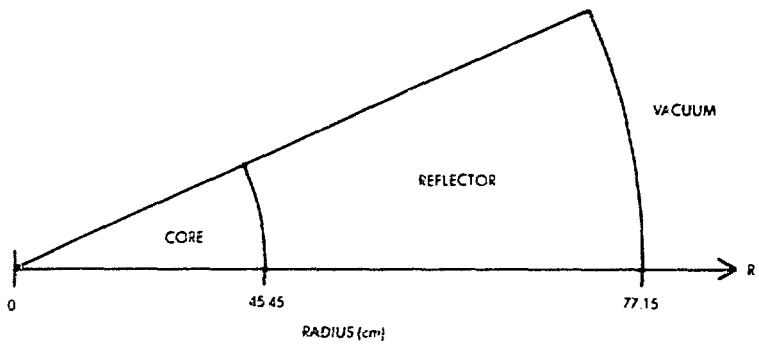

Figure 1. Spherical Model of ZEBRA-2 Assembly

2. Two-Dimensional Model Description

A two-dimensional (R-Z) cylindrical model of the ZEBRA 2 assembly is given in Figure 2. A zero return current boundary condition should be applied to the top and right side of the model; a symmetry boundary condition should be applied along the model bottom. The standard calculation mode is two-dimensional diffusion theory with mesh as follows: 40 radial and axial intervals in core; 30 intervals for the reflector thickness.

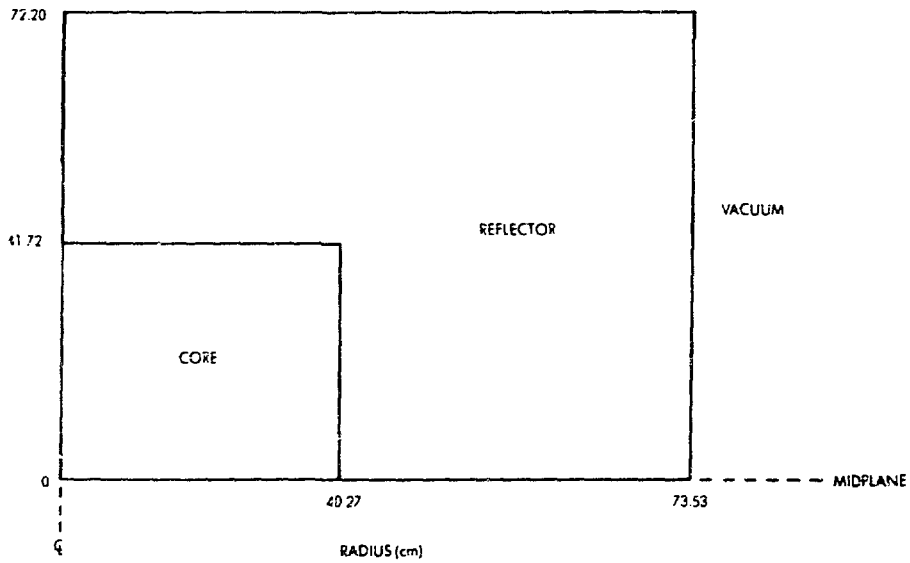

Figure 2. Two-Dimensional (R-Z) Model of ZEBRA-2 Assembly

Table 1.

ZEBRA 2 Region Compositions*

(Atoms/Barn-cm)

Material	Core	Reflector
U-235	0.002526	0.000298
U-238	0.015667	0.041269
H	0.00030876	-
O	0.0001544	-
Fe	0.0036485	0.003323
Cr	0.000864	0.000864
Cu	0.000004	0.000004
Mo	0.000008	0.000008
Mn	0.000064	0.000064
Ni	0.000483	0.000483
Aℓ	0.000019	0.000019
Ti	0.000016	0.000016
Si	0.000054	0.000054
V	0.000005	0.000005
C	0.037992	0.000042

*Revised: Private communication, R. W. Smith (AEEW) to H. Alter, 11/70

D. Experimental Data

1. Experimental Critical Mass

Experimental Critical Mass	418±1 Kg U-235
Corrections for Irregularities	-2.6±0.3
Finite Fuel Plate Thickness (Fuel + Diluent)	+3.1±6.2
Homogeneous Cylinder Critical Mass	418.5±6 Kg U-235
Experimental Eigenvalue	1.000±0.002

2. Experimental Spectral Indices at Core Center Relative to σ_f U-235

σ_f (U-238)	= 0.0320±0.0005	σ_c (U-238)	= 0.136±0.001
σ_f (U-233)	= 1.453±0.014	σ_c (Au)	= 0.298±0.015
σ_f (U-234)	= 0.153±0.016	σ_c (Mn)	= 0.026±0.002
σ_f (U-236)	= 0.093±0.014	σ_c (Ta)	= 0.401±0.040
σ_f (Pu-239)	= 0.987±0.010	σ_c (Na)	= 0.0013±0.0001
σ_f (Pu-240)	= 0.237±0.004	σ_c (B-10)	= 1.58±0.07
σ_f (Np-237)	= 0.214±0.002		

3. Material Worths at Core Center

Material	Reactivity Coefficient (10^{-5} Δk/k/mole)	Material	Reactivity Coefficient (10^{-5} Δk/k/mole)
U-235	68.4±0.7	Au	-15±1
U-238	-5.3±0.3	Cu	-1.8±0.1
Pu-239	97.3±1.2	Fe	-0.6±0.1
Pu-240	22±4	Cr	-0.6±0.1
B-10	-94±3	Ni	-1.2±0.1
B	-20±1	Mn	-0.85±0.10
Li-6	-39±2	Na	0.14±0.10
Li	-4.2±0.4	Al	-0.27±0.10
Ta	-23.2±0.4	C	0.31±0.05
Hf	-20.9±0.4	H	15±1

The reactivity coefficients given in D.3 are values for effective zero size samples as quoted in the references.[1][2] The conversion from inhours to $\Delta k/k$, as calculated by ZEBRA personnel for that assembly is 480 Ih = 0.01 $\Delta k/k$.

4. Rossi Alpha

At delayed critical, $\alpha = -2.82 \pm 0.05 \times 10^4 \text{ sec}^{-1}$. Also extrapolation to zero alpha gave 339 inhours per dollar.

F. Comments and Documentation

ZEBRA 2 was a cylindrical critical assembly. The experimental information was detailed in report AEEW-R410.[1] Another report, AEEW-R373[2] contains results of investigations into sample size effects upon material worth measurements. Comment was received from R. W. Smith[3] regarding material composition changes in core and reflector and those revised material compositions are given in Table 1. Smith also advised that an allowance had been made for the moisture contamination of the graphite of approximately 700±200 p.p.m. hydrogen. The effect on k_{eff} is approximately 1.1% $\Delta k/k$.

The experimental critical mass was 418±1 Kg U-235. Corrections for edge irregularities and heterogeneity effects were -2.6+0.3 and +3.1±6.2 Kg U-235, respectively, resulting in homogeneous cylinder critical mass of 418.5±6 Kg U-235. Plates in the fuel elements in the ZEBRA assemblies form continuous planes perpendicular to the axis of the core. It was therefore possible to estimate corrections for heterogeneity ($\sim$ 1% in k) from infinite slab calculations. Applying a shape factor of 0.925±0.005 gives a homogeneous spherical critical mass of 387±6 Kg U-235. The corresponding critical sphere radius is 45.45±0.22 cm.

The correction to the S_4 eigenvalue result to extrapolate to an "S_∞" eigenvalue is estimated to be -0.0005. For example, if the k_{eff} (S_4) value was 1.0000, then the value for S_∞ would be 0.9995.

REFERENCES

1. A. M. Broomfield, et al., "The Second Core of ZEBRA", [illegible]
2. G. Ingram, et al., "Central Perturbation Cross Sections in ZEBRA Cores 1 and 2", AEEW-R 373 (1964).
3. Private Communication, R. W. Smith (AEEW) to H. Alter (11/70).

A. Benchmark Name and Type

ZPPR Assembly 02, a Demonstration Fast Reactor Benchmark Critical

B. System Description

ZPPR Assembly 02, Loading No. 90 was designed as a fast reactor benchmark critical experiment. Its composition and neutron spectrum are typical of an LMFBR. An R-Z representation of ZPPR Assembly 02 is shown in Figure 1. The reference loading contained equal volumes in the inner and outer core zones. The inner core zone was composed from a repetition of a one-drawer unit cell; the outer core zone utilized a two-drawer cell. Both inner and outer core zones contained some partial core drawers with 1/2 inch wide void channels (for poison rods) alongside, and the inner core contained movable control drawers. The region compositions in Tables I and II are not the unit cell compositions, but include the perturbation (in sodium and steel densities) due to the void channels and control drawers.

C.1 One-Dimensional Homogeneous Model Description

A one-dimensional radial model of ZPPR Assembly 02 is shown in Figure 2, including model dimensions, boundary conditions and suggested mesh. The atom densities in each region (atoms/barn-cm) are given in Table I. The perpendicular buckling to be used in all regions and groups is 5.92×10^{-4} cm.$^{-2}$ Diffusion theory is suggested with cross sections in any suitable fast reactor energy-group structure, but with groups no coarser than 0.5 lethargy width down to a lethargy of 12.5. A heterogeneity correction of +0.0175 $\Delta k/k$ should be applied to the calculated eigenvalue, to account for flux variations in the unit cells.

C.2 Two-Dimensional Model Description

The two-dimensional (R-Z) model of ZPPR Assembly 02 is shown in Figure 1, including model dimensions and suggested mesh. Zero return current boundary conditions are to be applied on the top, bottom and right boundaries. The atom densities in each region (atoms/barn-cm) are

given in Tables I and II. Diffusion theory is suggested with cross sections in any suitable fast reactor energy group structure*. The effects of heterogeneity should be included in the generation of the multigroup cross sections for each region, using the unit-cell descriptions in paragraph C.3.

C.3 Unit-Cell Descriptions

The outer dimensions of the ZPPR matrix tubes, determined from the total lattice dimensions, are a width of 5.5245 cm and a height of 5.7839 cm. The drawers inserted into the tubes have an inside cross section of 2 inches square for the loading of the various reactor-material plates. Thus, the total cell can be represented as a 2 x 2 inch loading area of plates inside a structural box, as illustrated in Figure 3. The arrangements of the plate columns used for the Assembly 02 core and blanket cells are shown in Figure 4.

Tables III and IV give average widths and compositions for the plate columns used in the core and blanket drawers. For the canned materials (fuel, sodium, and Na_2CO_3) a nominal thickness of 0.015 in. was chosen for the steel cladding, and the remainder of column width (1/4 in. or 1/2 in.) was assumed to be occupied by the fuel, Na, or Na_2CO_3-plate core. For all of the column materials, the densities were derived assuming the assigned widths, a height of 2 in. and a length of 18.036 in. (column length plus thickness of drawer front). Table IV includes the composition for the side structure of the cell (drawer plus matrix) homogenized over the true widths of the matrix wall plus drawer side plus slack. Compositions for the upper and lower regions of the cells as indicated in Figure 3 are given in Table V: These include the drawer front and bottom, matrix, edges and ends of the claddings, and in some cases shims on the bottom of the plate loadings.

---

*If the two-dimensional problems are run with a group structure that contains groups broader than 0.5 lethargy, these cross sections should be generated by regionwise collapsing, using representative spectra for each of the regions in Figure 1, from a structure that has no groups greater than 0.5 lethargy width down to a lethargy of 12.5.

Tables III and IV include a letter designation at the top for each of the different types of material columns. For cell calculations to be used in determining heterogeneously-averaged cross sections, the overall cell for each region can be viewed as a stack of vertical columns (5.08 cm high by 5.5245 cm total width) sandwiched between horizontal upper and lower plates of structure: The cell descriptions so conceived are as follows:

1. Inner Core Cell

The plate-loading pattern for core zone 1 is shown at the top in Figure 4 using the notations for column labels as given in Tables III and IV, the vertical constituents of the cell (including the side structure of the matrix and drawers) are as follows:

L B J H J F J A J F J H J B L

Column 2 of Table V gives the upper and lower structure atom densities for these drawers (which had steel shims on the bottom).

2. Outer Core Cell

As shown in the middle of Figure 4, the outer core cell was actually a two-drawer cell with three columns of fuel (giving a 1.5 ratio of fuel density of the outer zone relative to the inner zone). For simplicity, it is represented here as two cells, A and B:

Outer core A, with upper/lower structure in column 3 of Table V,
L F J A J E J H J B J G J E J A J F L.
Outer core B, with upper/lower structure in column 4 of Table V,
L J H J F J A J F J H J B J G J L.

3. Radial Blanket Cell

The loading pattern at the bottom left in Figure 4 was that used in the front 23 in. (to the

spring gap) in each half of the Inner Radial Blanket. The column notations for these regions would thus be

L C D J H J B B D J I J L.

For the back 16 in. of the Inner Radial Blanket (beyond the spring gap in each half of the assembly) the U_3O_8 was all in the form of 1/2 in. thick plates, giving the pattern of vertical constituents as

L C D J H J C D J I J L.

The upper/lower structure composition in column 5 of Table V applies to the overall average cell (full 34-in. length in each assembly half) of the Inner Radial Blanket.

The Outer Radial Blanket contained double columns of 1/4-in.-thick sodium in place of the 1/2-in.-thick Na above, giving the pattern for the front 23 in. as

L C D J G J J G J B B D J I J L,

and for the back 11 in. as

L C D J G J J G J C D J I J L.

4. Axial Blanket Cell

As indicated in Figure 4, a two-drawer cell was used for the axial blanket regions, the difference between the two drawers being a column (1/8 in.) of steel in place of a column of Fe_2O_3. Thus for the Fe_2O_3-loaded drawer, the pattern of vertical components would be

L B J H J E B D J H J B L,

and the steel-loaded drawer pattern would be

L B J H J K B D J H J B L.

The axial blanket behind the inner core contained steel shims at the bottom of the drawers, giving a high-density upper/lower structure region as indicated in column 6 of Table V.

The last column of Table V lists the upper/lower structure composition for the cell of the axial blankets behind the outer core.

The inclusion of all these cell descriptions is not to suggest that calculations are needed for each case to generate cell-averaged cross sections for all regions, but rather to point out the variances typically encountered in the construction of the critical assemblies and to show why the region compositions differ. One cell calculation each for the radial and axial blankets, with the patterns shown at the bottom of Figure 4, should be sufficient to obtain multigroup sets for use in all blanket and reflector regions.

It should also be mentioned that the homogenized compositions of the cell descriptions cited above will not agree exactly with the average region compositions given in Tables I and II because the column densities presented in Tables III and IV are averages of several lengths of plates, whereas the different regions involved variations of column plate-length patterns. Also, as indicated earlier, the core and axial blanket regions contain void channels and extra drawer steel homogenized into their compositions.

D. Experimental Data

1. Measured Keff = 1.0000 ± .0006

2. Experimental spectral indices at the core center, relative to σ_f (U-235) are as follows:

σ_f (U-233) = 1.446 ± 0.022
σ_f (U-234) = 0.1492 ± 0.0023
σ_f (U-236) = 0.0443 ± 0.0007
σ_f (U-238 = 0.0201 ± 0.0004
σ_f (Pu-239) = 0.9372 ± 0.0142
σ_f (Pu-240) = 0.1704 ± 0.0026

3. Material worths at the core center are as follows:

Material	Reactivity Coefficient 10^{-5} $\Delta k/k$/mole
Pu-239	28.29 ± 0.19
Pu-241	38.7 ± 4.9
U-235	20.86 ± 0.48
C	-0.1348 ± 0.0093
Na	-0.1172 ± 0.0056
Ta	-9.10 ± 0.18
B10	-22.37 ± 0.41
Fe	-0.1736 ± 0.0045
Cr	-0.174 ± 0.012
Ni	-0.2755 ± 0.0095
Al	-0.160 ± 0.014
Mn	-0.414 ± 0.018
W	-1.957 ± 0.009
Mo	-1.223 ± 0.052
Nb	-1.606 ± 0.060

E. Comments and Documentation

The radial dimensions for the core zones in Figures 1 and 2 have been adjusted to give a k = unity model with equal volumes in both zones. The adjustments account for the following corrections to the as-built loading:

1. Partial insertion of control rods
2. Subcriticality at operating power
3. The gap between the halves of the reactor
4. Uniform temperature representation (22.0°C average)

There were no control drawers spiked with extra fuel in this loading and the effect of smoothing the radial outlines of the inner and outer core was estimated to be negligible.

The total adjustment to the as-built Pu-239 + Pu-241 loading to derive the k = unity model was -8.5 ± 0.9 kg; with equal volume reductions in the inner and outer core zones, this gave the core radii shown in Figures 1 and 2. The radial blanket and reflector radii were adjusted to obtain the same thicknesses as in the as-built case. Overall, the loading uncertainty is about $\pm$ 1.5 kg of Pu-239 + Pu-241 (out of 1024 kg). This gives an uncertainty for the k = unity model of about $\pm$ 0.0006 $\Delta k/k$.

For the one-dimensional homogeneous model, the perpendicular buckling was determined in a CAESAR consistent-keff calculation. CAESAR is a diffusion theory code; a consistent-keff calculation alternates one-dimensional radial, axial and zero-leakage calculations until the bucklings give the same eigenvalue as in the two-dimensional model for both the radial and axial cases. 25 energy groups were employed.

The conversion from inhours to $\Delta k/k$ is 1015.7 Ih = .01 $\Delta k/k$. The calculated model was specified by Hess (ANL) and modified by Otter (AI).

1. R. E. Palmer, et al, "ZPPR-2 Benchmark Analyses to January 1971", ZPR-TM-51 (January 20, 1971)

2. R. E. Kaiser, et al, "Experimental Evaluations of the Critical Mass for ZPPR Assembly 2", ZPR-TM-47 (January 20, 1971)

3. ZPPR Staff, "ZPPR 2 Benchmark Experimental Data to January 1971", ZPR-TM-48 (January 20, 1971)

4. Private communication A. Hess to H. Alter, "Benchmark Model for ZPPR Assembly 02", January 1971.

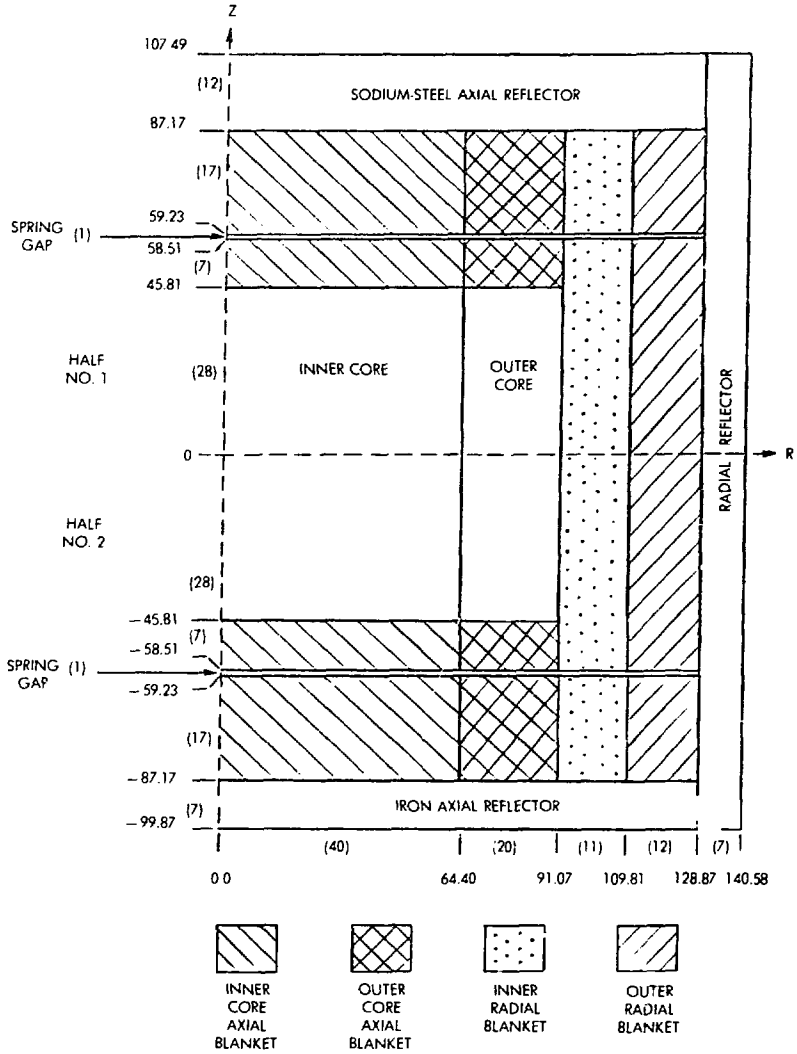

Figure 1. Benchmark Model of ZPPR Assembly 02.
Dimensions in cm; Suggested Number of Mesh Intervals in ( ).

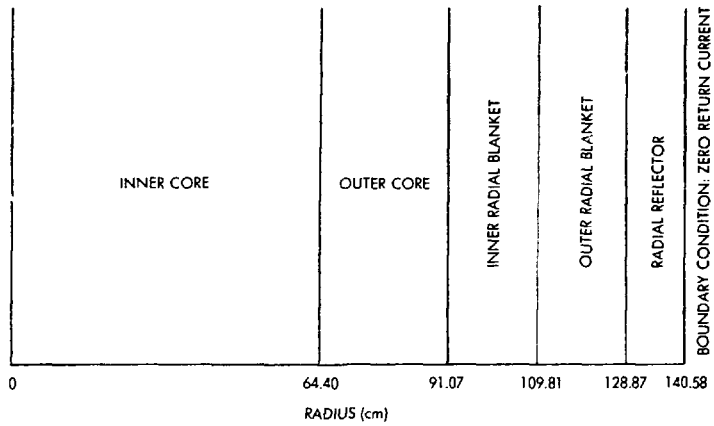

Figure 2. Radial Model of ZPPR Assembly 02.
Suggested Mesh: 40 Intervals, Inner Core; 20 Intervals Outer Core; 30 Intervals Across Inner/Outer Blankets and Reflector.

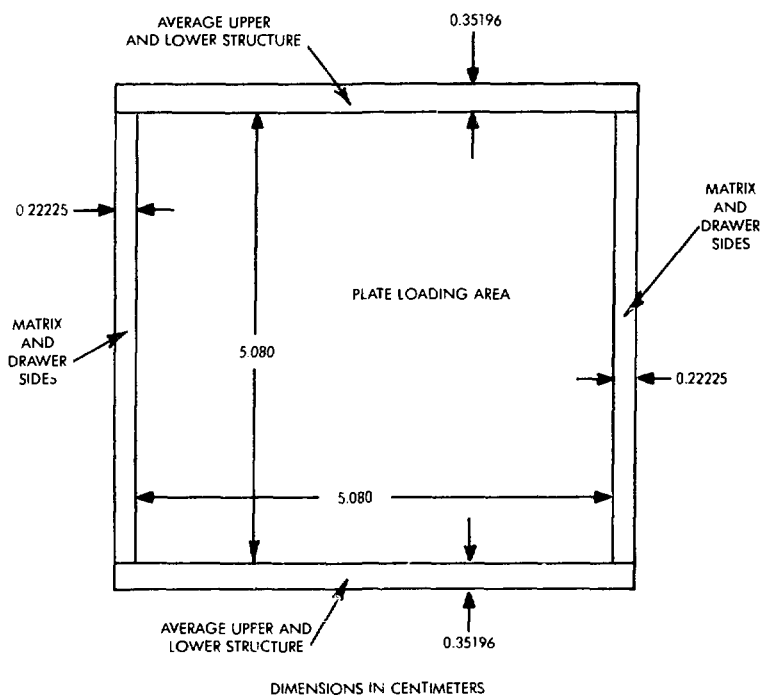

Figure 3. Geometry of ZPPR Unit-Matrix Cells

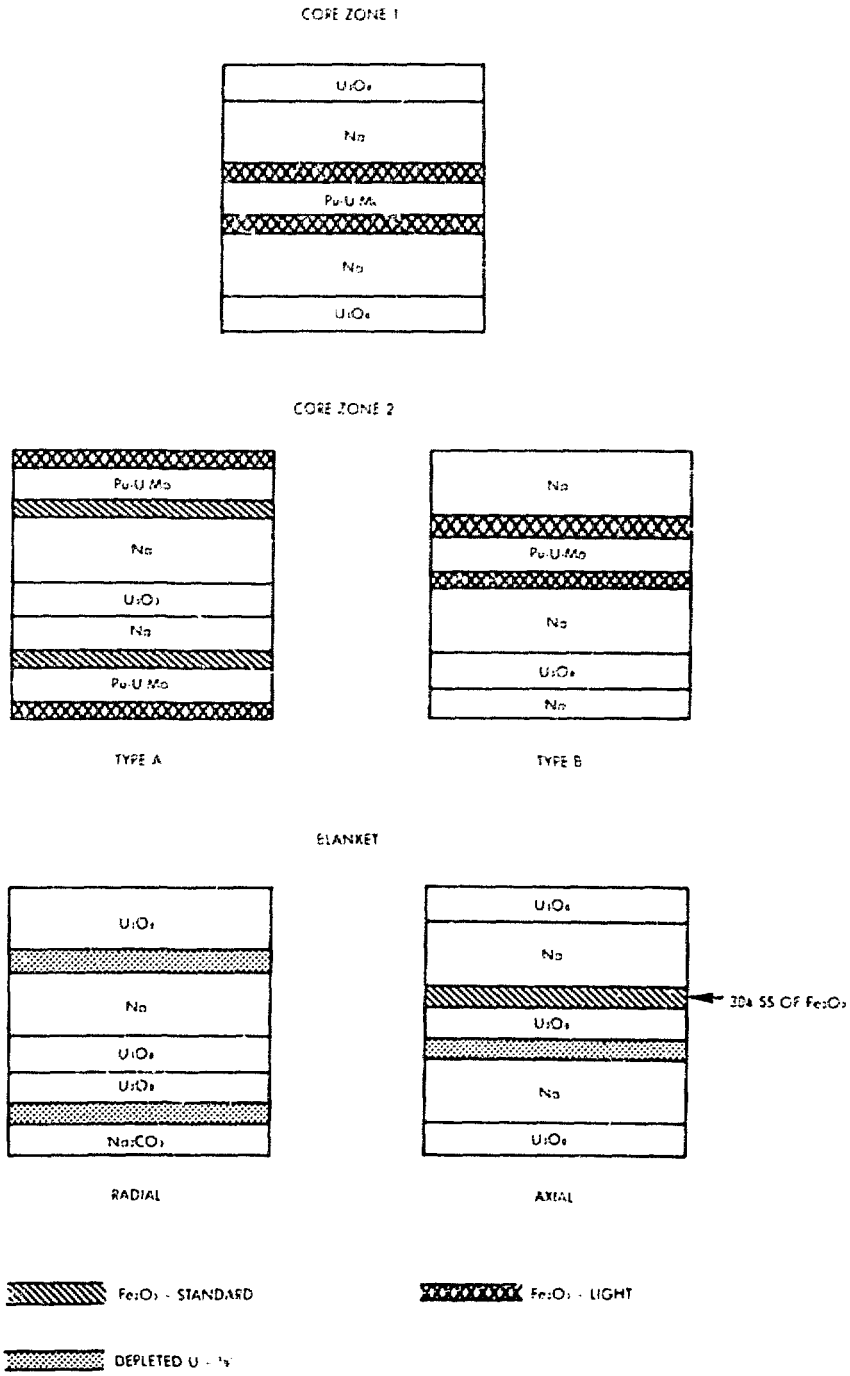

Figure 4. Cell-Loading Patterns for ZPPR Assembly 02

Table I

ZPPR Assembly 2, a Demonstration Fast Reactor Benchmark Critical

Radial Region Compositions at Axial Centerline (atoms/barn-cm)

Material	Inner Core	Outer Core	Inner Radial Blkt.	Outer Radial Blkt.	Radial Reflector
Pu 239	.0008433	.0012741			
Pu 240	.0001117	.0001687			
Pu 241	.0000153	.0000231			
Pu 242	.0000018	.0000028			
Pu 238	.0000006	.0000009			
Am 241	.0000029	.0000043			
U 235	.0000123	.0000115	.000024	.000024	
U 238	.0055549	.0051980	.011085	.011085	
C	.00003	.000023	.001013	.001013	.000558
O	.013116	.011761	.020132	.020133	
Na	.008796	.008564	.006398	.005963	
Al	.000003	.000004	.000002	.000003	
Fe	.012576	.013852	.006923	.007541	.075161
Cr	.002702	.002523	.001991	.002172	.001205
Ni	.001221	.001160	.000898	.000987	.000513
Mn	.000209	.000202	.000157	.000174	.000598
Cu	.000019	.00002	.000017	.000018	.000013
Mo	.000231	.000341	.000014	.000015	.000012
Si*	.000137	.000118	.000094	.000102	.000091
H	-	-	.000008	.000008	

*Includes minor concentrations of P and S

Table II

ZPPR Assembly 02, a Demonstration Fast Reactor Benchmark Critical

Region Compositions Off Axial Centerline (atoms/barn-cm)

Material	Axial Blanket Over Inner Core	Axial Blanket Over Outer Core	Spring Gaps	Sodium Steel Axial Reflector	Iron Axial Reflector
U 235	.000016	.000016			
U 238	.007036	.007057			
C	.000036	.000030	.000284	.000214	.000557
O	.013895	.014008			
Na	.008739	.008808		.008966	
Al	.000002	.000002	.000001	.000002	
Fe	.010751	.009355	.021133	.035713	.072271
Cr	.002835	.002418	.004393	.005347	.001639
Ni	.001275	.001095	.001503	.002412	.000706
Mn	.000230	.000205	.000279	.000611	.000623
Cu	.000017	.000017	.000030	.000017	.000014
Mo	.000014	.000014	.000023	.000014	.000013
Si*	.000150	.000119	.000182	.000305	.000114

*Includes minor concentrations of P and S

Table III. Specifications of Fuel, Fertile, and Iron Oxide Constituents of Core and Blanket Cells

Cell Component	Cores of Pu-U-Mo Alloy Plates	1/4 in. thick U_3O_8 Columns	1/2 in. thick U_3O_8 Columns	1/8 in. thick Depleted U Columns	Standard Fe_2O_3 Columns	Light Fe_2O_3 Columns
Label	A	B	C	D	E	F
Thickness (cm)	0.5588	0.6350	1.2700	0.3175	0.3175	0.3175
Atom Densities (atoms/barn-cm)						
Pu 238	.000006	- -	- -	- -	- -	- -
Pu 239	.009501	- -	- -	- -	- -	- -
Pu 240	.001258	- -	- -	- -	- -	- -
Pu 241	.000173	- -	- -	- -	- -	- -
Pu 242	.000021	- -	- -	- -	- -	- -
Am 241	.000032	- -	- -	- -	- -	- -
U 235	.000060	.000034	.000035	.000103	- -	- -
U 238	.026988	.015646	.016189	.045778	- -	- -
Mo	.002436	- -	- -	- -	- -	- -
O	- -	.041691	.042901	- -	.055404	.046632
Fe	- -	- -	- -	- -	.036869	.031735

Table IV. Specifications of Sodium, Sodium Carbonate, Cladding and Reactor-Structure Constituents of Core and Blanket Cells

Cell Component	Cores of 1/4 in. Na Columns	Cores of 1/2 in. Na Columns	Cores of 1/4 in. Na_2CO_3 Columns	Cladding of Fuel, Na and Na_2CO_3 Plates	1/8 in. thick Stainless Steel Column	Structure Side Wall, Matrix and Drawer
Label	G	H	I	J	K	L
Thickness, cm	0.5588	1.1938	0.5588	0.0381	0.3175	0.22225
Atom Densities, (atoms/barn-cm)						
Na	.022302	.023300	.022291	- -	- -	- -
C	- -	- -	.011140	- -	.000270	.000162
O	- -	- -	.033438	- -	- -	- -
Fe	- -	- -	- -	.055936	.058032	.035911
Cr	- -	- -	- -	.016276	.016146	.010303
Ni	- -	- -	- -	.008189	.007303	.004510
Mn	- -	- -	- -	.001176	.001584	.000875
Si*	- -	- -	- -	.000778	.000981	.000501
Mo	- -	- -	- -	.000043	- -	.000086
Cu	- -	- -	- -	.000093	- -	.000096
Al (H)	- -	- -	.000094	.000067	- -	- -

*Includes minor concentrations of S and P

Table V. Compositions of Upper and Lower Cell Structure

Material	Average Compositions of Upper and Lower Structural Regions [a] for Core and Blanket Cells, atoms/barn-cm					
	Cell for Inner Core	Cell for Outer Core A	Cell for Outer Core B	Cell for Inner Radial Blanket	Cell for Axial Blanket of Inner Core	Cell for Axial Blanket of Outer Core
Fe	.039436	.028733	.028801	.024899	.036611	.035240
Cr	.011337	.008237	.008268	.007141	.010693	.007347
Ni	.004960	.003643	.003482	.003128	.004703	.003259
Mn	.000860	.000680	.000683	.000551	.000814	.000621
Si*	.000607	.000335	.000338	.000330	.000580	.000332
Mo	.000054	.000050	.000055	.000060	.000059	.000059
Cu	.000072	.000074	.000074	.000065	.000068	.000068
Al	.000008	.000009	.000009	.000003	.000007	.000007
C	.000148	.000097	.000097	.000096	.000144	.000094

[a]Region dimensions as illustrated in Figure 3.

*Includes minor concentrations of P and S.

FAST REACTOR BENCHMARK NO. 12

A. ZPR-6 Assembly 7 - A Plutonium Oxide Fueled Fast Critical Assembly.

B. System Description:

The ZPR-6 consists of two halves, each a horizontal matrix of 2.2 in. square stainless steel tubes into which are loaded stainless steel drawers containing fuel and diluent materials of various types. Assembly 7 is a large (3100 liter) fast critical assembly with a soft spectrum and other characteristics representative of current LMFBR designs. It has a single fuel zone with a length-to-diameter (L/D) ratio of approximately unity; it has a simple one-draw unit cell; and it is blanketed both axially and radially with depleted uranium. The assembly's spectrum characteristics, simple geometric configuration, and simple unit cell make it well suited for a benchmark assembly.

The unit cell, which is shown in Fig. 1 is identical to that of a companion benchmark assembly; ZPR-6 Assembly 6A, except that the fuel is Pu/U/Mo (28 w/o plutonium, 69.5 w/o uranium and 2.5 w/o molybdenum) rather than enriched uranium. The plutonium is 11.5 w/o ^{240}Pu. A cross sectional view of the as-built reference assembly, which had an excess reactivity of 96.2 Ih, is shown in Fig. 2 and the equivalent cylindricalized representation of the as-built system is shown in Fig. 3.

C. Model Description:

1. One-Dimensional Model: A one-dimensional model with spherical geometry has been used in the analysis of many measurements in the assembly. The spherical model was defined with reference to a two-dimensional finite cylindrical model, which will be described in Section C.2. The homogeneous spherical model was defined by first determining a blanket thickness and then searching for a core radius that gives the spherical reactor the same k_{eff} as the homogeneous two-dimensional cylinder. The blanket dimensions and compositions were defined as the weighted average of the axial and radial blanket dimensions and compositions in which the weighting was done on the basis of the relative leakages into the axial and the radial blankets (as given by the two-dimensional calculations). The resulting core radius and blanket thickness for the homogeneous spherical model were 88.16 and 33.81 cm, respectively. The appropriate compositions for use with the spherical model are given in Table I. The spherical model is expect to introduce approximately a 0.1% uncertainty in k_{eff}.

An energy group structure with 27 groups, as given in Table II, is suggested. Such a structure has sufficient detail at low energies to afford accurate computations of material worths and Doppler effects.

Because of the simplicity of the two-region, homogeneous spherical model, the macroscopic flux distributions across the

reactor may be computed with diffusion theory and a relatively coarse mesh of 2 cm should be adequate.

Central material reactivity worths and Doppler reactivity worths may be computed by perturbation tehory. If the material sample is optically thin and if the material is contained in the core, the homogeneous core cross sections for the material are appropriate to the sample. If the material sample is optically thin and, if the material is not contained in the core, then infinite dilution cross sections are appropriate for the sample.

The major flaw in the homogeneous spherical model for this geometrically simple system is in the neglect of heterogeneities in the unit cell. Sections D and F indicate the uncertainties arising from the use of homogeneous cross sections. The error in material worth or Doppler worth introduced by flux distortions depends strongly upon the nature of the sample.

2. Other More Complicated Models: A two-dimensional finite cylindrical representation of the system is closer to the physical configuration than a spherical representation. The as-built loading was thus corrected for both excess reactivity and edge smoothing. The spring gap was homogenized into the axial blanket and the radial blanket height was defined to be the same as the core plus axial blanket heights. Resulting region dimensions are given in Table III.[1]

The corresponding compositions for the zero-excess, uniform cylindrical model are given in Table IV. The "exact core region", at the center of the assembly, is simply a region in which material concentrations are known more accurately than in the rest of the core.

D. Experimental Data:

1. Measured Eigenvalues: The measured eigenvalue corresponding to the models of Section C is 1.0000 ± 0.001. Calculations indicate a 0.0166 heterogeneous-homogeneous correction[2] and a 0.0018 S_8-diffusion correction.

2. Unit-Cell Reaction Rates: Detailed unit-cell measurements of the capture and fission in ^{238}U and fission in U^{238} and ^{239}Pu were made. Activation foils of ^{238}U, ^{235}U, and ^{239}Pu were used to measure the rates within the fuel and U_3O_8 plates, such that the actual cell-averaged values of the reaction rates could be obtained. To be clear, these unit-cell reaction rate values correspond to the reactions actually taking place in the unit-cell in the assembly, and not, for example, to a cell-average defined as the value of the flux at every point in the cell multiplied by the cross section of the foil material. We use the term to refer to the flux and volume weighted reaction rates as they actually occur in the unit-cell. Hence, a per atom unit-cell reaction rate ratio is converted to the actual ratio of the number of reactions taking place in the cell simply by multiplying

the former ratio by the appropriate atom density ratio.

The details of the technique used for counting the activated foils and reducing the data to absolute reaction rates are identical with those used in Ref. 3. The absolute calibrations were made with three separate and independent techniques: (1) by absolute fission chambers with identical foils on their faces to those used in the unit-cell measurements, with the fission chambers placed in the reactor at the same spectral position; (2) by thermal irradiation of identical foils in ATSR thermal column; and (3) by absolute radiochemical analysis of some of the foils that were actually used in the unit-cell measurement. The excellent agreement among the various calibration methods made possible the small uncertainty, $1\sigma = 2\%$, in the measured reaction rate ratios.

For the plate cell environment, the unit cell in which the reaction ratios were measured differed somewhat from the "normal unit-cell" of Fig. 1. In the "experimental" unit-cell, instead of the normal 1/4 in. thick Pu/U/Mo plate, two thinner Pu/U/Mo plates were used to permit foils to be placed at the center of the fuel column so that an integration of the reaction rates through the fuel plate could be made. Each of the plates had a 0.015 in. stainless steel cladding and a 0.095 in. core thickness. The effect of this substitution for the normal fuel plate was to reduce the fuel content of the experimental unit-cell (33% less Pu-Mo, 15% less ^{238}U) and to increase

its stainless steel content by 7.5%. The measured reaction rate ratios for ^{238}U Capture-to-^{239}Pu fission, ^{238}U fission-to-^{239}Pu fission, and ^{235}U fission-to-^{239}Pu fission are given in Table V along with calculated correction factors (to be applied to the measured values) for heterogeneities.[1,2]

3. Material Worths at the Center of the Core: Central reactivity worths of several materials were measured in a small cavity with use of the radial sample changer. The uranium and plutonium samples were thin annuli clad on the outside with stainless steel. The other samples were generally unclad cylinders. The samples were held in thin-walled stainless steel sample holders and the reactivity worth of the sample was obtained by the difference in the reactivity worth (relative to void) of the sample holder between when it is empty and when it holds a sample. Further descriptions of the samples and the measurements are given in Ref. 4. Table VI gives the experimental worths of the isotopes, the weights and identifications of the samples from which they were obtained, and the calculated results.

E. Calculated Results:

The calculations described in this section were made using ENDF/B-III data and the standard one-dimensional, homogeneous spherical model of the assembly. The fundamental mode option of the SDX[5] code was used to compute homogeneous cross sections. This model yielded a multiplication constant of 0.9772 for the critical system. The addition

of the heterogeneity and transport corrections (Section D.1) gives a k_{eff} of .9956.

The calculated values for the reaction rate ratio values for the normal plate unit cell are given in Table VII.

The central worth calculations based on the homogeneous spherical model central fluxes are given in Table VII. The basic calculations used first-order perturbation theory.

F. Comments and Documentation:

To assess the limitations of the homogeneous, spherical Benchmark model the multiplication constant, reaction rate ratios and central reactivity worths were calculated with a one-dimensional spherical heterogeneous model and with a two-dimensional finite cylindrical, heterogeneous model. In this way, the errors from homogenization can be separated from the errors from the simplified geometric representation. The heterogeneous cross sections were computed with the plate unit-cell option in the SDX code, which uses equivalence theory in the narrow resonance approximation to obtain resonance cross sections and integral transport methods to obtain spatial weighting factors. The model used to represent the unit cell in these SDX problems is described in Ref. 7. For the one-dimensional model, the heterogeneous cross sections were obtained with the fundamental mode option of SDX; for the two-dimensional model, the space-dependent option was used.

The results of calculations with the three models are compared in Table VII. The one- and two-dimensional heterogeneous models are in good agreement. The difference in k_{eff} is due to both the use of fundamental mode cross sections in the spherical model and spherical model's being defined with ENDF/B-I data. From comparison of the homogeneous and heterogeneous results, heterogeneities account for a difference of about 1.7% in the multiplication constant. For the reaction rate ratios and the material worths of the homogeneous results are in surprisingly good agreement although they do show the changes in ^{10}B and ^{238}U worths expected from the spectrum difference.

For the central worth measurements, the conversion factor 1% $\Delta k/k$ = 1007 Ih was used to convert the measured periods to the desired reactivity units. The delayed neutron data of Keepin[8] were used in computing this conversion factor.

References

1. C.E. Till, L. G. LeSage, R. A. Karam, et al., "ZPR-6 Assemblies 6A and 7: Benchmark Speicifications for the Two Large Single-Core-Zone Critical Assemblies - ^{235}U-Fueled Assembly 6A and Plutonium-Fueled Assembly 7 - LMFBR Demonstration Reactor Benchmark Program", Applied Physics Division Annual Report, July 1, 1970 to June 30, 1971, 86-101, ANL-7910.

2. B. A. Zolotar, E. M. Bohn, and K. D. Dance, "Benchmark Tests and Comparisons Using ENDF/B Version III Data", Applied Physics Division Annual Report, July 1, 1971 to June 30, 1972, ANL-8010 (in press).

3. C. E. Till, J. M. Gasidlo, E. F. Groh, et al., "Null-Reactivity Measurements of Capture/Fission Ratio in ^{235}U and ^{239}Pu", Nucl. Sci. Eng. 40, 132 (1970).

4. L. G. LeSage, E. M. Bohn and J. E. Marshall, "Solium-Void and Small-Sample Reactivity Worth Measurements in ZPR-6 Assembly 7", Applied Physics Division Annual Report, July 1, 1970 to June 30, 1971, 141-154, ANL-7910.

5. W. M. Stacy, Jr., H. Henryson II, B. J. Toppel and B. A. Zolotar, "MC^2-2/SDX Development - Part II", Applied Physics Division Annual Report, July 1, 1971 to June 30, 1972, ANL-8010 (in press).

6. P. H. Kier, "Calculations of the Effects of Local Flux Distortions in Central Reactivity Worth Measurements in ZPR-6 Assembly 7", Applied Physics Division Annual Report, July 1, 1971 to June 30, 1972, ANL-8010 (in press).

7. J. E. Marshall, "The Unit-Cell Composition Model Developed for SDX Input Preparation and the Resulting Cell Speicifications for the ZPR/ZPPR Benchmark Assemblies". Applied Physics Division Annual Report, July 1, 1971 to June 30, 1972, ANL-8010 (in press).

8. G. R. Keepin, "Physics of Nuclear Kinetics", Addison-Wesley, Reading, Mass., 1965, Table 4-7.

TABLE I. Assembly 7 Spherical Model Atom Densities, atoms/barn-cm

Isotope	Core radius = 88.16 cm	Blanket thickness = 33.81 cm
^{239}Pu	0.00088672	-
^{240}Pu	0.00011944	-
^{241}Pu	0.0000133	-
^{235}U	0.0000126	0.0000856
^{238}U	0.00578036	0.0396179
Mo	0.0002357	0.0000038
Na	0.0092904	-
O	0.01390	0.000024
Fe	0.013431	0.004637
Cr	0.002842	0.001295
Ni	0.001291	0.0005635
Mn	0.000221	0.0000998

Table II. Specifications of 27-Group Structure

Group	ΔU	E_{upper}, keV	Group	ΔU	E_{upper}, keV
1	0.5	10000	14	0.5	15.034
2	0.5	6065.3	15	0.5	9.1188
3	0.5	3678.8	16	0.5	5.5308
4	0.5	2231.3	17	0.5	3.3546
5	0.5	1353.4	18	0.5	2.0347
6	0.5	820.85	19	0.5	1.2341
7	0.5	497.87	20	0.5	0.74851
8	0.5	301.97	21	0.5	0.45400
9	0.5	183.16	22	1	0.27536
10	0.5	111.09	23	1	0.10130
11	0.5	67.379	24	1	0.03727
12	0.5	40.868	25	1	0.01371
13	0.5	24.787	26	2	0.00504
			27	–	0.00063

Table III. Dimensions for the Zero-Excess Reactivity, Uniformly Loaded Cylindrical Version of ZPR-6 Assembly 7

Outer Core Radius, cm	80.30
"Exact Core" Region Radius, cm	24.34
Core Height, cm	152.56
Radial Blanket Thickness, cm	33.54
Radial Blanket Height, cm	221.10
Axial Blanket Thickness, cm	34.27
Core Volume, liters	3090

Table IV. Mean Atom Densities for the Zero-Excess Uniform Cylindrical Model of Assembly 7, atoms/barn-cm

	Exact Core	Outer Core	Axial Blanket	Radial Blanket
^{238}Pu	0.00000033	0.00000033	-	-
^{239}Pu	0.0008867	0.0008879	-	-
^{240}Pu	0.0001177	0.0001178	-	-
^{241}Pu	0.0000133	0.0000133	-	-
^{242}Pu	0.00000141	0.00000177	-	-
^{234}U	0.00000006	0.00000006	0.00000040	0.00000040
^{235}U	0.0000126	0.0000126	0.0000834	0.0000866
^{236}U	0.00000030	0.00000030	0.0000020	0.0000020
^{238}U	0.005777	0.005802	0.03859	0.04006
^{241}Am[a]	0.0000030	0.0000028	-	-
Mo	0.0002357	0.0002382	0.0000046[b]	0.0000034[b]
Na	0.0092904	0.009132	-	-
O[c]	0.01398	0.01482	0.000030[b]	0.000021[b]
Fe[d]	0.01297	0.01353	0.005652	0.004197
Cr	0.002709	0.002697	0.001579	0.00117
Ni	0.001240	0.001212	0.000691	0.0005082
Mn	0.000212	0.000213	0.000123	0.0000897

[a] ^{241}Pu decay to ^{241}Am corrected to 9/15/71

[b] Arising from SS304 impurities

[c] Includes ~0.005% from SS304 and Pu/U/Mo fuel impurities

[d] Includes ~0.0088% from heavy (atomic wt > Si) SS304 impurities and Pu/U/Mo fuel impurities.

Note: The number of digits in each density is a measure of the compositional precision. Nominally, the rightmost digit bounds the density according to a 2σ of 93% confidence interval.

Table V. Unit-Cell Reaction Rate Ratios in ZPR-6 Assembly 7

	Measurement (1σ = 2%)	Calculated Heterogeneity Correction Factors[a]
$^{28}c/^{49}f$	0.1400	1.023
$^{28}f/^{49}f$	0.02336	1.030
$^{25}f/^{49}f$	1.061	0.989

[a] homogeneous/heterogeneous

TABLE VI. Control Reactivity Worths Measured in a Central Cavity in ZPR-6 Assembly 7, 10^{-5} $\Delta k/k$/mole

Isotope	Isotopic Wt. in sample, gm	Sample[a] ident.	Sample-Size[b] Correction	Measured[c,d] Worth 1σ imprecision	Calculated[e] Worth
^{239}Pu	9.856	MB10	0.99	37.6 ± 0.40	47.12
^{235}U	14.702	MB21	1.01	31.10 ± 0.47	38.37
^{238}U	19.033	MB24	1.01	-2.58 ± 0.108	-2.801
^{10}B	0.1103	B(L)	1.03	-29.3 ± 0.63	-32.04
Na	17.044	NA(L2)	1.09	-0.155 ± 0.008	-0.189
Ta	18.647	TA-2		-7.739 ± 0.78	
C	33.441	C(L)		-0.1454 ± 0.0025	
Al	53.067	AL(L3)		-0.1800 ± 0.0045	
Fe	33.277	Fe-1		-0.2368 ± 0.0086	
Ni	37.916	Ni-1		-0.3770 ± 0.0108	
Cr	26.999	Cr-3		-0.2343 ± 0.0191	
Mo	43.393	Mo-1		-1.466 ± 0.010	

a. See Ref. 4 for a fuller description of samples
b. Integral transport calculation based on ENDF/B-I data and one-dimensional cylindrical representation central fluxes, see Ref. 6
c. Measured period converted to reactivity with use of conversion factor 1% $\Delta k/k$ = 1007 Ih
d. Corrected for sample-size effect where given
e. FOP calculation based on ENDF/B-III data and central spherical fluxes

TABLE VII. Comparison of Calculations for Assembly 7 with Several Models

		1-Dimensional Homogeneous	1-Dimensional Heterogeneous	2-Dimensional Heterogeneous
	k_{eff}	0.9772	0.9938	0.9924
Reaction Rates	$^{28}f/^{49}f$	0.02304	0.02313	0.02316
	$^{25}f/^{49}f$	1.0962	1.1143	-
	$^{28}c/^{49}f$	0.1570	0.1530	0.1531
Central[a] Worths	^{239}Pu	47.12	47.05	47.05
	^{235}U	38.37	38.67	38.69
10^{-5} $\Delta k/k$/mole	^{238}U	-2.801	-2.990	-2.985
	^{23}Na	-0.189	-0.193	-0.190
	^{10}B	-32.04	-34.52	-34.59

a. FOP calculations not corrected for sample size effects

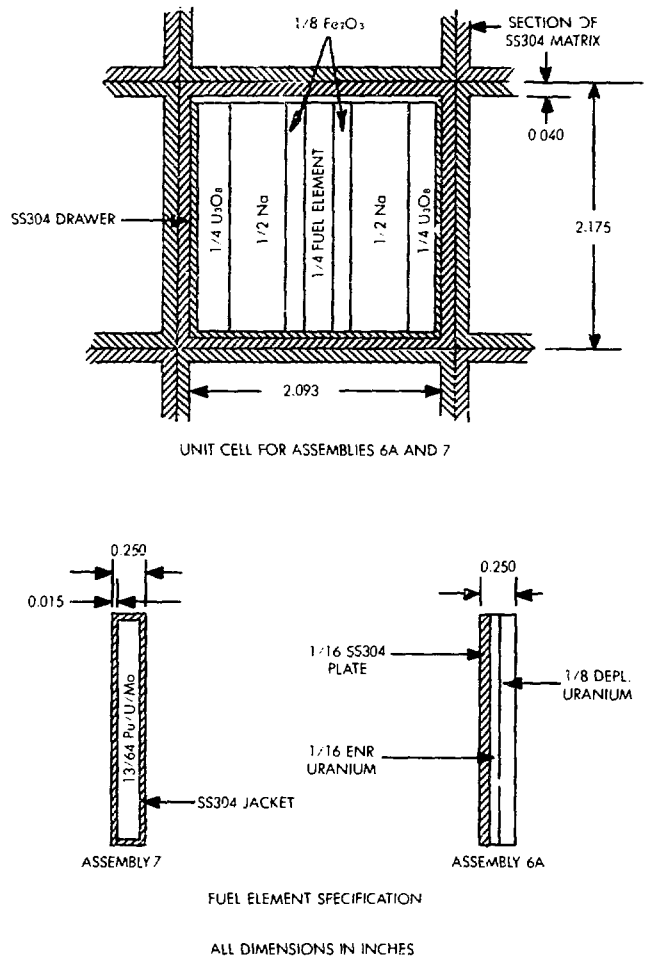

Figure 1. Cross Section of Unit-Cell Showing Matrix and Plate Loaded Drawer, ZPR Assemblies 6A and 7, ANL-Neg. No. 116-888.

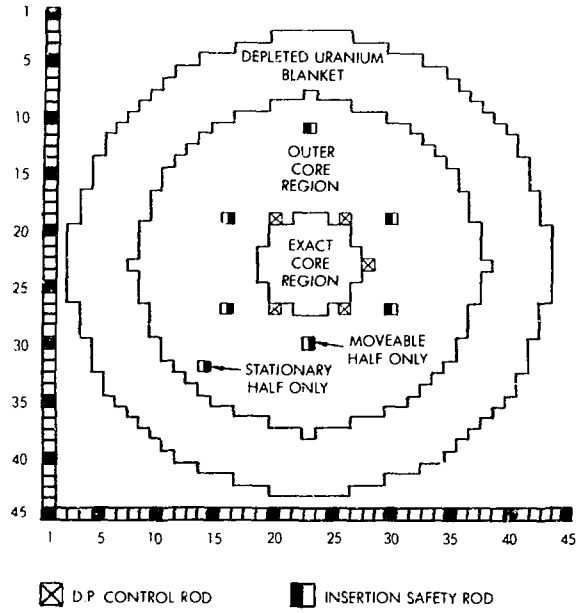

Figure 2. Radial Cross Section for the 96.2 Ih Excess Reactivity, As-Built ZPR-6 Assembly 7, ANL-Neg. No. 116-889.

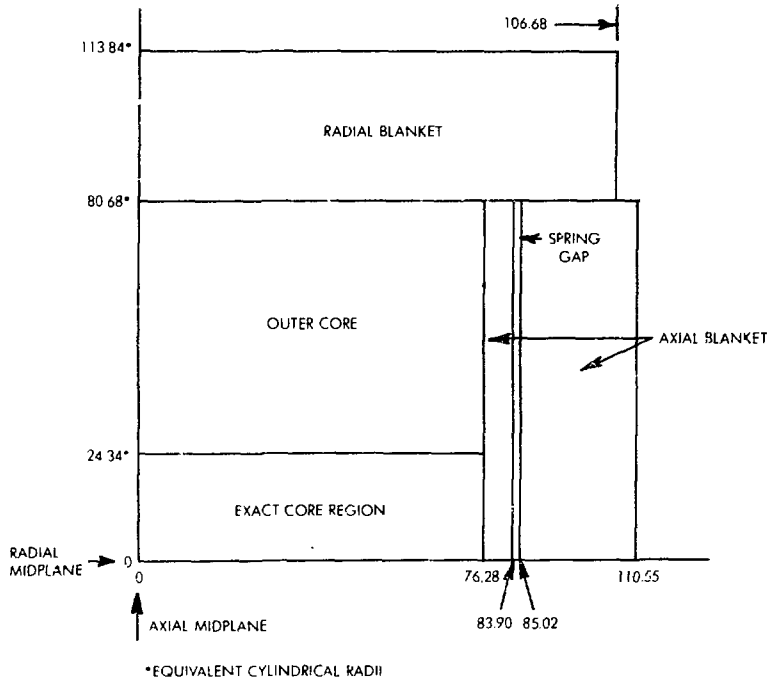

Figure 3. Axial Cross Section for the 96.2 Ih Excess Reactivity, As-Built ZPR-6 Assembly 7, ANL-Neg. No. 116-891.

FAST REACTOR BENCHMARK NO. 13

A. Benchmark Name and Type: ZPR-3-56B, and PuO_2 critical assembly with a nickel reflector.

B. System Description: This particular configuration of ZPR-3 was part of a series of critical experiments conducted to obtain data to evaluate calculational methods for the FTR. The core of assembly 56B was approximately a 615 liter cylinder fueled with Pu and U metal and UO_2 with carbonates and oxides added to simulate a PuO_2-UO_2 composition. Also, Na was added to simulate a homogenized FTR core. The reflector was composed of Ni, Na and steel.

Assembly 56B was selected for a benchmark because: 1) a rather complete set of precise measurements was performed on this relatively simple configuration; 2) this Ni reflected assembly can be compared with other Fe or U-238 reflected benchmarks; 3) and it has a relatively large PuO_2 driven core resembling the FTR.

C. Model Description:

1. One-Dimensional Model (sphere)

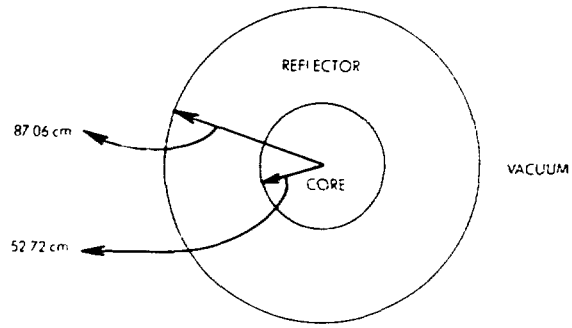

Suggestions:

Code..... 1-dimension transport theory with S_4.

Mesh..... 40 intervals in the core, 20 in the reflector.

2. Two-Dimensional Model (cylinder)

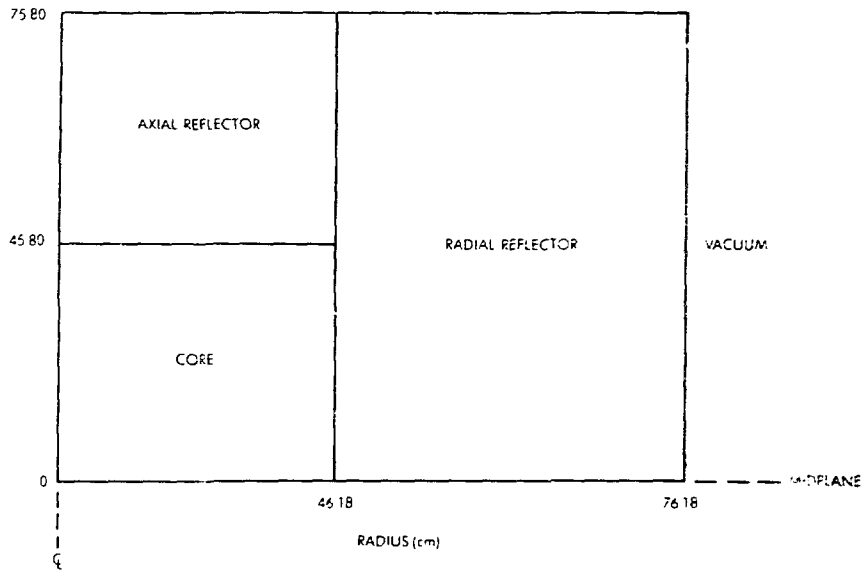

Suggestions:

Code..... 2-dimensional diffusion theory

Mesh..... 30 radial intervals, core

20 radial intervals, reflector

30 axial intervals, core

20 axial intervals, reflector

3. Atom Densities

Material	Density 10^{24} atoms/cc			
	Core	Radial Reflector	Axial Reflector	Spherical Reflector
U-235	0.000014			
U-238	0.006195			
Pu-239 & Pu-241	0.001358			
Pu-240 & Pu-242	0.000181			
O	0.015			
C	0.00103			
Na	0.008669	0.00657	0.01346	0.007879
Cr	0.0025	0.00188	0.0022	0.001941
Fe	0.0137	0.00759	0.00882	0.007824
Ni	0.00109	0.0476	0.0195	0.042261
Mo	0.00343			
Mn & Si	0.00022	0.0003	0.0003	0.0003

4. Techniques

All calculations should be performed with appropriately resonance-shielded cross sections. An acceptable multi-group structure is 26 half-lethargy width groups with E_{max} = 10 MeV.

D. Experimental Data: (All errors are one standard deviation)

1. Eigenvalue = 1.0000 ± .0014

2. Spectral Indices at Core Center

σ_f (U233) / σ_f (U235) = 1.478 ± 0.015

σ_f (U234) / σ_f (U235) = 0.195 ± 0.002

σ_f (U236) / σ_f (U235) = 0.0639 ± 0.0006

σ_f (U238) / σ_f (U235) = 0.0308 ± 0.0003

σ_f (Pu239) / σ_f (U235) = 1.028 ± 0.010

σ_f (Pu240) / σ_f (U235) = 0.282 ± 0.003

3. Material Worths at Core Center

Material	Reactivity Coefficient 10^{-5} $\Delta k/k$/mole
U-235	78.3 ± 2.2
U-238	-4.95 ± 0.22
Pu-239	100.5 ± 2.0
C	-0.338 ± 0.034
Na	-0.232 ± 0.109
Cr	-0.749 ± 0.073
Fe	-0.776 ± 0.029
Ni	-1.115 ± 0.037
B10	-79.2 ± 1.1
Ta	-24.54 ± 0.91

E. Comments and Documentation:

Since central fuel worths are sensitive to core volume and composition, the 1-D and 2-D models were set up to preserve these two experimental features. However, for the sake of simplicity, materials of low density and of little importance were either omitted or combined with other homogeneous material densities.

Correction factors were obtained in the following manner:

K_{eff} (2-D diffusion) - K_{eff} (1-D diffusion) = .0157

K_{eff} (1-D transport) - K_{eff} (1-D diffusion) = .0075

K_{eff} (heterogeneous) - K_{eff} (homogeneous) = .0102

2-D worths/1-D worths = 1.052.

The heterogeneity correction was obtained by adding the gross spatial self-shielding component (calculated using a 26-group S_{12} cell model with a homogeneous B^2 leakage) to the energy (resonance) self-shielding component (calculated using the Bell approximation).

If, for example, a 1-D transport calculation gave an eigenvalue of .9900, the corrected eigenvalue would be .9900 - .0157 (geometry correction) + .0102 (heterogeneity correction) = .9845. All 1-D central worths must be multiplied by 1.052 to account for geometric differences.

The experimental assembly 56B dimensions and compositions can be found in Reference 1, while the central indices and material worths

are given in Reference 2. The reactivity conversion parameter was calculated using the delayed neutron data of Masters (Reference 3) and found to be 1.13×10^5 $\Delta k/Ih$. The material worth values listed have been corrected for estimated sample size and composition effects.

References:

1. ANL-7561, Reactor Development Program Progress Report, March 1969, pages 8-15.

2. ANL-7577, Reactor Development Program Progress Report, April-May 1969, pages 17-35.

3. C. F. Masters et al, "The Measurement of Absolute Delayed-Neutron Yields from 3.1 and 14.9 MeV Fission," Nucl. Sci. & Eng., 36, 202-208 (1969).

FAST REACTOR BENCHMARK NO. 14

A. Benchmark Name and Type

SEFOR Doppler Benchmark, Core I

B. System Description

The SEFOR reactor was designed to provide a Doppler measurement in an environment that is representative of an operating LMFBR, with respect to the neutron spectrum, the fuel temperature range, the reactor composition and the fuel microstructure. Standard fuel for SEFOR was mixed oxide (20% PuO_2, 80% UO_2) in which the Pu contained a minimum amount of Pu-240 (~8% of the Pu) and the U was depleted in U-235. The fuel was contained in nominal one-inch diameter rods. Several guinea pig rods, having Pu concentrations 50% greater than the standard fuel, were included. Each of the fuel rods included an expansion gap located in the core region so as to minimize the reactivity effect of fuel axial expansion; hence, the Doppler effect contributed approximately 95% of the total SEFOR power coefficient and 90% of the energy coefficient. The measured Doppler coefficient reported here excludes the fuel axial expansion component.

Control of SEFOR was provided by the vertical movement of 10 nickel slab reflectors located radially outside the reactor vessel. Fine control of the position of two of these reflectors was provided; these were calibrated and used in the measurement of reactivity.

All of the SEFOR Doppler measurements used for this benchmark problem were made with the core loaded to its full size of 648 rods. This required the use of typically, 12 to 14 B_4C rods, distributed uniformly, in place of fuel rods to maintain the excess reactivity at full power to less than 50¢.

This benchmark is for SEFOR, Core I, which contained about 6 volume percent BeO. In Core II the BeO rods were replaced with steel rods, resulting in a harder spectrum. A benchmark problem for Core II has not been specified.

C.1 One-Dimensional Spherical Model Description

A one-dimensional spherical model of SEFOR is shown in Figure 1, including model dimensions and suggested mesh. The atom densities in each region (atoms/barn-cm) are given in Table I. A zero return current boundary condition should be applied at the outer boundary. Diffusion theory is suggested with cross sections in any suitable fast reactor energy-group structure, but with groups no coarser than 0.5 lethargy width down to a lethargy of 12.5. Correction factors to be made to the calculated values of k_{eff} and the Doppler coefficient are given in Section E.

Although this spherical model does not provide a very accurate description of SEFOR, it does give a computed Doppler coefficient within 2% and k_{eff} within 0.5% of that computed for the two-dimensional model (Section C.3), without the requirement of group-dependent bucklings.

C.2 One-Dimensional Axial Model Description

A one-dimensional axial model of SEFOR is shown in Figure 2, including model dimensions, suggested mesh and the composition number assigned to each region. The atom densities in each composition (atoms/barn-cm) are given in Table III. Zero return current boundary conditions should be applied at both boundaries. The set of group-dependent bucklings in Table II was found to give the Doppler coefficient within 2% and the k_{eff} within 0.5% of that computed for the two-dimensional model (Section C.3). It was not possible to find a constant buckling which produced both Doppler coefficient and k_{eff} values near to the two-dimensional results. Diffusion theory is suggested, with cross sections in any suitable fast reactor energy-group structure, but with groups no coarser than 0.5 lethargy width down to a lethargy of 12.5. Correction factors to be made to the calculated values are given in Section E.

C.3 Two-Dimensional Model Description

A two dimensional(R-Z) model of SEFOR is shown in Figure 3, including model dimensions, suggested mesh and composition number for each region. The atom densities in each composition (atoms/barn-cm) are given in Table III. Zero return current boundary conditions are to be applied on the top, right and bottom boundaries. Diffusion theory is suggested with cross sections in any suitable fast reactor energy-group structure.* Correction factor to be made to the calculated values are given in Section E.

C.4 Doppler Calculation Model

The isothermal Doppler coefficient should be computed in the following way:

$$T \frac{dk}{dT} = \frac{k_2 - k_1}{\ln \frac{T_2}{T_1}} = \frac{k_2 - k_1}{0.7006}$$

where

T_1 = 677°K (760°F), average fuel temperatures at zero power,
T_2 = 1365° K (2000°F), average fuel temperature at 20 MW,
k_1 = neutron multiplication factor with the fuel at T_1,
k_2 = neutron multiplication factor with the fuel at T_2.

It is suggested that a neutronics calculation be performed for the fuel at T_1, and that the value of $(k_2 - k_1)$ be obtained with first-order perturbation theory.

* If the two-dimensional problems are run with a group structure that contains groups broader than 0.5 lethargy, these cross sections should be generated by regionwise collapsing, using representative spectra for each of the regions in Figure 3, from a structure that has no groups greater than 0.5 lethargy width down to a lethargy of 12.5.

C.5 Cell Model Descriptions

Before comparing with experimental values for the Doppler coefficient and k_{eff}, the results of calculations with any of the three reactor models above must be corrected for effects not included in the models. These correction factors have been pre-calculated and are given in Section E. However, those computing this benchmark problem are encouraged to calculate their own correction factors. Descriptions of the fuel subassembly and B-10 cell are given below.

a. Fuel Subassembly.

Figure 4 shows a cross section of the fuel subassembly in the SEFOR core. This may be used, together with Composition 7 in Table III, (by computing volume fractions) to define a fuel cell for the calculation of heterogeneity effects. The fuel is mixed UO_2 - PuO_2. The 10 mil gap indicated in Figure 4, outside the channel wall, is sodium filled, so the value of 3.16 cm defines the effective cell outer dimension. Dimensions given in Figure 4 are for 70°F. Expansion to 350°F, to be consistent with Table III, will slightly increase the effective outer cell dimension, but will not change the material volume fractions.

b. B-10 Cell.

The benchmark problem contains 12 B_4C rods, essentially spaced evenly throughout the core. The B_4C rods replace fuel rods and are of the same diameter. A radial cell is defined by a single B_4C rod, surrounded by 1/12 of the core (Composition 7), homogeneously mixed.

D. Experimental Data

1. Measured k_{eff} = 1.0000
2. Isothermal Doppler coefficient [3] = $T \frac{dk}{dT}$ = -0.0080±0.0010

The Doppler measurements were made by determining the reactivity change in SEFOR as the power was increased from a nominal zero power to full power of 20 MW, while holding the coolant temperature constant.[2] The reactivity change was determined from the positions of calibrated reflector control rods.

Components of the reactivity change due to thermal expansion were computed and subtracted from the total to arrive at the Doppler component. (The Doppler component is >90% of the total.) Then measured and computed fuel temperatures and temperature distributions were used to obtain an equivalent, full-core, isothermal Doppler coefficient. The standard deviation of ±0.0010 includes the effects of uncertainties in other reactivity components and in fuel temperatures and temperature distributions. The measured Doppler coefficient of -0.0080 has been substantiated with both sub-prompt and super-prompt transient measurements made at several initial power levels between 0 and 10 MW, and the uncertainty has been reduced from ±0.0014 due to the transient measurements.

E. Computed Correction Factors

The correction factors in Table IV are defined as the absolute changes which should be made to the computed U-238 Doppler coefficient and to k_{eff}. For example, a computed Doppler coefficient $T \frac{dk}{dT}$ of -0.0075 would be corrected for resonance heterogeneity to -0.0080, since this correction factor is -0.00050. The correction factors were obtained as follows.

a. Resonance Heterogeneity.

A Bell-approximation correction was made to the microscopic cross sections for a radial cell defined by a fuel pin surrounded by 1/6 of the non-fuel subassembly materials, homogenized.

b. Subassembly Heterogeneity.

The effect of coarse-group flux variations across the subassembly (Figure 4) was computed for a radial cell model of the subassembly, with the BeO rod at the center.

c. B-10 Heterogeneity.

The effect of coarse-group flux variations about a B_4C pin was computed for a radial cell model defined by one B_4C pin surrounded by 1/12 of the core.

d. Reactor Expansion.

This correction factor is due to the effect of expanding the reactor from the dimensions given in Figure 3, for 350°F, to the isothermal temperature of 760°F. Although the average fuel temperature was greater than 760°F during the measurements, the SEFOR design minimizes the fuel expansion effect, and a correction for this in the basic problem was not necessary. (Both the measured and calculated Doppler coefficient exclude the fuel expansion effect.)

e. Control Effect.

The atom densities in Table III for composition 13 assume that 1.25 sections of reflector control were lowered and the void uniformly distributed. Since 1.56 sections of lowered reflector is a better description of the zero power condition, this correction accounts for both the difference in the number of sections lowered and the substantial heterogeneity effect of a single reflector.

f. Non-cylinder Effect.

This factor corrects for the irregularity of the core radial boundary. The value given here was computed earlier and reported in Reference 1.

g. Diffusion Theory Error.

This error was computed by comparison of the diffusion theory results from the spherical model with the extrapolation to S_∞ from spherical calculations in S_4, S_6, S_8 and S_{12}. It has been estimated that the inclusion of the anisotropic scattering effect using S_n-P_ℓ calculations will reduce k_{eff} by 0.001 over that obtained using S_n with transport-corrected P_0 cross sections, but this has not been verified by direct computation.

F. Comments and Documentation

The one-dimensional spherical model was derived as follows.

Region 1. The volume of this region was chosen to be equal to the volume of the portions of Compositions 2 and 3 in Figure 4 which lie

within the core ($41.800 \leq Z \leq 132.957$ cm). The composition of the region is the appropriate volume-weighted average of compositions 2 and 3 (Table III).

Region 2. The composition of this region is the volume-weighted average of compositions 6, 7 and 8 (Figure 4 and Table III). The radius of the region is 51.055 cm when the volume of these regions is conserved, but was reduced to 49.75 cm for the spherical model to produce the same k_{eff} as obtained for the two-dimensional model.

Region 3. The composition of this region is the volume-weighted average of Compositions 1,3,4,5,9,10,11,12,13 and 14 with the exception of the range $41.800 \leq Z \leq 94.243$ cm for Composition 3 and the range $0 \leq Z \leq 11.800$ cm for Compositions 4, 11, 12 and 14. The thickness of this region was chosen to preserve the volume of these component regions when Region 2 had a radius of 51.055 cm; the thickness of Region 3 was not changed when the radius of Region 2 was decreased.

Region 4. The composition of this region is the volume-weighted average of the remaining material from Figure 4 and Table III. The thickness of the region was chosen the same way as used for Region 3.

The composition and geometry of the one-dimensional axial model is identical to the two-dimensional model (Figure 3) for $4.226 \leq R \leq 44.118$. The spectrum of the perpendicular bucklings for the core regions and the constant perpendicular bucklings for the regions outside of the core were taken from computed results of the two-dimensional model. The magnitude of the perpendicular bucklings for the core regions was adjusted to produce the same k_{eff} as obtained from the two-dimensional model.

The value of β_{eff} (delayed neutron fraction) used to generate $T \frac{dk}{dT}$ from reactivity measurements is 0.00327.

G. References

1. L. D. Noble, et. al., "Results of SEFOR Zero Power Experiments", General Electric Co., GEAP-13588 (March 1970).
2. L. D. Noble, et. al., "SEFOR Core I Test Results to 20 MW", General Electric Co., GEAP-13702 (March 1971).
3. D. D. Freeman, "SEFOR Experimental Results and Applications to LMFBR's", General Electric Co., GEAP-13929 (January 1973).

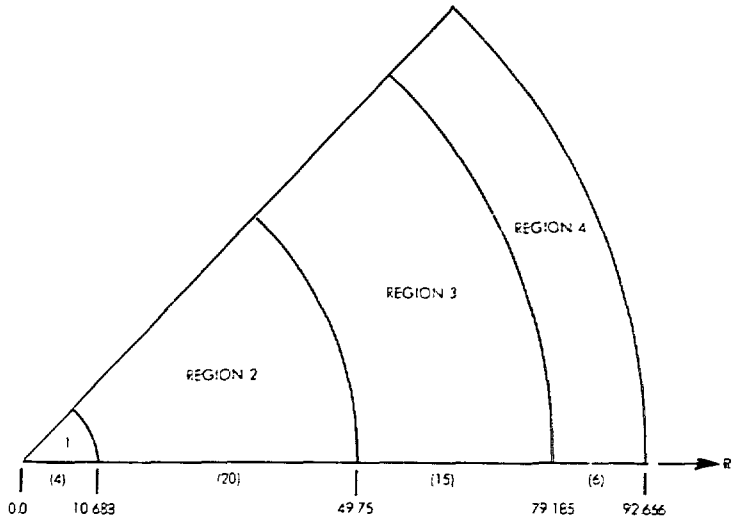

Figure 1. SEFOR Doppler Benchmark Spherical Model.
Dimensions in cm; Suggested Number of Mesh Intervals in ( ).

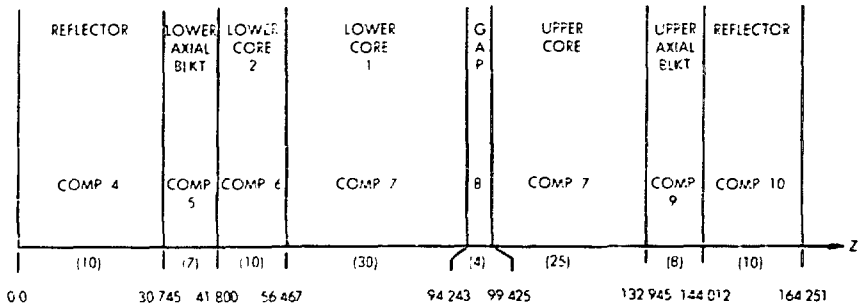

Figure 2. SEFOR Doppler Benchmark Axial One-Dimensional Model.
Dimensions in cm; Suggested Number of Mesh Intervals in ( ).

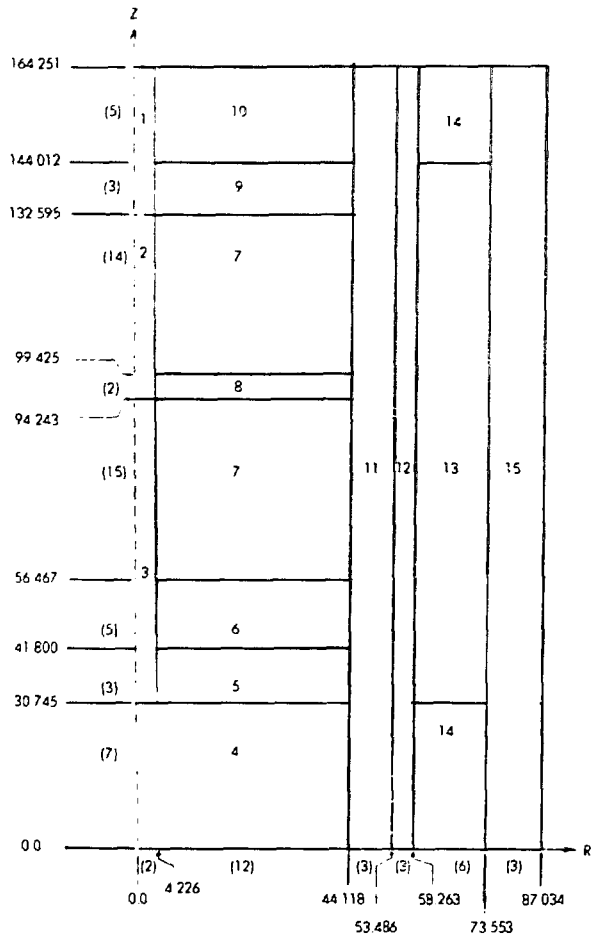

Figure 3. SEFOR Doppler Benchmark Two-Dimensional Model. Dimensions in cm; Suggested Number of Mesh Intervals in ( ).

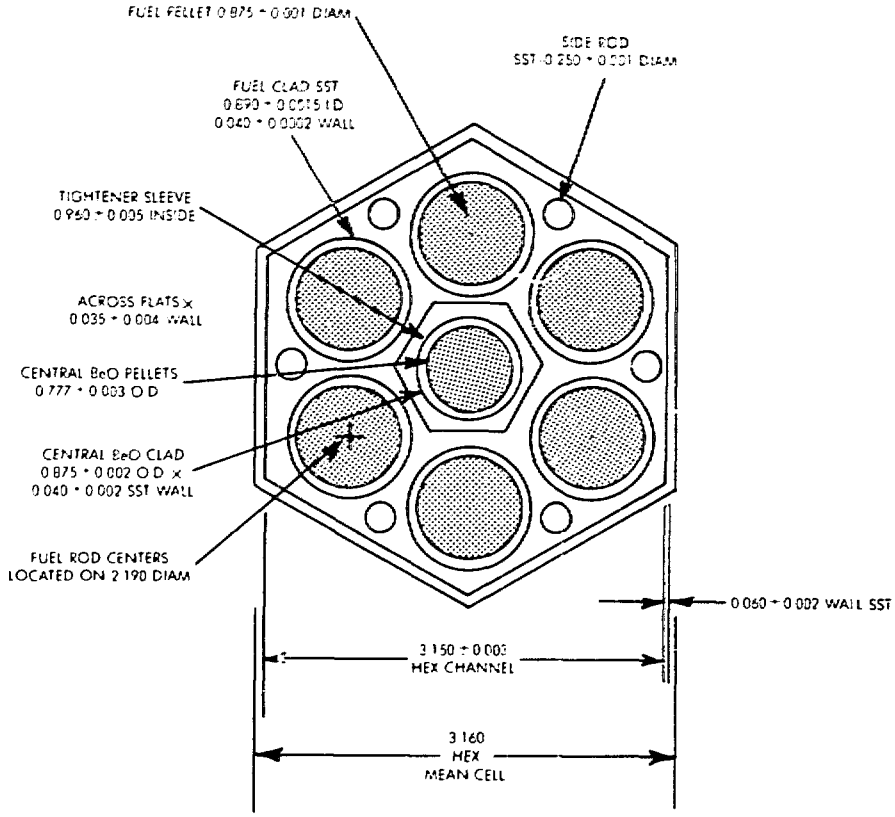

Figure 4. SEFOR Fuel Subassembly

TABLE I

SEFOR Doppler Benchmark:
Spherical Model Region Compositions (atoms/barn-cm)

Material	Region 1	Region 2	Region 3	Region 4
Fe	1.3574-2*	1.3886-2	5.8932-3	7.8587-3
Cr	3.9574-3	3.9511-3	2.8913-3	2.4623-3
Ni	2.0292-3	2.3580-3	3.0178-2	1.3315-3
Na	1.6615-2	6.8099-3	5.4493-3	1.3070-3
Si	-	3.6011-3	1.8327-5	-
O	-	2.0991-2	1.2597-4	-
Mo	-	1.1999-4	1.5605-5	-
B-10	-	6.1100-5	-	5.7684-3
B-11	-	2.4600-4	-	2.3100-2
U-235	-	1.5374-5	1.1724-7	-
U-238	-	6.9808-3	5.3438-5	-
Pu-239	-	1.5901-3	-	-
Pu-240	-	1.4355-4	-	-
Al	-	7.6770-5	-	7.2200-3
C	-	-	2.2330-3	6.5800-3

* a.bcde-n = a.bcdex10^{-n}

TABLE II

SEFOR DOPPLER BENCHMARK
AXIAL MODEL PERPENDICULAR BUCKLINGS (CM^{-2})

Lethargy Range	B_r^2 (Regions 3,4,5,6)	B_r^2 (Regions 1,8)	B_r^2 (Regions 2,7)
0 - 2	2.3-3*	1.2-3	1.4-3
2 - 4	1.8-3	1.2-3	1.4-3
4 - 6.5	1.7-3	1.2-3	1.4-3
6.5 - 9.0	1.3-3	1.2-3	1.4-3
9.0 - 10	-1.2-3	1.2-3	1.4-3
10 - ∞	-3.5-3	1.2-3	1.4-3

* a.b-n = a.bx10^{-n}

TABLE III

SEFOR DOPPLER BENCHMARK REGION COMPOSITIONS (ATOMS/BARN-CM)
FOR ONE-DIMENSIONAL AXIAL AND TWO-DIMENSIONAL MODELS

Material	Comp. 1	Comp. 2	Comp. 3	Comp. 4	Comp. 5	Comp. 6	Comp. 7	Comp. 8
Fe	1.0894-2*	7.0745-3	1.8373-2	1.4172-2	1.2837-2	1.4151-2	1.3567-2	1.7529-2
Cr	3.1760-3	2.0624-3	5.3564-3	4.4759-3	3.6373-3	4.0151-3	3.8493-3	5.1711-3
Ni	1.6285-3	1.0575-3	2.7465-3	2.3799-3	3.9552-2	2.3604-2	2.2629-3	3.6597-3
Na	1.6615-2	1.6615-2	1.6615-2	1.6900-2	6.9576-3	6.8099-3	6.8099-3	6.8099-3
Be	-	-	-	-	2.3175-4	2.6840-3	3.7769-3	3.7769-3
O	-	-	-	-	1.8660-3	2.0700-2	2.1795-2	1.0742-2
Mo	-	-	-	-	1.2014-4	1.2436-4	1.1915-4	1.1916-4
B-10	-	-	-	-	-	6.1110-5	6.1110-5	6.1110-5
B-11	-	-	-	-	-	2.4600-4	2.4600-4	2.4600-4
U-235	-	-	-	-	1.7800-6	1.5850-5	1.5850-5	7.4820-6
U-238	-	-	-	-	8.1126-4	7.1970-3	7.1970-3	3.3938-3
Pu-239	-	-	-	-	-	1.6895-3	1.6895-3	-
Pu-240	-	-	-	-	-	1.5220-4	1.5220-4	-
C	-	-	-	-	-	7.6770-5	7.6770-5	7.6770-5
Al	-	-	-	-	-	-	-	-

* a.bcde-n = a.bcdex10^{-n}

TABLE III (CONTINUED)

SEFOR DOPPLER BENCHMARK REGION COMPOSITIONS (ATOMS/BARN-CM)
FOR ONE-DIMENSIONAL AXIAL AND TWO-DIMENSIONAL MODELS

Material	Comp. 9	Comp. 10	Comp. 11	Comp. 12	Comp. 13	Comp. 14	Comp. 15
Fe	1.3748-2	1.8825-2	1.7345-2	9.4740-3	2.0489-3	9.0930-3	7.0523-3
Cr	3.9047-3	5.9192-3	5.3140-3	2.7620-3	5.9730-4	2.6590-3	2.2274-3
Ni	3.8953-2	3,1479-3	3.8328-3	1.4160-3	6.2400-2	8.3240-3	1.1843-3
Na	6.8702-3	1.3526-2	1.4842-2	-	-	-	-
Be	3.2470-4	-	-	-	-	-	-
O	1.9589-3	-	-	-	-	-	-
Mo	1.1797-4	1.2872-4	-	-	-	-	-
B-10	-	-	-	-	-	-	6.8040-3
B-11	-	-	-	-	-	-	2.7216-2
U-235	1.7800-6	-	-	-	-	-	-
U-238	8.1126-4	-	-	-	-	-	-
Pu-239	-	-	-	-	-	-	-
Pu-240	-	-	-	-	-	-	-
C	-	-	-	-	-	-	8.5149-3
Al	-	-	-	1.1790-2	2.1303-2	-	7.5555-3

* a.bcde-n = a.bcdex10^{-n}

TABLE IV

SEFOR DOPPLER BENCHMARK CORRECTION FACTORS

		$\Delta\left(T \frac{dk}{dT}\right)$	$\frac{\Delta k}{k}$
a.	Resonance Heterogeneity	-0.00050	+0.00247
b.	Subassembly Heterogeneity	-0.00009	+0.00111
c.	B-10 Heterogeneity	-0.00014	+0.00096
d.	Reactor Expansion	+0.00012	-0.00470
e.	Control Effect	∿0.0	-0.00519
f.	Non-cylinder Effect	∿0.0	-0.00300
	Total Correction to 2-D Transport Theory Results	-0.00061	-0.00835
g.	Diffusion Theory Error	-0.00004	+0.00686
	Total Correction to Diffusion Theory Results	-0.00065	-0.00149

FAST REACTOR BENCHMARK NO. 15

A. ZPR-6 Assembly 6A - A Uranium Oxide Fueled Fast Critical Assembly.

B. System Description:

The ZPR-6 consists of two halves, each a horizontal matrix of 2.2 in. square stainless steel tubes into which are loaded stainless steel drawers containing fuel and diluent materials of various types. Assembly 6A is a large (4000 liter) fast critical assembly with a soft spectrum and other characteristics representative of current LMFBR designs. It has a single fuel zone with a length-to-diameter (L/D) ratio of 0.84; it has a simple one-drawer unit cell; and it is blanketed both axially and radially with depleted uranium.[1] The assembly's spectrum characteristics, simple geometric configuration and simple unit cell make it well suited for a benchmark assembly.

The unit cell, which is shown in Fig. 1, is identical to that of a companion benchmark assembly; ZPR-6 Assembly 6A, except that the fuel is enriched uranium (5.4 w/o ^{238}U) rather than a plutonium-bearing alloy. A cross sectional view of the as-built reference assembly, which had an excess reactivity of 75.1 Ih, is shown in Fig. 2 and the equivalent cylindricalized representation of the as-built system is shown in Fig. 3.

C. Model Description:

1. One-Dimensional Model: A one-dimensional model with spherical geometry has been used in the analysis of many measurements in this assembly. The spherical model was defined with reference

to a two-dimensional finite cylindrical model, which will be described in Section C.2. The homogeneous spherical model was defined by first determining a blanket thickness and then searching for a core radius that gives the spherical reactor the same k_{eff} as the homogeneous two-dimensional cylinder. The blanket dimensions and compositions were defined as the weighted average of the axial and radial blanket dimensions and compositions in which the weighting was done on the basis of the relative leakages into the axial and radial blankets (as given by the two-dimensional calculations). The resulting core radius and blanket thickness for the homogeneous spherical model were 95.67 cm and 33.81 cm respectively. The appropriate compositions for use with the spherical model are given in Table I. The spherical model is expected to introduce approximately a 0.05% uncertainty in k_{eff}.

An energy group structure with 27 energy groups, as given in Table II, is suggested. Such a structure has sufficient detail at low energies to afford accurate computations of material worths and Doppler effects.

Because of the simplicity of the two-region, homogeneous spherical model the macroscopic flux distributions across the reactor may be computed with diffusion theory, and a relatively coarse mesh of 2 cm should be adequate.

Central material reactivity worths and Doppler reactivity worths may be computed by perturbation theory. If the material sample is optically thin and if the material is contained in the core, the homogeneous core cross sections for the material are appropriate to the sample. If the material sample is optically thin and if the material is not contained in the core, then infinite dilution cross sections are appropriate for the sample.

The major flaw in the homogeneous spherical model for this geometrically simple system is in the neglect of heterogeneities in the unit cell. Sections D and F indicate the uncertainties arising from the use of homogeneous cross sections. The error in material worth or Doppler worth introduced by flux distortions depends strongly upon the nature of the sample.

2. Other More Complicated Models: A two-dimensional finite cylindrical representation of the system is closer to the physical configuration than a spherical representation. The as-built loading was thus corrected for both excess reactivity and edge smoothing. The spring gap was homogenized into the axial blanket and the radial blanket height was defined to be the same as the core plus axial blanket. A portion of the outer core region was fueled with 1/8 in. thick enriched uranium fuel plates instead of the standard 1/16 in. thick plates. The reactivity effect of the difference in heterogeneities of the two types of plates was accounted for. The resulting region dimensions and compositions

for the zero-excess reactivity, uniform, two-dimensional model are given in Tables III and IV, respectively. The "exact core region", at the center of the assembly, is simply a region in which material concentrations are known more accurately than in the rest of the core.

D. Experimental Data:

1. Measured Eigenvalues: The measured eigenvalue corresponding to the models of Section C is 1.0000 ± 0.0005. Calculations indicate a 0.0073 heterogeneous-homogeneous correction.[2] The transport theory correction was not computed but it would be less than the 0.0018 effect in Assembly 7.

2. Unit-Cell Reaction Rates: Detailed unit-cell measurements of the capture and fission in ^{238}U and fission in ^{235}U were made. Activation foils of ^{238}U and ^{235}U were used to measure the rates within the fuel and U_3O_8 plates, such that the actual cell-averaged values of the reaction rates could be obtained. To be clear, these unit-cell reaction rate values correspond to the reactions actually taking place in the unit-cell in the assembly, and not, for example, to a cell-average defined as the values of the flux at every point in the cell multiplied by the cross section of the foil material. We use the term to refer to the flux and volume weighted reaction rates as they actually occur in the unit-cell. Hence, a per atom unit-cell reaction rate ratio is converted to the actual ratio of the number of reactions taking place in the cell simply by multiplying the former ratio by the appropriate atom density ratio.

The details of the technique used for counting the activated foils and reducing the data to absolute reaction rates are identical with those used in Ref. 3. The absolute calibrations were made with three separate and independent techniques: (1) by absolute fission chambers with identical foils on their faces to those used in the unit-cell measurements, with the fission chambers placed in the reactor at the same spectral position; (2) by thermal irradiation of identical foils in the ATSR thermal column; and (3) by absolute radiochemical analysis of some of the foils that were actually used in the unit-cell measurements. The excellent agreement among the various calibration methods made possible the small uncertainty, $1\sigma \cong 2\%$, in the measured reaction rate ratios. These are given in Table V along with calculated factor (to be applied to the measured value) for heterogeneities.[2]

3. Material Worths at the Center of the Core: Central reactivity worths of several materials were measured in a 2 x 2 x 1 in. cavity with use of the axial sample changer. The samples were plates that were placed in a stainless steel can. The reactivity worth of a sample was obtained from the difference in the reactivity worth (relative to void) of the empty and the sample-bearing can. Further descriptions of the measurements are given in Ref. 4. Table VI gives the experimental worths of the isotopes, their weights in the samples and the calculated results.

E. Calculated Results:

The calculations described in this section were made using ENDF/B

version III data and the standard one-dimensional, homogeneous spherical model of the assembly. The fundamental mode option of the SDX code[5] was used to compute homogeneous cross sections. This model yielded a multiplication constant of 0.9853, which is increased to 0.9926 by inclusion of the heterogeneity correction. In Table VII, are given the calculated values for the reaction rate ratios and the central material worths. First-order perturbation theory was used in the worth calculations.

F. Comments and Documentation:

To assess the limitations of the homogeneous spherical Benchmark model, the multiplication constant, reaction rate ratios and central reactivity worths were calculated also with a one-dimensional spherical heterogeneous model and a two-dimensional finite cylindrical heterogeneous model. In this way, the errors from homogenization can be separate from the errors from the simplified geometric representation. The heterogeneous cross sections were computed with the plate unit-cell option in the SDX code, which uses equivalence theory in the narrow resonance approximation to obtain spatial weighting factors. The model used to represent the unit cell in these SDX problems is described in Ref. 6. For the one-dimensional model, the heterogeneous cross sections were obtained with the fundamental mode option of SDX; for the two-dimensional model, the space-dependent option was used.

The results of the calculations with the three models are compared in Table VII. The one- and two-dimensional heterogeneous models are in good agreement. From comparison of the homogeneous and heterogeneous

results, heterogeneities account for a difference of 0.0073 in the multiplication constant. Heterogeneities do not affect appreciably the reaction rate ratios or the calculated worths of ^{239}Pu and ^{235}U but they have a 5% effect of the calculated worths of ^{238}U and ^{10}B and a large effect on the worth of sodium.

For the central worth measurements, the conversion factor, 1% $\Delta k/k$ = 449 Ih was used to convert the measured periods to the desired reactivity units. The delayed neutron data of Keepin[7] were used in computing the conversion factor.

References

1. C. E. Till, L. G. LeSage, R. A. Karam et. al., "ZPR-6 Assemblies 6A and 7: Benchmark Specifications for the Two Large Single-Core-Zone Critical Assemblies - ^{235}U-Fueled Assembly 6A and Plutonium-Fueled Assembly 7 - LMFBR Demonstration Reactor Benchmark Program," Applied Physics Division Annual Report, July 1, 1970 to June 30, 1971, 86-101, ANL-7910.

2. B. A. Zolotar, E. M. Bohn and K. D. Dance, "Benchmark Tests and Comparisons Using ENDF/B Version III Data," Applied Physics Division Annual Report, July 1, 1971 to June 30, 1972, ANL-8010 (in press).

3. C. E. Till, J. M. Gasidlo, E. F. Groh, "Null-Reactivity Measurements of Capture/Fission Ratio in ^{235}U and ^{239}Pu," Nucl. Sci. Eng. 40, 132 (1970).

4. R. A. Karam, W. R. Robinson, G. S. Stanford and G. K. Rusch, "ZPR-6 Assembly 6A, A 4000-Liter UO_2 Fast Core", Applied Physics Division Annual Report, July 1, 1969 to June 30, 1970, 175-183, ANL-7710.

5. W. M. Stacy, Jr., H. Henryson II, B. J. Toppel, and B. A. Zolotar, "MC^2-2/SDX Development - Part II," Applied Physics Division Annual Report, July 1, 1971 to June 30, 1972, ANL-8010 (in press).

6. J. E. Marshall, "The Unit-Cell Composition Model Developed for SDX Input Preparation and the Resulting Cell Specifications for the ZPR/ZPPR Benchmark Assemblies," Applied Physics Division Annual Report, July 1, 1971 to June 30, 1972, ANL-8010 (in press).

7. G. R. Keepin, "Physics of Nuclear Kinetics," Addison-Wesley, Reading, Mass., 1965, Table 4-7.

Table I Assembly 6A Spherical Model Atom Densities, atom/barn-cm

Isotope	Core	Blanket
^{235}U	0.001153	0.0000356
^{238}U	0.0053176	0.0395508
Na	0.0092904	-
O	0.01390	0.000023
Fe	0.013431	0.0044669
Ni	0.001291	0.0005407
Cr	0.002842	0.001247
Mn	0.000221	0.0000960

Table II. Specifications of 27-Group Structure

Group	ΔU	E_{upper}, keV	Group	ΔU	E_{upper}, keV
1	0.5	10000	14	0.5	15.034
2	0.5	6065.3	15	0.5	9.1188
3	0.5	3678.8	16	0.5	5,5308
4	0.5	2231.3	17	0.5	3,3546
5	0.5	1353.4	18	0.5	2,0347
6	0.5	820.85	19	0.5	1,2341
7	0.5	497.87	20	0.5	0.74851
8	0.5	301.97	21	0.5	0.45400
9	0.5	183.16	22	1	0.27536
10	0.5	111.09	23	1	0.10130
11	0.5	67.379	24	1	0.03727
12	0.5	40.868	25	1	0.01371
13	0.5	24.787	26	2	0.00504
			27	-	0.00068

Table III. Dimensions for the Zero-Excess Reactivity, Uniformly-Loaded Cylindrical Version of Assembly 6A

Outer core radius, cm	91.34
"Exact Core" region radius, cm	24.34
Core height, cm	152.56
Radial blanket thickness, cm	28.61
Axial blanket thickness, cm	34.22
Core Volume, liters	3999

Table IV. Atom Densities for the Zero-Excess Uniform Cylindrical Model of Assembly 6A atoms/barn-cm

	Exact Core	Outer Core	Axial Blanket	Radial Blanket
^{234}U	0.000011	0.000011	0.0000004	0.0000004
^{235}U	0.001153	0.001149	0.0000836	0.0000866
^{236}U	0.0000056	0.0000056	0.0000020	0.0000020
^{238}U	0.005801	0.005784	0.03865	0.04006
Mo	0.000011	0.000011	0.0000040[a]	0.0000034[a]
Na	0.0092904	0.009202	-	-
O[b]	0.01390	0.01474	0.000026[a]	0.000022[a]
Fe	0.01342	0.01399	0.004931	0.004197
Ni	0.001291	0.001264	0.0005977	0.0005082
Cr	0.002842	0.002841	0.001378	0.001172
Mn	0.000221	0.000222	0.000107	0.0000897

[a] Arising from SS305 impurities

[b] Includes ∿0.0088% due to heavy (atomic wt $\geq$ Si) SS304 impurities

Note: The number of digits in each density is a measure of the compositional precision. Nominally, the rightmost digit bounds the density according to a 2σ or 93% confidence interval.

Table V. Unit Cell Reaction Rate Ratios in Assembly 6A

	Measurement	Heterogeneity correction factor[a]
$^{28}f/^{25}f$	0.02411 ± 0.00072	1.016
$^{28}c/^{25}f$	0.1378 ± 0.0041	1.011

[a] calculated homogeneous/heterogeneous

Table VI. Central Reactivity Worths Measured in a Central Cavity in ZPR-6 Assembly 6A, 10^{-5} $\Delta k/k$/mole

Isotope	Isotopic wt in sample, gm	Sample-Size Correction	Measured[c,d] Worth 1σ imprecision	Calculated[e] Worth
^{239}PU	41.23	-	30.40 ± 1.06	33.16
^{235}U	4.20	-	21.86 ± 0.25	24.73
^{238}U	1151.49	1.07[a]	-1.866 ± 0.005	-2.223
^{23}Na	51.38	-	0.0082± 0.0021	-0.0140
^{10}B	29.29	1.60[b]	-29.28 ± 1.30	-26.09
Ta	833.69	-	-5.038 ± 0.004	
C	101.98	-	0.1033± 0.0005	

a. integral-transport calculation

b. by experiment

c. period/reactivity conversion factor 1% $\Delta k/k$ = 449 Ih

d. corrected for sample size effect where given

e. FOP calculation based on ENDF/B-III data and homogeneous, spherical fluxes

Table VII. Comparison of Calculations with Several Models for Assembly 6A

		1-Dimensional Homogeneous	1-Dimensional Heterogeneous	2-Dimensional Heterogeneous
k_{eff}		0.9853	0.9926	0.9920
Reaction Rates	$^{28}f/^{25}f$	0.02196	0.02161	
	$^{28}c/^{25}f$	0.1434	0.1418	
Central[a] Worths,	^{239}Pu	33.16	33.65	33.32
	^{235}U	24.73	25.50	25.27
10^{-5} $\Delta k/k$/mole	^{238}U	-2.223	-2.341	-2.317
	Na	-0.0140	-0.0343	-0.0331
	^{10}B	-26.09	-27.40	-27.12

[a] FOP Calculations not corrected for sample size effects

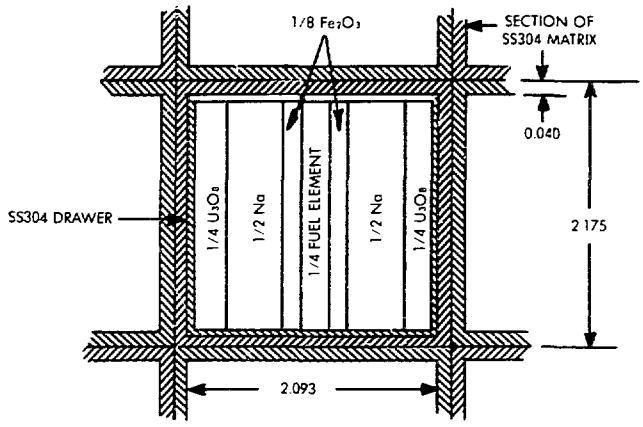

UNIT CELL FOR ASSEMBLIES 6A AND 7

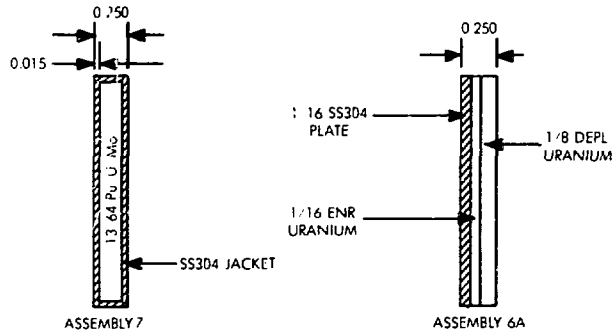

FUEL ELEMENT SPECIFICATION

ALL DIMENSIONS IN INCHES

Figure 1. Cross Section of Unit-Cell Showing Matrix and Plate Loaded Drawer, ZPR Assemblies 6A and 7, ANL-Neg. No. 116-888.

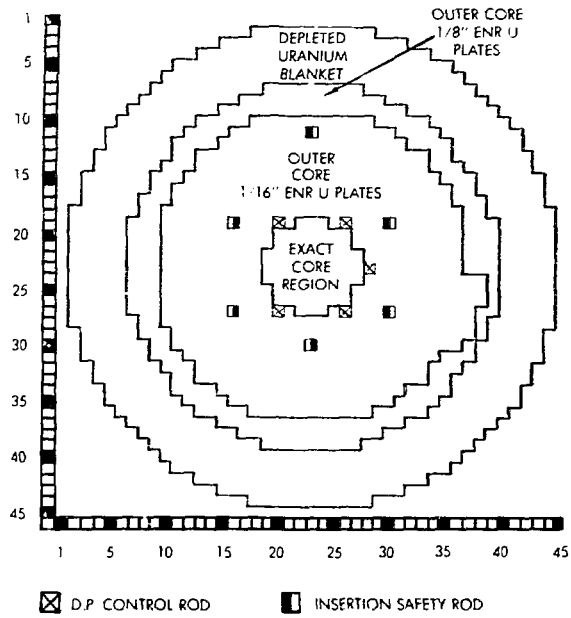

Figure 2. Radial Cross Section for 75.1 Ih Excess Reactivity, As-Built ZPR-6 Assembly 6A, ANL-Neg. No. 116-890.

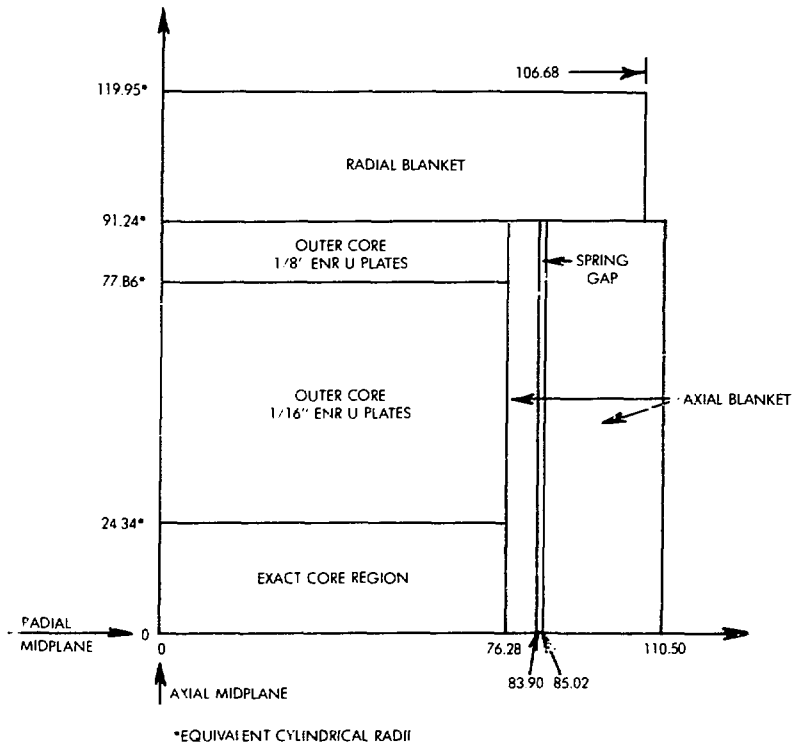

Figure 3. Axial Cross Section for 75.1 Ih Excess Reactivity, As-Built ZPR-6 Assembly 6A, ANL-Neg. No. 116-892.

CROSS SECTION EVALUATION WORKING GROUP SHIELDING BENCHMARK COMPILATION

by

CSEWG Shielding Subcommittee

June 1974

CSEWG SHIELDING BENCHMARK CONTENTS

I. Introduction

The CSEWG Shielding Benchmarks have been published or are in the process of being published as formal laboratory reports that are widely available. For these cases only a compilation of references will be given.

II. References to Shielding Benchmarks Published as Laboratory Reports

SDT1. Iron Broomstick Experiment - An Experimental Check of Neutron Total Cross Sections (ORNL-3876, ENDF-166, Revised)

SDT2. Oxygen Broomstick Experiment - An Experimental Check of Neutron Total Cross Sections (ORNL-3868, ENDF-167, Revised)

SDT3. Nitrogen Broomsitck Experiment - An Experimental Check of Neutron Total Cross Sections (ORNL-3869, ENDF-168, Revised)

SDT4. Sodium Broomstick Experiment - An Experimental Check of Neutron Total Cross Sections (ORNL-3870, ENDF-169, Revised)

SDT5. Stainless Steel Broomstick Experiment - An Experimental Check of Neutron Total Cross Sections (ORNL-3871, ENDF-170,(Revised))

SDT6. Experiment on Secondary Gamma-Ray Production Cross Sections Arising from Thermal-Neutron Capture in Iron, Stainless Steel Nitrogen and Sodium (ORNL-3957, ENDF-176)

SDT7. Experiment on Secondary Gamma-Ray Production Cross Sections Averaged Over a Fast-Neutron Spectrum for Iron, Stainless Steel, Oxygen, and Sodium (ORNL-3974, ENDF-177)

SDT9. Neutron Attenuation Measurements in a Mockup of the FFTF Radial Shield (AI-AEC-13048, ENDF-181)

SDT10. Calculational Models for LLL Pulsed Spheres (UCID-16372) - ^{6}Li, ^{7}Li, Be, C, N, O, Mg, Aℓ, Ti, Fe, Pb, ^{235}U, ^{233}U, ^{239}Pu

SDT11. The ORNL Benchmark Experiment for Neutron Transport Through Iron and Stainless Steel, Part 1 (ORNL-TM-4222, ENDF-188)

SDT12. The ORNL Benchmark Experiment for Neutron Transport Through Sodium (ORNL-TM-4223-189)

III. References to Shielding Benchmarks in Preparation as Laboratory Reports

SDT8. Experiment on the ZPPR Mock-up of the FTR Reactor plus Shield (ANL; Write-up by LASL)

CROSS SECTION EVALUATION WORKING GROUP
THERMAL REACTOR BENCHMARK COMPILATION

June 1974

CSEWG Data Testing Subcommittee
Thermal Data Testing Group

THERMAL REACTOR BENCHMARK CONTENTS

I. INTRODUCTION

The validation of nuclear data files in the calculation of thermal reactor benchmarks is an important objective of CSEWG. At this time no special introductory material has been written for the thermal reactor benchmarks but much of the introductory material for the section on Fast Reactor Benchmarks is appropriate.

THERMAL REACTOR BENCHMARKS NOS. 1-5

A. Benchmark Name and Type: ORNL-1 through ORNL-4, ORNL-10, unresolved spheres of ^{235}U.

B. System Description

This series of benchmarks consists of five unreflected spheres of ^{235}U (as uranyl nitrate) in H_2O, three of them poisoned with boron. Critical compositions and volumes were determined. These benchmarks are useful for testing H_2O fast scattering data, the ^{235}U and thermal absorption of hydrogen.

C. Model Description

Benchmarks ORNL-1 through ORNL-4 are of radius 34.595 cm; ORNL-10 has radius 61.011 cm.

	Concentration, 10^{24} atoms/cm^3				
Material	ORNL-1	ORNL-2	ORNL-3	ORNL-4	ORNL-10
^{10}B	0.0	1.0286×10^{-6}	2.0571×10^{-6}	2.5318×10^{-6}	0.0
H	0.066228	0.066148	0.066070	0.066028	0.066394
O	0.033736	0.033800	0.033865	0.033902	0.033592
N	1.869×10^{-4}	2.129×10^{-4}	2.392×10^{-4}	2.548×10^{-4}	1.116×10^{-4}
^{234}U	5.38×10^{-7}	6.31×10^{-7}	7.16×10^{-7}	7.62×10^{-7}	4.09×10^{-7}
^{235}U	4.8066×10^{-5}	5.6206×10^{-5}	6.3944×10^{-5}	6.7959×10^{-5}	3.6185×10^{-5}
^{236}U	1.38×10^{-7}	1.63×10^{-7}	1.84×10^{-7}	1.97×10^{-7}	2.20×10^{-7}
^{238}U	2.807×10^{-6}	3.281×10^{-6}	3.734×10^{-6}	3.967×10^{-6}	1.985×10^{-6}

It is suggested that the multiplication factor be calculated with multigroup $S_n (n \geq 4)$ or equivalent P_ℓ theory.

The measured k values (Ref. 1) and "corrected" experimental k values (Ref. 2) are shown below. The corrections were evaluated by Staub et al. to account for newer β values, the thin aluminum shells, distortion of the spherical shape, fill tubes and room return.

D. Experimental Data

	Measured k	Corrected Measured k
ORNL- 1	1.00118	1.00026
2	1.00073	.99975
3	1.00090	.99994
4	1.00028	.99924
10	1.00129	1.00031

E. Comments and Documentation

The experiments are described in Ref. 1. The experimental k values are for a sphere without container. Reference 2 presents a detailed analysis of these systems including a discussion of cross section sensitivities and uncertainties in the analysis, both systematic and random.

References:

1. R. Gwin and D. W. Magnuson, "Eta of ^{233}U and ^{235}U for Critical Experiments," Nucl. Sci. Eng. 12, 364 (1962).
2. A. Staub et al., "Analysis of a Set of Critical Homogeneous U-H_2O Spheres," Nucl. Sci. Eng. 34, 263 (1968).

THERMAL REACTOR BENCHMARKS NOS. 6-9

A. Benchmark Name and Type: TRX-1 through TRX-4, H_2O- moderated uranium lattices.

B. System Description

These benchmarks are H_2O moderated lattices of slightly enriched (1.3%) uranium rods with diameters of .4915 cm in a triangular pattern. Measured lattice parameters include ρ^{28}, δ^{25}, δ^{28}, and C*; B^3 was measured for TRX-1 and TRX-2, but not for TRX-3 and TRX-4 which are two-region lattices. These lattices directly test cross sections for ^{238}U fast fission. They are sensitive to ^{238}U inelastic scattering, the ^{235}U fission spectrum and the H_2O cross sections.

C. Model Description

1. Infinite Lattice Calculation

a. Physical Properties (Cylindrical Geometry)

Region	Outer Radius, cm	Isotope	Concentration 10^{24} Atoms/cm^3
Fuel	0.4915	^{235}U	6.253×10^{-4}
		^{238}U	4.7205×10^{-2}
Void	0.5042	-	
Clad	0.5753	Al	6.025×10^{-2}
Moderator	*	^{1}H	6.676×10^{-2}
		^{16}O	3.338×10^{-2}

*Lattice spacings of 1.8060, 2.1740, 1.4412, and 2.8824 cm, respectively, for TRX-1 through TRX-4.

b. Suggested Method of Calculation

Monte Carlo, multigroup $S_n (n \geq 4)$ or equivalent P_ℓ, or integral transport theory. An accurate treatment of resonance absorption is essential.

2. Leakage Calculation

a. To account for leakage use a homogenized multigroup B_ℓ calculation with a total buckling $B^2 = .0057\ cm^{-2}$ for TRX-1 and $B^2 = .005469\ cm^{-2}$ for TRX-2. This is not suitable for TRX-3 and TRX-4 which are two-region lattices.

b. An alternative treatment of leakage, applicable to all four lattices, is to cylinderize them and calculate radial shapes explicitly using multigroup S_n or P_ℓ theory. In all four lattices the axial buckling is $.000526\ cm^{-2}$; all are fully reflected. Core perimeters are as nearly circular as possible.

TRX-1: 764 fuel rods

TRX-2: 578 fuel rods

TRX-3: A hexagonal array of 169 UO_2 rods was removed from the center of the driver lattice (pitch 1.806 cm), leaving 1432 rods. A hexagonal array of 217 metal rods (pitch 1.4412 cm) was centered in the opening.

TRX-4: Every other rod of the TRX-3 inner lattice was removed, leaving 61 metal rods (pitch 2.8824 cm). 1809 UO_2 driver rods were now required.

Dimensions of Cylinderized TRX Lattices

Composition	Outer Radius (cm)			
	TRX-1	TRX-2	TRX-3	TRX-4
Homogenized test Lattice cells	26.2093	27.4419	11.1467	11.8198
Water gap	-	-	12.3268	12.3268
Homogenized driver lattice cells	-	-	37.9406	42.1717
Reflector		large		

Properties of UO_2 Driver Lattice (TRX-3 and TRX-4)

Region	Outer Radius, cm	Isotope	Concentration 10^{24} Atoms/cm^3
Fuel	.4864	^{235}U	3.112×10^{-4}
		^{238}U	2.3127×10^{-2}
		^{16}O	4.6946×10^{-2}
Void	.5042	-	
Clad	.5753	Al	6.025×10^{-2}
Moderator	*	^{1}H	6.676×10^{-2}
		^{16}O	3.338×10^{-2}

*Triangular pitch lattice with spacing of 1.8060 cm.

D. Experimental Data

	TRX-1	TRX-2	TRX-3	TRX-4
Pitch, cm	1.8060	2.1740	1.4412	2.8824
Water/fuel vol. ratio	2.35	4.02	1.00	8.11
Number of rods	764	578	217	61
B^2, 10^{-4} cm^{-2}	57 ± 1	54.69 ± .36	-	-
ρ^{28}	1.311 ± .02	.830 ± .015	3.01 ± .05	.466 ± .01
δ^{25}	.0981 ± .001	.0608 ± .0007	.230 ± .003	.0352 ± .0004
δ^{28}	.0914 ± .002	.0667 ± .002	.163 ± .004	.0452 ± .0007
C*	.792 .008	.646 ± .002	1.255 ± .011	.526 ± .004

Note: Parameters correspond to thermal cutoff of 0.625 eV and were measured at core center.

ρ^{28} = ratio of epithermal-to-thermal ^{238}U captures.

δ^{25} = ratio of epithermal-to-thermal ^{235}U fissions.

δ^{28} = ratio of ^{238}U fissions to ^{235}U fissions.

C* = ratio of ^{238}U captures to ^{235}U fissions.

E. Comments and Documentation

Parameter measurements are described in Ref. 1 and 2. Measurements of thermal disadvantage factors (Ref. 3) and fast advantage factors (Ref. 4) are also available. Reference 5 shows some additional details about the lattices, fuel rods, etc. Cadmium cutoff energies and foil perturbation were given careful attention.

REFERENCES

1. J. Hardy, Jr., D. Klein and J. J. Volpe, "A Study of Physics Parameters in Several Water-Moderated Lattices of Slightly Enriched and Natural Uranium," WAPD-TM-931, March 1970.

2. J. Hardy, Jr., D. Klein and J. J. Volpe, Nucl. Sci. Eng., 40, 101 (1970).

3. J. J. Volpe, J. Hardy, Jr., and D. Klein, Nucl. Sci. Eng. 40, 116 (1970).

4. J. Hardy, Jr., D. Klein and R. Dannels, Nucl. Sci. Eng. 26, 462 (1966).

5. J. R. Brown et al., "Kinetics and Buckling Measurements in Lattices of Slightly Enriched U or UO_2 Rods in H_2O," WAPD-176 (Jan. 1958).

THERMAL REACTOR BENCHMARKS NOS. 10-12

A. Benchmark Name and Type: MIT-1, MIT-2, and MIT-3, D_2O-moderated uranium lattices.

B. System Description

These benchmarks consist of D_2O-moderated lattices of natural uranium rods with diameters of 2.565 cm positioned in a triangular lattice pattern. The associated lattice spacings are 11.43, 12.70, and 14.605 cm. Measured lattice parameters include B^2, ρ^{28}, δ^{25}, δ^{28}, and C*. These lattices are useful for testing D_2O cross section data and cross sections for thermal and eqithermal ^{235}U fission, thermal and epithermal ^{238}U neutron capture, and ^{238}U fast fission.

C. System Description

1. Infinite Lattice Calculation

a. Physical Properties (Cylindrical Geometry):

Region	Outer Radius, cm	Composition Isotope	Concentration 10^{24} Atoms/cm^3
Fuel	1.283	^{235}U	3.441×10^{-4}
		^{238}U	4.745×10^{-2}
Clad	1.354	Al	6.049×10^{-2}
Moderator	*	^{1}H	1.850×10^{-4}
		^{2}H	6.641×10^{-2}
		^{16}O	3.321×10^{-2}

*Lattice spacings of 11.43, 12.70 and 14.605 cm (benchmarks MIT-1, MIT-2, and MIT-3 respectively).

b. Suggested Method of Calculation:

Monte Carlo S_n ($n \geq 4$) or integral transport theory. An accurate treatment of resonance absorption is essential.

2. Axial Leakage Calculation

To account for leakage use the following geometric bucklings in B_ℓ calculations with $\ell \geq 1$:

Benchmark	Pitch, cm	B^2, 10^6 cm^{-2}
MIT-1	11.43	848
MIT-2	12.70	865
MIT-3	14.605	815

A less desirable way to account for axial leakage is to use the following critical heights, h:

Benchmark	h, cm	λ_{tr} cm
MIT-1	103.8	2.845
MIT-2	102.9	2.769
MIT-3	106.2	2.692

These heights have been derived from measured material bucklings using

$$B^2 = \frac{(\pi)^2}{(h + \epsilon)^2}$$

when the extrapolation distances, ϵ, have been determined using the relation

$$\epsilon = 0.71\ \lambda_{tr}$$

The values for the transport mean free patch λ_{tr} were obtained using leakage corrected integral transport theory and ENDF/B-III cross sections.

D. Experimental Data

Parameter	Pitch, cm 11.43	12.70	14.605
B^2, 10^6 cm^{-2}	848 ± 10	865 ± 10	815 ± 8
ρ^{28}	0.498 ± 0.008	0.394 ± 0.002	0.305 ± 0.004
δ^{25}	0.447 ± 0.0019	0.031 ± 0.003	0.0248 ± 0.0010
δ^{28}	0.0597 ± 0.0020	0.0596 ± 0.0017	0.0583 ± 0.0012
C^*	1.017 ± 0.023	0.948 ± 0.020	0.859 ± 0.016

Note: Parameters correspond to thermal cutoff of 0.625 eV.

ρ^{28} = ratio of epithermal-to-thermal ^{238}U captures

δ^{25} = ratio of epithermal-to-thermal ^{235}U fissions

δ^{28} = ratio of ^{238}U fissions to ^{235}U fissions

C^* = ratio of ^{238}U captures to ^{235}U fissions

F. Comments and Documentation

The physical properties of the lattices and the experimental facilities are described in Ref. 1. The measured lattice parameters are documented in Ref. 2. With regard to the latter, no mention is made of the cadmium cutoff energy to be associated with the δ^{25}, ρ^{28} measurements. Apparently the experiments employed 20 mil Cd covers (3), (4); hence the values reported in Ref. 2 correspond to a cutoff energy of approximately 0.55 eV. The experimental values for δ^{25} and ρ^{28} recorded here have been adjusted from a 0.555 eV cutoff energy to a 0.625 eV cutoff using ENDF/B cross sections.

REFERENCES

1. P. F. Palmedo et al., "Measurements of the Material Bucklings of Lattices of Natural Uranium Rods in D_2O," NYO-9660 (MITNE-13) (1962).
2. T. J. Thompson et al., "Heavy Water Lattice Project Final Report," MIT-2344-12 (1967).
3. Irving Kaplan et al., "Heavy Water Lattice Project Annual Report, September 30, 1963," NYO-10,212 (MITNE-46) (1963).
4. M. J. Driscoll, Private communication (Oct. 1972).

THERMAL REACTOR BENCHMARKS NOS. 13-17

A. Benchmark Name and Type: PNL-1 through PNL-5, unreflected plutonium spheres.

B. System Description

This series of benchmarks consists of five unreflected spheres of plutonium nitrate solutions with hydrogen/^{239}Pu atom ratios ranging from 131 to 1204. Critical volumes for the various solutions were measured. In one experiment the critical buckling was determined. These benchmarks are useful for testing H_2O scattering data, cross sections for thermal neutron capture and fission by ^{239}Pu, and the ^{239}Pu fission spectrum.

C. Model Description

PNL-1 and PNL-2 have H/^{239}Pu atom ratios of 700 and 131 respectively; each contains 4.6 wt. % ^{240}Pu and has an effective radius of 19.509 cm.

	Concentration, 10^{24} atoms/cm^3	
Material	PNL-1	PNL-2
H	.06563	.05416
O	.03456	.03977
N	6.216×10^{-4}	4.720×10^{-3}
^{239}Pu	9.373×10^{-5}	4.141×10^{-4}
^{240}Pu	4.501×10^{-6}	1.988×10^{-5}

Benchmarks PNL-3 and PNL-4 have H/^{239}Pu atom ratios of 1204 and 911 respectively; each contains 4.20 wt. % ^{240}Pu and has an effective radius of 22.70 cm.

Material	Concentration, 10^{24} atoms/cm^3 PNL-3	PNL-4
H	.06495	.06041
O	.03441	.03712
N	7.393×10^{-4}	2.775×10^{-3}
Fe	1.294×10^{-6}	1.520×10^{-6}
^{239}Pu	5.395×10^{-5}	6.633×10^{-5}
^{240}Pu	2.355×10^{-5}	2.895×10^{-6}

Benchmark PNL-5 has an effective radius of 20.1265 cm, a H/^{239}Pu atom ratio of 578 and contains 4.17 wt. % ^{240}Pu.

Material	Concentration, 10^{24} atoms/cm^3
H	.06028
O	.03710
N	2.737×10^{-3}
Fe	1.930×10^{-6}
^{239}Pu	1.043×10^{-4}
^{240}Pu	4.520×10^{-6}

It is suggested that multiplication constants k be calculated using S_n theory ($n \geq 4$) with approximately 50 mesh points per sphere. A group structure should be selected which adequately represents fast leakage phenomena as well as thermal events. Pu-240 resonance absorption is significant in these calculations.

D. Experimental Data

The compositions and dimensions specified above were experimentally derived for criticality (k = 1). A geometric buckling of 0.02182 ± 0.00015 cm^{-2} was derived for PNL-1.

F. Comments and Documentation

The experimental conditions associated with benchmarks PNL-1 and PNL-2 are given in (1). Recent calculations for these two benchmarks with ENDF/B-II data are described in (2). Reference 3 documents the experimental conditions associated with PNL-3, PNL-4, and PNL-5. In all five experiments the plutonium nitrate solutions were enclosed in stainless steel walled spheres. The effective radii quoted above in the Physical Properties Section were derived by the experimenters (1), (3) and specify critical sizes for solutions without stainless steel walls.

REFERENCES

1. R. C. Lloyd et al., "Criticality Studies with Plutonium Solutions," Nuc. Sci. and Eng. 25, 165 (1966).
2. L. E. Hansen and E. D. Clayton, "Theory-Experiment Tests Using ENDF/B Version II Cross-Section Data," Trans. Amer. Nuc. Soc. 15, 309 (June 1972).
3. F. E. Kruesi et al., "Critical Mass Studies of Plutonium Nitrate Solution," HW-24514 (1952).